STUDIES OF NON REFLECTING BOUNDARY CONDITIONS AND THEIR APPLICATIONS

Thesis

Submitted in Partial Fulfillment of the Requirements

for the Degree of

DOCTOR OF PHILOSOPHY

by

RAJIV CHATURVEDI

Department of Mechanical Engineering

Indian Institute of Technology, Bombay

October, 1999.

Approval

Thesis entitled: Studies of Non Reflecting Boundary Conditions and their Applications

by Rajiv Chaturvedi

is approved for the degree of DOCTOR OF PHILOSOPHY.

Examiners:

_ _ _ _ _ _ _ _ _ _ _ _ _ _ _ _

_ _ _ _ _ _ _ _ _ _ _ _ _ _ _ _

_ _ _ _ _ _ _ _ _ _ _ _ _ _ _ _

_ _ _ _ _ _ _ _ _ _ _ _ _ _ _ _

Supervisor:

Prof. D. P. Roy

_ _ _ _ _ _ _ _ _ _ _ _ _ _ _ _

Chairman:

_ _ _ _ _ _ _ _ _ _ _ _ _ _ _ _

Date:

_ _ _ _ _ _ _ _ _ _

Place:

_ _ _ _ _ _ _ _ _

Course Work

Indian Institute of Technology, Bombay, India

Certificate of Course Work

This is to certify that Mr. Rajiv Chaturvedi was admitted to the candidacy of Ph. D. degree on the 4^{th} of January, 1993, after successfully completing all the courses required for the Ph. D. degree program. The details of the course work done are given below.

Sr. No.	Course No.	Course Name	Credits
(1)	ME 660	Numerical Methods and Computational Techniques for Fluid Flow Problems	6
(2)	MES 601	Seminar	4
(3)	MA 404	Elements of Partial Differential Equations	Audit
(4)	ME 613	Finite Element and Boundary Element Methods	Audit
(5)	MA 403	Real Analysis	Audit
		Total Credits	10

I.I.T. Bombay Dy. Registrar (Academic)

Dated:

Acknowledgement

I would like to thank my guide **Prof. D. P. Roy** for his constant help and valuable advice throughout the course of this endeavour without which this would have been but an effort in futility.

Rajiv Chaturvedi

1999

Abstract

In order to model infinite or very large spatial domains by smaller finite computational domains accurately for wave propagation problems, Non Reflecting Boundary Conditions (NRBC) must be imposed at the artificial truncation boundary. This dissertation deals with modeling of unbounded media using NRBC's. The reported work consists of formulation and application of NRBC's for two different classes of problems. Depending on the governing differential equations, the approach towards formulating an NRBC as well as the NRBC itself are different.

In the first part, formulation and well posedness analysis of a class of NRBC's for the time dependent scalar wave equation has been carried out. These NRBC's are then applied to a problem of large heat exchangers in nuclear/ process industries. A methodolgy is developed to compute the pressure field in the moderator of a pressurized heavy water reactor after a high pressure tube has failed. The method affords significant economic improvement for computation by reducing the spatial domain of computation. NRBC's simulate the behaviour of the large expanse of low pressure fluid outside the computational domain. Reflections from multiple tubes in the domain are considered. Transient phase of the solution is concentrated upon. Computer experimentation is carried out on the placement of truncating boundaries. In this part of the work, the governing differential equation is comparatively simple, but the geometry is complex.

In the second part of the work, three new NRBC's for the compressible Navier Stokes equations are proposed. They are characterised by two tunable parameters, and by the way they handle the term containing the pressure at the subsonic outflow boundary of the truncated domain. Their performance is investigated by applying them to a simple geometry of a semi infinite flat plate placed in a uniform transonic stream of air. Steady state solution is sought by means of time marching. The effect of the NRBC applied and of the two parameters on rate of convergence is studied. The criteria of minimum spurious reflections from the subsonic outflow boundary is related

to the minimum steps required for convergence to steady state. Spurious reflections are graphically observed. We deal with a non linear set of governing differential equations and boundary conditions but a simple geometry in this part of the work.
Keywords: non reflecting boundary condition, absorbing boundary condition, wave equation, compressible Navier Stokes equations, full Navier Stokes equations, transonic flow, compressible flow, truncation boundary, artificial boundary, unbounded domain, unbounded media, pressurized heavy water reactor, NRBC, PHWR.

Contents

List of Figures

List of Tables

Nomenclature

In some cases, the same symbol has been used to represent more than one quantities. All symbols are defined where they appear in the text, reference to text is therefore suggested.

Abbreviations	
b.c.	boundary condition
BEM	boundary element method
CFL	Courant Friedrichs Lewy
deg	degrees (for angle measurements)
FEM	finite element method
g.d.e.	governing differential equation
IBVP	initial boundary value problem
MoC	method of characteristics
NRBC	non reflecting boundary condition
NRBC's	non reflecting boundary conditions
NS	Navier Stokes
o.d.e.	ordinary differential equation
p.d.e.	partial differential equation
PHWR	pressurized heavy water reactor
PML	perfectly matched layer
UKC	uniform Kreiss condition
Chapters 1 and 2	
ρ	mass density
u	perpendicular displacement; x-velocity component; any field variable

$\dot{u}$	partial derivative of u with respect to time
r	radial coordinate measured from some point in the interior domain
ω	cyclic frequency
x, y, z	space coordinates
t	time
c	phase velocity
k	$= \omega/c$
d	spatial dimension ($= 1$, 2 or 3)
∞	super/sub-script denotes the unbounded medium or the free stream values
$[S^{\infty}(\omega)]$	dynamic-stiffness matrix
ϕ	any field variable
$\phi(0, x)$	$= \phi_0(x)$, the initial condition on ϕ
f, g	functions in D'Alembert's solution of the wave equation
$\vec{x}$	(t, x)
i	$\sqrt{-1}$
ξ	wave number
ζ	$= (\omega, \xi)$, the wave vector
θ	angle of incidence on the truncation boundary
$R(\theta)$	reflection coefficient (fractional amplitude of reflected wave)
C, k	constants in the well-posedness condition
$r(z)$	a rational approximation $P(z)/Q(z)$
N, M	integers
$f_{(N,M)}(z)$	Pade approximation of order (N, M) to a function $f(z)$

$P_N(z)$	polynomial of order N, numerator in the order (N, M) rational approximation
$Q_M(z)$	polynomial of order M, denominator in the order (N, M) rational approximation
α, β	angles, parameters
V	functional in variational method used for deriving NRBCs
$w(\theta)$	weight function
Chapter 3	
B	artificial truncation boundary, it must not reflect
Ω	the entire domain
$\partial\Omega_j$	boundaries (subspaces) of Ω, j is an integer
$\partial(\partial\Omega_j)$	intersection of two boundaries, a corner in two space dimensions (subspace of $\partial\Omega_j$)
p	perturbation in pressure
a_∞	speed of sound in undisturbed medium
i,j	grid indices in x and y directions respectively, they appear as subscripts. i also denotes $\sqrt{-1}$.
k	index for time, appears as superscript
Δx, Δy	steps in x and y directions
Δt	the step in time
λ	stability factor (Courant Friedrichs Lewy criteria) for the time marching numerical scheme, subscripts x and y denote its value in the two space directions
α	the free parameter of certain NRBCs
α_j	multiple paramerters in certain NRBCs to tune them for better performance
R	reflection coefficient, subscript denotes the NRBC referred to

θ	the actual angle of incidence of the waves
ξ, η, τ	parameters in the single mode solution used in the Uniform Kreiss Condition to test well posedness, dispersion relation relates ξ to η and τ
Chapter 4	
T	temperature
E	specific total energy
p	pressure
u	x-component of velocity
v	y-component of velocity
ρ	mass density
U	conserved quantities in Navier Stokes equations
F, G	flux vectors in Navier Stokes equations
ϕ	denotes each of the dependent variables (u, v, ρ, T) in Navier Stokes equations
μ	coefficient of viscosity
k	coefficient of heat conductivity
c_p	specific heat at constant pressure
c_v	specific heat at constant volume
γ	c_p/c_v
Re	Reynolds number
Pr	Prandtl number
M	Mach number
c	local speed of sound in the fluid
ref	denotes a reference quantity for non dimensionalization
∞	denotes a free stream quantity
ϵ	value of the convergence criteria

λ	stability factor for the time marching numerical scheme,
	subscripts x and y denote its value for the grid
	in the two space directions
$\mathbf{R}$	real part of a complex quantity
i	$\sqrt{-1}$, also grid index in the x- direction
β	stretching coefficient for the grid
s	x distance from the leading edge of the plate
v_{edge}	value of v at the edge of the boundary layer
N_{conv}	number of steps required to reach convergence
α	the multiplicative free parameter in the newly proposed
	NRBCs, single parameter of Rudy and Strikwerda NRBC
z	the second parameter which appears as the power in
	the newly proposed NRBCs

Chapter 1

Introduction

1.1 Introductory remarks

Considerations of computer memory and time in the numerical solution of differential equations (partial and ordinary) posed over a spatial domain of infinite or very large extent leads one to truncating the domain to a smaller (interior) region of interest. In such a situation, the question of the condition to be imposed at the truncation boundary becomes important, especially when the phenomenon under consideration is that of wave propagation. A wrong boundary condition (b.c.) in such a case physically amounts to a non-existing nonhomogeneity in the medium; computationally it leads to spurious reflection of waves into the interior domain. In order to model infinite or very large domains by smaller finite computational domains accurately for wave propagation problems, Non Reflecting Boundary Conditions (NRBC) must be imposed at the truncation boundary. NRBC's do not allow waves that originate in the interior region and strike the truncation boundary to be reflected back into the interior, thus modeling the actual physics.

In spite of finite computer resources and the fact that the initial value problem (IVP) involving wave phenomenon may be posed over an infinite spatial domain, an NRBC is not strictly necessary for computing the correct numerical solution for a limited spatial region, in the time domain. One can approach the computer solution in the following way, too. The requirement that in the far field the disturbance is small is sufficient for computational purposes. However, because the waves are outgoing at infinity, such a formulation requires a progressive domain expansion with time so that the size of the computational domain is always larger than the domain of influence of the wave phenomenon. The result is high computational costs especially when the

spatial domain of interest is only a small part of the entire spatial domain. Once again, the usefulness of truncated domains with NRBC's applied at the truncation boundary is apparent. For the case of solution being sought for elliptic equations, the above alternative approach is not feasible at all.

Researchers have studied NRBC's from a theoretical viewpoint and also for their applications to various phenomena. In the following pages, a review of literature pertaining to NRBC's is provided.

This dissertation deals with problems in the time domain. The theme is modeling of unbounded media using NRBC's.

1.2 Modeling of unbounded media

As mentioned above, the problem to be handled is that of an infinite/ semi-infinite/ large medium. Often, a bounded structure is also present together with the unbounded medium. The 'finite' surface is usually the structure-medium interface. When this system is excited by a time varying load, the structure interacts dynamically with the unbounded medium. To determine the resulting response, a 'dynamic unbounded medium and structure interaction' analysis is required in general. One often also has to deal with the special case of steady state analysis, obtained from the time dependent problem by assuming, for example, a cyclic steady state.

Time dependent problems requiring the modeling of an infinite domain can be classified as those related to wave propagation and those related to diffusion. Examples in wave propagation are soil-structure interaction, fluid-structure interaction, and many aspects of acoustics, electromagnetism, geophysics, etc. Some problems with this kind of geometry that can be mentioned in connection with diffusion type problems are heat conduction and consolidation of soil. Further, statics (elliptic governing differential equations) as a special case of the time dependent problem (both wave propagation and diffusion) is important.

In such unbounded medium and structure interaction analysis (which can be either dynamic or static) numerical modeling of the structure with, for instance, finite elements is comparatively well developed, but that of unbounded medium is still an

active field of research. The aim of this research is to be able to solve practical problems *efficiently* and accurately. If the unbounded medium is non linear, the problem becomes still more difficult.

Note that the loading can arise either through the unbounded medium or from the structure. The region of interest in the spatial domain is the near (interior) region around the structure, it is here that one wants to compute a solution. The far (exterior) region excluded is generally assumed to be regular in literature.

In this situation, the waves that result propagate from the structure-medium interface towards infinity (in the unbounded medium). The boundary condition applicable at infinity is a *radiation condition*, named so because this condition must be such that it does not allow energy to be *radiated* from infinity towards the structure.

1.2.1 Radiation condition

The solution (as it is in reality) for the unbounded domain must be unique. Let us consider the problem of wave propagation in an elastic medium of unbounded size. The governing differential equations (g.d.e.) of elasto-dynamics will apply for such a medium. Boundary conditions applicable are those on the structure-medium interface and on the free surface, if present. But these are not sufficient to define a unique solution. Theory leads to the so called 'radiation condition' applicable in the limit of the spatial distance (from the structure-medium interface) tending to infinity. Related references are Sommerfeld [1949], Sommerfeld [1964] and Gurtin [1972].

The development of a radiation condition is based on analysis in the *frequency domain*. Why should it be so can be explained based on the following discussion.

In the *time domain*, the additional condition required for uniqueness can be based on the *domain of influence* of the wave propagation phenomena. For a specific instant of time the domain of influence is defined as that part of the unbounded medium that is enclosed by the fastest propagating wave front, note that the domain of influence expands with time. Outside the domain of influence, the medium is at rest up to infinity.

Hence, for a *finite* time, the response of the unbounded medium can be deter-

mined from that of a sufficiently large (larger than the domain of influence) bounded medium. A vanishing displacement outside the domain of influence would suffice. But this condition would be time dependent, and will require large spatial domains so that the truncation boundary lies outside the domain of influence. When a solution is required for larger times, one may need to consider *progressively expanding* domains or a very large domain to start with. In case the condition of vanishing displacement is applied within the domain of influence, spurious (non physical) reflections that result from such a truncation boundary will spoil the solution in the domain of interest. Note that for two and three dimensional spatial domains (neglecting frictional dissipation), as a wave generated at the structure-medium interface travels *outwards*, it's amplitude attenuates; the converse is true for incoming fronts. Thus the effect of the spurious reflections will not be negligible in most situations. This kind of modeling, namely, choosing the truncation boundary outside the domain of influence is termed the technique of 'extended mesh'.

Instead of considering the region *outside* the domain of influence for modeling purposes, one can consider the ever expanding *interface* of the domain of influence and the rest of the medium. One can then proceed as follows. Consider an infinitesimal area dA on the boundary of the domain of influence. Since the element is considered on the boundary of the domain of influence, the region into which the wave front propagates is initially at rest. A load per unit area p acts in the direction perpendicular to it for an infinitesimal interval of time dt. The wave front travels a distance of $c\ dt$ (outwards), and the increase in the domain of influence is therefore $c\ dt\ dA$. Applying the law of conservation of momentum for the interval dt (and neglecting friction), we get

$$p\ dA\ dt = \rho\ c\ \dot{u}\ dA\ dt \tag{1.1}$$

where ρ is the mass density, u the displacement perpendicular to dA, and $\dot{u}$ the corresponding velocity. Thus, the response perpendicular to the boundary of the domain of influence is modeled by a dashpot of coefficient per unit area ρc (the *impedance*). Similar conclusion will hold for tangential directions. In the above, it must be remembered that for an infinitesimal increase in time, an additional part of the unbounded

medium adjacent to the wave front is incorporated in the domain of influence. The energy required for this is supplied by the structure-medium interface. Thus the structure experiences the so called *radiation damping*. The difficulties of this approach, especially for two and three dimensions, are obvious. For one dimension, where there is only the normal direction to the domain of influence, placing a dashpot of the kind described above is more feasible.

The above two approaches are based on the concept of the domain of influence. Instead of being tied down to the domain of influence, which involves analysis in the time domain as seen above, one can consider the entire unbounded domain. A so called radiation condition is the outcome of such an approach. A radiation condition is formulated at an infinite distance from the structure-medium interface, *in the frequency domain*. The condition guarantees uniqueness of the solution. As is indicated by the fact that analysis is carried out in the frequency domain, the condition of vanishing displacement at infinity is *not* sufficient for wave propagation problems. A radiation condition states that 'no energy is radiated from infinity towards the interior domain'– the unbounded medium acts as an energy sink and never as an energy source. Sommerfeld [1949], Sommerfeld [1964] or Gurtin [1972] may be looked up for the details of the derivation for the scalar wave equation.

As is obvious, the formal expression for the radiation condition will depend on the governing differential equation (g.d.e.) for the unbounded medium. It is easier to formulate a radiation condition for linear g.d.e.'s as compared to non linear ones. For the scalar wave equation,

$$\frac{\partial^2 u}{\partial t^2} = c^2 \nabla^2 u \tag{1.2}$$

the radiation condition (Sommerfeld radiation condition) for an infinite medium is formulated in terms of the radial coordinate r, measured from some point in the interior domain. The condition is:

$$\lim_{r \to \infty} r^{\frac{(d-1)}{2}} [u(\omega)_{,r} + \frac{i\omega}{c} u(\omega)] = 0 \tag{1.3}$$

In the time domain, the above can be expressed as:

$$\lim_{r\to\infty} r^{\frac{(d-1)}{2}}[u_r + \frac{1}{c}\, u_t] = 0 \tag{1.4}$$

In the above, u is the field variable (later we choose it to be pressure), $u(\omega)$ is the displacement amplitude for the frequency ω, t is time, c the phase velocity, d the spatial dimension (= 1, 2 or 3) and r the radial coordinate. Note that the Sommerfeld radiation condition is applicable only at infinity, it implies that waves at infinity are outgoing. This condition can not be used at finite distances from the source. Sommerfeld radiation condition is useful when an analytical solution over the entire spatial domain is possible.

1.2.2 Substructure *vs.* direct method of modeling the domain

As far as the bounded structure of finite dimension is concerned, methods exist to model and discretize it using one of the domain procedures, introducing a finite number of degrees of freedom. This part of analysis is well understood.

In order to model the unbounded medium, one of the following methods can be used to reduce it to finite dimensions. A surface that encloses the structure is chosen. This surface is called the *interaction horizon*, and it divides the domain into the interior domain of interest, in which we are trying to obtain the numerical solution, and the exterior domain which is the rest of the unbounded medium. In the case of the *substructure method*, the interaction horizon is chosen to coincide with the structure medium interface. In this case, one will have to enforce a *rigorous* boundary condition (b.c.) to achieve sufficient accuracy. It may not always be possible to obtain a rigorous b.c. The other case of the *direct method* is when one chooses the interaction horizon to be an *artificial boundary* lying in the unbounded medium. This boundary truncates the unbounded medium into an interior part and an exterior part, and an appropriate boundary condition must be *devised* to model the fact that the medium is actually unbounded. This boundary condition is usually approximate and *simpler* compared to the rigorous b.c. of the substructure method. Accuracy of the results also depend on how far the artificial truncation boundary is chosen in the unbounded domain. When the phenomenon under consideration is that of wave propagation, Non Reflecting

Boundary Conditions (NRBC) are required at the truncation boundary to model the combination of an infinite domain and a radiation condition.

An investigation into the physics at the interaction horizon is illuminating. Consider the truncated domain using either of the two approaches above. The discretization of this domain leads to a finite number of degrees of freedom. Discretization will result in a finite number of nodes introduced on the interaction horizon. A boundary condition formulated for such a node represents the interaction force – displacement relationship of the exterior medium; this boundary condition can thus roughly be looked upon as a stiffness relationship. The important fact is: in time domain analysis the exact form of this stiffness relationship is *global in space and time.* That is to say, the interaction force of a specific degree of freedom at a specific time depends on the displacements corresponding to all degrees of freedom at all previous times from the start of the excitation onwards.

The above statement can be explained as follows. Consider a unit impulse displacement at any node. This results in interaction forces at all nodes (spatial coupling) and also at later time (temporal coupling). Formally, one can express $R(t)$, the interaction force vector of the nodes on the interaction horizon (truncation boundary) at a specific time t in terms of the convolution integral of the unit impulse response matrix of the unbounded domain ($S^{\infty}(t)$), and the corresponding displacement vector $u(t)$. The unbounded domain is assumed linear for convenience.

$$R(t) = \int_0^{\infty} [S^{\infty}(t-\tau)]u(\tau)d\tau \tag{1.5}$$

The above expression must be regarded only as a formal expression, emphasizing the global nature of the interactions on the boundary in general. The superscript ∞ in above denotes the unbounded medium. In the frequency domain, the relationship can be formally denoted for frequency ω as:

$$R(\omega) = [S^{\infty}(\omega)]u(\omega) \tag{1.6}$$

The matrix $[S^{\infty}(\omega)]$ is fully coupled, it is called the dynamic-stiffness matrix.

For the substructure method, the above relationship will have to be expressed rigorously, resulting in a similar accuracy as that for the discretized structure. As

already mentioned, this may not always be possible. The computational effort required due to the global coupling in the exact form of the interaction force and displacement relationship of the unbounded medium is also large.

The computational effort can be reduced by constructing a simple but, in general, an approximate form in place of the above. In the time domain, this simpler but approximate stiffness relationship is usually *local in space and time.* This form is used in conjunction with the direct method described above; an NRBC is nothing but this form. The phrase 'local in space and time' means that information is used only from the nodes in the vicinity of the specific node on the truncation boundary (interaction horizon), and only at a specific time, or, at most, during a limited past time. Using the direct method, one can thus obtain transient response directly in the time domain without calculating convolution integrals.

1.2.3 Note on rigorous (substructure) modeling

As already discussed, rigorous b.c.'s are required for substructure modeling. The interaction force and displacement relationship must be established for the nodes on the structure medium interface. This relationship must represent the significant dynamic features of the unbounded medium lying on the exterior of the interface. That is to say, the radiation condition that ensures that no energy is radiated from infinity towards the structure must be satisfied. For certain situations, an analytical expression can be obtained which incorporates the radiation condition. This expression can be used as a fundamental solution to formulate the boundary integral equation. In the boundary element method (BEM) a discretized form of the boundary integral equation is used: only the boundary has to be discretized as the governing differential equations are satisfied exactly. Hence, the spatial dimension is reduced by one. Compared with a domain procedure (for example, FEM) mesh generation is simpler and the system of equations to be solved is smaller. Since the radiation condition is satisfied as a part of the fundamental solution, the method is exact in the limit of the the boundary elements becoming infinitesimal. The main drawback, as is obvious, is that the fundamental solution is not available most of the time. The method is mainly limited to

homogeneous, isotropic (and linear) full space problems. In other cases, fundamental solution either is not available or is complicated. Another disadvantage is that the non-symmetric coefficient matrices of the final system of equations are difficult to evaluate as singularities and special functions (not encountered in the FEM) arise. Also, for boundaries that extend to infinity, for example, free surfaces (interfaces between two different materials), only a finite part can be discretized. This truncation, if required, is a source of error.

1.2.4 Modeling using NRBC's

When employing the direct method of analysis, a boundary condition is formulated on the artificial truncation boundary introduced in the unbounded medium. The radiation condition that has to be enforced at infinity is replaced by a highly 'Non Reflecting' boundary condition on the artificial truncation boundary at a finite distance from the structure. The NRBC is usually approximate, but sufficiently accurate for numerical calculations. It is, in general, local in space and time and formulated directly in the time domain.

There are many theoretical approaches to formulate NRBC's for the particular problem at hand. As is obvious, depending on the properties of the unbounded medium, i.e., the governing differential equation satisfied by it, the NRBC will be different. In addition, for the same unbounded medium (hence the same g.d.e.), different approaches towards formulating an NRBC will result in different expressions for it. The efficacy of a particular NRBC can be judged on the basis of how much of the spurious reflection it is able to suppress for the waves arising in the interior domain and striking the artificial truncation boundary. This fact is hardly surprising because an NRBC generally is an approximation, and there can be many approximations to the same situation. Thus, NRBC's express a large variety in the equations they arise from, their conceptual basis, mathematical formulation, and numerical implementation.

The above observations are highlighted in the problems considered in this dissertation, one of which deals with the scalar wave equation (linear g.d.e.), and the other with the compressible Navier Stokes' (NS) equations (nonlinear system of partial

differential equations).

It may be noted however, that in cases when the NRBC's we are dealing with arise from the same g.d.e. (for example the linear scalar wave equation), many of the NRBC's obtained through different approaches may turn out to be equivalent, corresponding to the same kind of differential equations but with varying coefficients. In the literature review that follows, some of these approaches and their equivalence are considered.

In addition to the NRBC procedure, other methods are also available for modeling the unbounded medium, for example, *infinite elements* used in conjunction with the FEM. Here, the shape functions for the infinite element are expressed in terms of decay functions representing the wave propagation towards infinity. The method is used in the frequency domain wherein the phase velocity and decay rate are specified. An analysis directly in the time domain is not feasible because shape functions can *not* represent the displacements which can exhibit any spatial pattern in the time domain. The infinite element method is approximate, an error caused by modeling of the unbounded medium remains as the element size becomes infinitesimally small. Further, while deciding on the shape function for the infinite element, the analytical solution over the (regular) unbounded domain utilizing the radiation condition for the medium can be made use of.

1.2.5 Paraxial wave equations and NRBC's

In order to gain an understanding as to how NRBC's may be formulated, the method of obtaining NRBC's via the vehicle of paraxial wave equations is considered below. The method is described for the mathematically simplest of the mediums, for which the linear wave equation holds. Consider the one dimensional wave equation for the wave field $\phi(x,t)$, where x and t are the space and time coordinates respectively, and c is the phase speed:

$$\frac{1}{c^2}\frac{\partial^2\phi}{\partial t^2} = \frac{\partial^2\phi}{\partial x^2} \tag{1.7}$$

The well known D'Alembert's general solution for this equation is

$$\phi(t,x) = f(x-ct) + g(x+ct) \tag{1.8}$$

where the initial data

$$\phi(0,x) = \phi_0(x) \tag{1.9}$$

and

$$\frac{\partial \phi}{\partial t} = \phi_{t_0}(x) \tag{1.10}$$

determines the functions f and g for the particular solution:

$$f = \frac{1}{2}(\phi_0 - \frac{1}{c}\int^x \phi_{t_0}(s)ds) \tag{1.11}$$

$$g = \frac{1}{2}(\phi_0 + \frac{1}{c}\int^x \phi_{t_0}(s)ds) \tag{1.12}$$

Now each of the two functions $f(x-ct)$ and $g(x+ct)$ is a solution to the wave equation 1.7. The solution $f(x-ct)$ describes a pulse of shape given by the function f travelling along the x axis towards right at a constant phase speed c. It is the right propagating wave. The solution $g(x+ct)$ describes a left propagating wave (along the x axis). By selecting the initial data appropriately, one can generate each type of wave.

In addition, the functions $f(x-ct)$ and $g(x+ct)$ *separately* satisfy the *simpler* differential equations:

$$(\frac{1}{c}\frac{\partial}{\partial t} - \frac{\partial}{\partial x})g(x+ct) = 0 \tag{1.13}$$

and

$$(\frac{1}{c}\frac{\partial}{\partial t} + \frac{\partial}{\partial x})f(x-ct) = 0 \tag{1.14}$$

Equation 1.13 is a partial differential equation which allows only a left propagating wave in 1 dimension, while partial differential equation 1.14 allows only a right propagating wave in 1 dimension. Thus, there are *simpler* equations that can serve in place of the wave equation 1.7, if we are concerned only with wave propagation in some *preferred* direction.

From equation 1.14, solutions of equation 1.7 that correspond to wave propagation in the positive x direction are solutions of the equation:

$$(\frac{1}{c}\frac{\partial}{\partial t} + \frac{\partial}{\partial x})\phi = 0 \tag{1.15}$$

while from equation 1.13, solutions propagating in the negative x direction are solutions of

$$(\frac{1}{c}\frac{\partial}{\partial t} - \frac{\partial}{\partial x})\phi = 0 \tag{1.16}$$

Consider the waves in a linear horizontal string described by the one dimensional wave equation 1.7. ϕ then corresponds to the vertical displacement of the string about a fixed horizontal line. Suppose the string is pinned at its right end, while the left end is free. A pulse can be launched in the string by flicking the free end of the string, this pulse travels right towards the fixed end. This being a unidirectional wave, it is a *special* solution of the wave equation and will be a solution of equation 1.15 *until it encounters the fixed end on the right.* Then the wave gets reflected and the left travelling reflected wave starts interfering with the right travelling initial wave. The solution from then onwards consists of a combination of left and right travelling waves, and is a solution of the *full* wave equation 1.7.

Unbounded string

If the above string were infinite, the wave would propagate only in the positive x direction, forever. In this situation, one would need to solve only the equation 1.15.

Modeling the unbounded string for a computer generated solution

If it were required to compute the solution for the unbounded string situation described in the above paragraph on a computer, one will have to take into account the finite resources available for computation. One possibility is to place an artificial boundary at some *distant* point $x = L$. A boundary condition would then be required at the artificial boundary to pose this Cauchy problem. The question as to an appropriate boundary condition to be imposed therefore arises. Requiring $\phi(t, L) = 0$ results in the situation of the pinned string described above. Unphysical reflected waves are propagated back into the computational domain $[0, L]$, and interfere with the solution that is required to be computed.

Even for the multidimensional case the argument that waves are attenuated in amplitude as they travel farther and farther off, so that it is possible to choose the artificial boundary sufficiently far away and apply a boundary condition of the kind

$\phi(t, L) = 0$ at large L is not correct. This is so because as the reflected waves from the artificial boundary travel inwards (and the wavefront becomes smaller circles/ spheres), the amplitude of the reflected waves increases.

What is needed is a condition at the artificial boundary that does *not* generate such reflections- an NRBC. For the simple one dimensional case being considered, the answer is obvious; use the one way wave equation 1.15 itself as the condition at the boundary $x = L$, in conjunction with the governing differential equation 1.7 for the domain, i.e.,

$$(\frac{1}{c}\frac{\partial \phi}{\partial t} + \frac{\partial \phi}{\partial x})(t, L) = 0 \tag{1.17}$$

Paraxial wave equations

A paraxial wave equation is a simplification to a more complicated wave equation that can be used to describe a particular class of *unidirectional* waves in that medium. The unidirectional waves being referred to are thus a solution to the *full* as well as the paraxial equations. Often, a paraxial equation is an approximate expression. Paraxial approximations change the classification type of the equation, and hyperbolic equations are often changed to a parabolic form. Hence, paraxial approximations are also known as parabolic approximations in literature. Paraxial approximations arise as serious approximations in their own right in many fields, for example, geophysics and electromagnetism. Here our concern is with their use in constructing NRBC's. Equations 1.15 and 1.16 are examples of *paraxial* wave equations. The following material based on the one dimensional wave equation 1.7 serves to provide a viewpoint on how to derive paraxial approximations, and can be generalized to other equations describing wave phenomena.

Linear operator factorization

The general solution 1.8 follows directly from the following *factorization* of the operator in the one dimensional wave equation 1.7

$$[\frac{1}{c^2}\frac{\partial^2}{\partial t^2} - \frac{\partial^2}{\partial x^2}] \equiv [\frac{1}{c}\frac{\partial}{\partial t} - \frac{\partial}{\partial x}][\frac{1}{c}\frac{\partial}{\partial t} + \frac{\partial}{\partial x}] \tag{1.18}$$

From the above factorization it is clear that the solutions to equations 1.15 and 1.16 will also solve equation 1.7. This suggests that the theory of linear operator factorization is the key to the construction of paraxial equations and NRBC's, of course for *linear g.d.e.'s*. An even simpler approach to this problem is described below, which suffices to obtain results for *constant coefficient* linear systems.

A simpler approach in lieu of linear operator factorization

Consider the single complex mode

$$u_\zeta(\vec{x}) = \exp(i\langle\vec{x},\zeta\rangle) \tag{1.19}$$

where $\vec{x} = (t, x)$, and $\zeta = (\omega, \xi)$ is the wave vector. In the expression for ζ, ω is the cyclic frequency and ξ the wave number. In order that this special function is a solution of the wave equation 1.7 the following relation must be satisfied

$$\xi^2 = \frac{\omega^2}{c^2} \tag{1.20}$$

The above (equation 1.20) is a polynomial equation. It can be factored as

$$(\xi - \frac{\omega}{c})(\xi + \frac{\omega}{c}) = 0 \tag{1.21}$$

which is analogous to equation 1.18. Thus there are two basic mode solutions

$$u_{\zeta+}(t, x) = \exp[i\omega(x - \frac{t}{c})] \tag{1.22}$$

$$u_{\zeta-}(t, x) = \exp[i\omega(x + \frac{t}{c})] \tag{1.23}$$

where the first one (equation 1.22) is the right propagating wave, and the second (equation 1.23) is the left propagating wave.

For these special (single mode) solutions, we have the formal correspondence from the analogy pointed out above

$$\omega \longleftrightarrow -i\frac{\partial}{\partial t} \quad \xi \longleftrightarrow -i\frac{\partial}{\partial x} \tag{1.24}$$

That is to say, the two factors in equation 1.21 give rise to the differential operators in equations 1.15 and 1.16.

This formal technique can easily be extended to the wave equation in two space dimensions

$$\frac{1}{c^2}\frac{\partial^2\phi}{\partial t^2} = \frac{\partial^2\phi}{\partial x^2} + \frac{\partial^2\phi}{\partial y^2} \tag{1.25}$$

Equation 1.25 has the special *fundamental mode solution* (equation 1.19) with $\vec{x}$ and ζ now given by $\vec{x} = (t, x, y)$ and $\zeta = (\omega, \xi, \eta)$ if

$$\xi^2 + \eta^2 = \frac{\omega^2}{c^2} \tag{1.26}$$

The relationship given in 1.26 has the following *one parameter* family of solutions

$$\xi = -\frac{\omega}{c}\cos(\theta)\ , \quad \eta = -\frac{\omega}{c}\sin(\theta) \tag{1.27}$$

Hence the single mode solutions (corresponding to equation 1.19 for the 1 dimensional wave equation) are given by

$$u_\zeta(t, x, y) = \exp(i(\omega t + \xi x + \eta y)) \tag{1.28}$$

that is,

$$u_\zeta(t, x, y) = \exp(i\frac{\omega}{c}(ct - x\cos(\theta) - y\sin(\theta))) \tag{1.29}$$

The above solutions, equation 1.29, represent plane wave fronts travelling in two dimensions. θ, the parameter, in above is interpreted as follows. The surfaces of constant phase (the wave fronts) are planes that make an angle θ with the x axis.

Suppose it is required to find a paraxial equation that describes waves travelling in a direction determined by θ. Following the one dimensional case, we solve equation 1.26 for ξ:

$$\xi = \pm\frac{\omega}{c}\sqrt{(1 - (\frac{c\eta}{\omega})^2)} = \pm\lambda(\omega, \eta) \tag{1.30}$$

Defining z as the quantity in the inner brackets and utilizing equation 1.27:

$$z = \frac{c\eta}{\omega} = -\sin(\theta)\ , \tag{1.31}$$

the quantity under the radical sign can be written as $\sqrt{1-z^2}$. z is small if θ is small. Thus the quantity under the radical sign in equation 1.30 can be approximated for the case of *plane wave solutions that are at a small angle to the x axis.* Note that the one dimensional case did not require any approximations, the analysis there was exact. *Approximations are required when space dimensions are greater than one.*

This approximation can be carried out in a number of ways, Taylor expansion has been used below.

$$\sqrt{1-z^2} = 1 - \frac{z^2}{2} + O(z^4) \quad (|z| < 1) \tag{1.32}$$

We can use different orders of approximate forms for equation 1.30, from equation 1.32 we get two approximate forms (using the plus sign only):

$$\xi = \frac{\omega}{c} \tag{1.33}$$

and

$$\xi = \frac{\omega}{c} - \frac{c\eta^2}{2\omega} \tag{1.34}$$

The analogy to equation 1.24 is the following correspondence for the two dimensional case:

$$\omega \longleftrightarrow -i\frac{\partial}{\partial t}\ , \quad \xi \longleftrightarrow -i\frac{\partial}{\partial x}\ , \quad \eta \longleftrightarrow -i\frac{\partial}{\partial y} \tag{1.35}$$

Substituting the correspondences 1.35 into equations (approximate forms) in 1.33 and 1.34, we obtain the required (approximate) paraxial equations that describe plane wave solutions *close to the x axis.*

$$(\frac{\partial\phi}{\partial x} - \frac{1}{c}\frac{\partial\phi}{\partial t}) = 0 \tag{1.36}$$

and

$$(\frac{\partial^2\phi}{\partial t\partial x} - \frac{1}{c}\frac{\partial^2\phi}{\partial t^2} + \frac{c}{2}\frac{\partial^2\phi}{\partial y^2}) = 0 \tag{1.37}$$

The first of these, equation 1.36, is nothing but equation 1.16 for the one dimensional case, i.e., the result when $z = 0$. This corresponds to the first order approximation. The second order approximation, equation 1.37, is a new equation.

Consider the use of either of these equations (1.36 or 1.37) as a boundary condition. Let a single mode solution propagating to the left in the region $x < 0$ strike the artificial boundary at $x = 0$ where a boundary condition given by one of the two paraxial equations 1.36 or 1.37 derived above is imposed. The result is the solution of the form

$$u_\zeta(t,x,y) = \exp\left[i\frac{\omega}{c}(ct + x\cos(\theta) + y\sin(\theta))\right] + R(\theta)\exp\left[i\frac{\omega}{c}(ct - x\cos(\theta) + y\sin(\theta))\right] \tag{1.38}$$

where the second term is the reflected wave from the boundary; $R(\theta)$, called the *reflection coefficient*, is the amplitude of the reflected wave. For the first order NRBC, equation 1.36, applied at $x = 0$, the reflection coefficient is

$$R(\theta) = \frac{1 - \cos(\theta)}{1 + \cos(\theta)} \tag{1.39}$$

For $\theta = 0$, the situation reduces to the exact case of one dimensional analysis, and the reflection coefficient is zero as expected. For angles of incidence other than zero, there is a reflected wave. This is expected in view of the fact that this NRBC is a first order approximation.

For the second order NRBC, equation 1.37, applied at $x = 0$, the reflection coefficient is improved as far as the performance of the boundary as a non reflecting one is concerned. It now is

$$R(\theta) = -\left[\frac{1 - \cos(\theta)}{1 + \cos(\theta)}\right]^2 \tag{1.40}$$

The better the approximation to the function $(1-z^2)^{1/2}$ for use in equation 1.30, the smaller will be the reflection coefficient and the greater the range of θ for which the NRBC will be applicable. If we proceed with the approximations based on the Taylor series expansion, as we did above, it might be supposed that keeping the $O(z^4)$ term in equation 1.32 will result in a better NRBC. The reflection coefficient certainly is reduced, but it is still to be ensured that the resulting Initial Boundary Value Problem (IBVP) is *well posed*. Verifying well posedness requires further analysis of the IBVP.

Well posedness of an IBVP The IBVP is said to be well posed if a solution exists, is unique, and depends continuously on the intial data. This is equivalent to the existence of constants C and k for which

$$\|\phi(t)\| = C\exp(kt)\|\phi_0\| \tag{1.41}$$

where ϕ is the solution of a Initial Boundary Value Problem, with the initial data given as

$$\phi(t=0,x,y) = \phi_0(x,y) \tag{1.42}$$

Use of single mode solutions for the IBVP of the kind expressed in equations 1.19 and 1.29 for analyzing the well posedness of (linear) IBVP's, results in the Kreiss condition (Kreiss [1970]) which has been used to investigate the well posedness of some IBVP's formulated in the following chapters.

Approximations other than Taylor expansion Analysis of higher order Taylor's approximations to $\sqrt{(1-z^2)}$ to formulate NRBC's for the g.d.e. (wave equation) under consideration can be shown to result in ill posedness. This results in the motivation for investigating methods of approximating $\sqrt{(1-z^2)}$ other than the Taylor expansions.

The key to constructing local paraxial equations (and NRBC's) by the above procedure is to express the term $\sqrt{(1-z^2)}$, and hence the relationship 1.30, in a polynomial form. A more general method is to use *rational approximations* rather than *polynomial approximations* for the term under the square root symbol.

Padé approximations

The most commonly used rational approximations are Padé approximations. Here, given a function $f(z)$ with a Taylor series

$$f(z) = f_0 + zf_1 + z^2f_2 + z^3f_3 + ... + z^kf_k + ... \tag{1.43}$$

a rational function is sought which has a Taylor series which agrees with that of $f(z)$ up to some power of z. The rational function $f_{(N,M)}(z)$, called the (N,M) Padé approximant of the function $f(z)$, is defined as

$$f_{(N,M)}(z) = \frac{P_N(z)}{Q_M(z)} \tag{1.44}$$

where $P_N(z)$ and $Q_M(z)$ are polynomials of degrees N and M respectively. Further,

$$f(z) - f_{(N,M)}(z) = O(z^{(N+M+1)}) \tag{1.45}$$

The $(1,1)$ Padé approximant of the function $\sqrt{(1-z^2)}$, is

$$f_{(1,1)}(z) = \frac{1 - \frac{3}{4}z^2}{1 - \frac{1}{4}z^2} \tag{1.46}$$

This results in the paraxial wave equation for left propagating waves in two dimensional space of the following form

$$\frac{1}{c}\frac{\partial^3\phi}{\partial t^3} + \frac{\partial^3\phi}{\partial t^2 \partial x} - \frac{3}{4}c\frac{\partial^3\phi}{\partial t \partial y^2} - \frac{c^2}{4}\frac{\partial^3\phi}{\partial x \partial y^2} = 0 \tag{1.47}$$

The NRBC to be applied on the y axis to stop the waves from being reflected is

$$\left(\frac{1}{c}\frac{\partial^3\phi}{\partial t^3} - \frac{\partial^3\phi}{\partial t^2 \partial x} - \frac{3}{4}c\frac{\partial^3\phi}{\partial t \partial y^2} + \frac{c^2}{4}\frac{\partial^3\phi}{\partial x \partial y^2}\right)(t, x = 0, y) = 0 \tag{1.48}$$

The IBVP resulting from the above NRBC can be shown to be well posed, Engquist and Majda [1977, 1979].

A rational approximation

$$r(z) = \frac{P(z)}{Q(z)} \tag{1.49}$$

can be obtained by methods other than Padé's. Wagatha [1983] has developed the procedure of using variational criterion on the reflection coefficient in order to obtain the optimum approximation. The reflection coefficient for the general approximation 1.49 is

$$R(\theta) = \frac{c\cos(\theta)\ \ Q(-\sin(\theta)) - P(-\sin(\theta))}{c\cos(\theta)\ \ Q(-\sin(\theta)) + P(-\sin(\theta))} \tag{1.50}$$

for which two possible functionals to which a variational criterion can be applied are

$$V_1[P,Q] = \int_\alpha^\beta R^2(\theta)\ w(\theta)\ d\theta \tag{1.51}$$

and

$$V_2[P,Q] = \int_{\alpha}^{\beta} \mid R(\theta) \mid \; w(\theta)\, d\theta \tag{1.52}$$

which involve an arbitrary weight function $w(\theta)$. α and β define the prarticular range of θ values of interest, $\alpha < \theta < \beta$.

Trefethen and Halpern [1986] have provided a number of general results for rational approximations used in formulating paraxial equations based on analyses of the kind described above.

The methodology and the results detailed above can be generalized to *variable coefficient linear differential equations*. Instead of the simple approach based on analogy defined in equations 1.24 and 1.35, one then has to use Fourier transforms and the theory of *pseudo differential operators*, the latter being a generalization of linear differential operators. Factorization of differential operators again plays an important part in the derivations. However, whatever method one adopts to arrive at a paraxial approximation, and through it an NRBC, well posedness of the resulting IBVP remains an issue to be established.

It must be borne in mind that the above description of the method of obtaining NRBC's via the vehicle of paraxial equations is not applicable to all situations. For instance, in the case of non linear governing partial differential equations, these techniques are *not* directly applicable in general. Nor is well posedness analysis readily possible by an application of the criteria mentioned above (namely, the Kreiss criteria). One may first linearize the equations under consideration and hope that the results for the linearized equations give sufficiently valid indicators for the original non linear equations. Or issues of well posedness and an *optimum* NRBC may be settled *á-posteriori on the basis of numerical experimentation*. For that matter, the procedure of formulating an NRBC itself may not be as formalized as that for the linear case described above. This aspect is illustrated in chapter 4 of this dissertation where new NRBC's are proposed for compressible Navier Stokes equations.

1.3 Problems considered in this dissertation

In this dissertation, NRBC's have been formulated and used for two different problems. The first involves the time dependent wave equation in two dimensions for a complex geometry, the second deals with transonic flow of a Newtonian fluid over a flat plate. The first one is a second order linear partial differential equation with constant coefficients, the second one consists of *compressible* Navier Stokes equations which are nonlinear. It will be seen that the particular NRBC for a given situation is dependent on the system of governing differential equations, and for each situation one may need to adopt a different procedure to formulate a correct NRBC. In the case where the g.d.e. is linear, the procedure to arrive at an NRBC can, in general, be better formalized compared to the nonlinear case. Similar assertion can be made with respect to the well posedness analysis of the new IBVP that results when the original problem posed over an unbounded spatial domain is replaced by the one posed in terms of NRBC's.

1.4 Organization of this dissertation

The first chapter of this dissertation contains an introduction to NRBC's, to the situations in which they arise, and the advantage of using them. An outline of the method of deriving NRBC's from paraxial equations which was the seed for development of research in this field, is provided. Other methods that have been used to model infinite media are mentioned in the passing, they are discussed in greater detail in the second chapter. Also contained in this chapter is an overview of the work presented in the remainder of this dissertation.

The second chapter provides a literature review pertaining to NRBC's. Other methods for modeling infinite media and also methods other than the use of paraxial equations for obtaining NRBC's are reported. A wide range of governing differential equations for which methods for modeling infinite media have been studied are covered.

The third and the fourth chapters report the work carried out by the author in this field. This work consists of formulation and application of NRBC's for two different classes of problems. The first involves the time dependent wave equation

in two dimensions for a complex geometry. The second deals with transonic flow of a Newtonian fluid over a flat plate. The first one is a second order linear partial differential equation with constant coefficients, the second one consists of *compressible* Navier Stokes equations which are nonlinear. Chapters three and four cover the work on these two problems, respectively.

The third chapter deals with the formulation and well posedness analysis of a particular class of NRBC's for the time dependent scalar wave equation. These NRBC's are then applied to a problem of great importance– to that of large heat exchangers in nuclear and process industries. The pressure field in the moderator of an Indian 500 MWe Pressurized Heavy Water Reactor (PHWR) in the event of a single coolant channel failure is obtained. The effect of this incident on channels in the *immediate* neighbourhood of the channel that fails needs to be investigated to determine their likelihood of failure in turn. However, the moderator domain itself is much *larger* compared to the *small* immediate neighbourhood of interest while the time over which this response is of interest is relatively small. This is an indication that the truncation of the domain to an interior region and application of NRBC at the truncation boundary may be fruitfully applied to model the situation. NRBC's are applied to the moderator boundary while a perfectly reflecting boundary is assumed for the channels.

In the fourth chapter, *new* NRBC's for the compressible Navier Stokes equations are formulated. The results of the application of these NRBC's to transonic flow of air over a flat plate are then presented. Results are compared with similar work available in literature.

The fifth chapter concludes the dissertation.

Chapter 2

Literature Survey

2.1 Introduction

2.1.1 Mathematical models for waves and NRBC's

To borrow from Whitham (Whitham [1974]) 'wave motion can be studied at any technical level'. Indeed, mathematical equations containing description of wave motion range from simple algebraic equations to partial differential equations- hyperbolic, parabolic and elliptic. The wave equation, one of the first equation that one encounters when dealing with phenomena of wave propagation, is also the first prototype of hyperbolic partial differential equations one is exposed to. Paraxial approximations to wave equations that describe propagation of waves in one direction only are usually parabolic partial differential equations. If we factor out the time dependence of the form $e^{i\omega t}$, for example, from the hyperbolic wave equation (a simple physical example would be stationary waves on a string), an elliptic partial differential equation (the *reduced* wave equation) results which describes the variation of the amplitude of the oscillating medium at various locations in space. Further, each of these types of governing differential equations may be either linear or non-linear.

Depending on the kind of the governing differential equation, the approach towards developing an NRBC would differ. For some cases even an exact NRBC is available, for others, heuristic arguments may be used to obtain an NRBC. These arguments may be justified based on linearization of equations, numerical experimentation for simple geometries, etc.

Further, for the same set of governing differential equations, a number of approaches may exist to develop an NRBC, each resulting in a different NRBC. In such

a situation one would be interested in knowing how do these NRBC's perform vis-a-vis their ability to compute the correct solution efficiently. In this situation, one may also be interested in knowing how these NRBC's relate to each other.

The following survey of literature elaborates on these perspectives.

2.1.2 General remarks on literature on NRBC's

Work in the field of devising, implementing and using NRBC's has been carried on in numerous fields: acoustics, gas dynamics, hydrodynamics, elctrical engineering, civil engineering, geophysics, meteorology, environmental sciences, quantum mechanics, plasma physics, mechanical and aeronautical engineering, etc. As already mentioned, situations differ in the governing equations (media in which the wave motion occurs) under consideration; in addition they may differ in geometrical complexity. Methods used for discretization also differ– usually finite difference or finite element methods are used. Analytical solutions– when they exist– serve as useful benchmarks to determine the accuracy and efficiency of the NRBC formulation. In fact, some methods to obtain an NRBC use the analytical solution to the problem for simple geometries.

Since researchers in such a wide variety of fields have worked in this area, many a times the work done and references cited have been confined to the particular area of interest of the research worker. Indeed, the nomenclature used for NRBC's themselves shows a rich variety– they have been referred to in the literature by a variety of names, some of which are listed below:

1. absorbing boundary conditions
2. radiating boundary conditions
3. transparent boundary conditions
4. one way boundary conditions
5. transmitting boundary conditions
6. free space boundary conditions

7. open boundary conditions
8. silent boundary conditions
9. on surface radiation conditions
10. paraxial boundary conditions
11. non reflecting boundary conditions

The term 'Non Reflecting Boundary Conditions' has gained some sort of general acceptance in recent times, Givoli [1991]. The term is used with the understanding that it means boundary conditions that prevent *spurious* reflections from being generated at the subspace (boundary) they are applied at, while not affecting the true physical reflections that are a part of the actual solution. The choice of words in the previous sentence will be of relevance in situations when one wants to model geometries where waves may enter the computatinal domain from outside. An example can be the case of two shock waves originating inside the domain Ω and colliding outside it, resulting in physical waves coming back into the computational domain. As far as actual reflections within Ω are concerned, it is understood that all such reflectors have been appropriately modeled.

The unifying features in this variety are (a)the goal to obtain a boundary that is transparent to the relevant waves, (b) their use to truncate the spatial domain to a smaller region of interest and, (c) to a small extent, the techniques used to devise such a boundary.

In order to be of use, an NRBC must satisfy at least some of the following requirements:

Requirements for the continuous problem

1. The governing differential equation on the domain Ω and the boundary condition(s) imposed on the boundary (subspace of the domain) B together form a *well posed mathematical problem.*

2. The problem as expressed above must form a good approximation to the original problem on the infinite spatial domain.

Requirements for the approximate discrete problem

1. The amount of spurious reflection generated by the boundary condition must be small.

2. The boundary condition must be compatible with the numerical method employed (finite differences, finite elements,...).

3. The numerical method employed, together with the boundary condition used, must result in a stable numerical scheme.

4. The boundary condition must be easy to implement numerically.

5. For time marching schemes to obtain a steady state solution, the boundary condition must facilitate a fast convergence to steady state.

The requirements enumerated above are not independent of each other. The extent to which a combination of them is satisfied affects the performance vis-a-vis other requirements, too. The main object in devising an NRBC is to reduce spurious reflections to a minimum in an efficient way. If the artificial boundary is very far away from all sources and scatterers in the domain, most of the NRBC's perform well. This is as expected. But then, for time dependent problems, one may as well choose a very large domain (or a progressively expanding one) so that in the period of time for which the solution is required spurious reflections do not reach the spatial domain of interest in which the solution is being sought. This would be an inefficient way of solving the problem. A good NRBC will perform well even when placed close to a source or scatterer.

Steady state solutions can be sought for in either of the two ways– by dropping the time dependence in the governing equations or by time marching techniques. For the former, the requirement of an efficient NRBC that can be placed at a finite distance from the sources and scatterers in the domain is even more necessary as the dropping

of terms involving time derivatives imply that disturbances introduced anywhere in the domain affect all other points in it instantaneously. For the latter (time marching to steady state), the last of the requirements mentioned above (requirement 5) becomes significant. A problem of this kind is considered and studied in chapter 4 of this dissertation.

As will be seen below (section 2.2.4), NRBC's have also been formulated for the discretized governing equations rather than the continuous ones. In such a situation, requirements number 1 and 2 listed above for the continuous problem will be applicable to the discretized problem.

2.2 NRBC's for Scalar Wave Equation

The scalar wave equation is obtained on the basis of the acoustic assumption:

$$u_{tt} = c^2 \nabla^2 u \tag{2.1}$$

for the field quantity u, wave speed c and time t. The special case of time harmonic waves (cyclic steady state) results in the *reduced* wave equation:

$$\nabla^2 u + k^2 u = 0 \tag{2.2}$$

where u has been assumed to have the form

$$u(\vec{x}, t) = \tilde{u}(\vec{x}) e^{-i\omega t} \tag{2.3}$$

In the above, e is the base of the natural logarithms, ω is the cyclic frequency of the wave, $k = \omega/c$, and $i = \sqrt{-1}$. $\vec{x}$ denotes (x, y, z), and $\tilde{u}$ is the amplitude of u.

The forms of the radiation condition applicable at infinity for equations 2.1 (scalar wave equtaion) and 2.2 (reduced wave equation) are, respectively,

$$\lim_{r \to \infty} r^{\frac{(d-1)}{2}} (u_r + \frac{1}{c} u_t) = 0 \tag{2.4}$$

and

$$\lim_{r \to \infty} r^{\frac{(d-1)}{2}} (u_r - iku) = 0 \tag{2.5}$$

r is the spatial coordinate and d the number of space dimensions in the above.

2.2.1 The One Dimensional Case

For the 1-d case, the radiation condition given by equation 2.4 is written as

$$u_t + cu_x = 0 \tag{2.6}$$

This is exact for all $x \in R$, and not just at infinity. Physically this means that a semi-infinite longitudinally vibrating rod, for example, can be truncated at any point by substituting for the eliminated part a dashpot of strength $1/c$. Waves striking the dashpot will be fully absorbed and no spurious reflections will be generated. Kuhlemeyer and Lysmer [1973] have used this condition in conjunction with the finite element method (FEM). Halpern [1982] has studied this NRBC for various finite difference approximations. Foreman [1986] examined analogous NRBC's for one dimensional linearized shallow water equations.

The one dimensional case can not be generalized to two and three dimensions in a straightforward manner. Constructing NRBC's for the wave equation for two and three space dimensions has been a rich field of research, of which the work by Engquist and Majda has been one of the most quoted one in literature. It is described below.

2.2.2 Engquist and Majda NRBC

Engquist and Majda [1977, 1979] have developed *approximate* NRBC's of progressively increasing order. For equation 2.1 in two space dimensions, the first two of these are:

$$E_1 u \equiv \left(\frac{\partial}{\partial x} - \frac{1}{c}\frac{\partial}{\partial t} \right) u = 0 \tag{2.7}$$

$$E_2 u \equiv \left(\frac{1}{c}\frac{\partial^2}{\partial x \partial t} - \frac{1}{c^2}\frac{\partial^2}{\partial t^2} + \frac{1}{2}\frac{\partial^2}{\partial y^2} \right) u = 0 \tag{2.8}$$

on B, the truncation boundary. x and y are the Cartesian coordinates. They used rational approximations of varying orders to the expression of the form $\sqrt{1-s^2}$ to obtain equations that allow wave propagation only in one direction. The procedure used by them has been outlined in section 1.2.5.

The NRBC E_1 is perfectly non reflecting at the angle of incidence zero. NRBC E_2 performs better than E_1.

Engquist and Majda have also generalized the above NRBC's to the situation where the wave equation has coefficients dependent on the spatial coordinates, i.e., where the medium is inhomogeneous upto the truncation boundary. For the case of inhomogeneous medium the second order NRBC, in addition to the second order derivatives of the kind in the NRBC E_2 above, contains third order derivatives, too. Whenever an NRBC contains higher order derivatives as compared to the governing differential equation in a direction perpendicular to the boundary, one can not use the expression as a 'boundary condition' directly. This results in some difficulty in implementing the NRBC, additional modifications need to be carried out before using it as a boundary condition.

Engquist and Majda have also derived NRBC's in polar coordinates, where the truncation boundary is a circle of radius R. In order to achieve this, they have considered the wave equation in polar coordinates as a special case of wave equation in rectangular coordinates with variable coefficients. Other approaches for getting the expressions for NRBC's in coordinate systems other than Cartesian can be: (1) developing the NRBC's in the non-rectangular system from the start, or (2) using coordinate transformations to convert NRBC's from one system to the other. E_1 and E_2 in polar coordinates are:

$$E_1 u \equiv \left(\frac{\partial}{\partial r} + \frac{1}{c}\frac{\partial}{\partial t} + \frac{1}{2R} \right) u = 0 \tag{2.9}$$

$$E_2 u \equiv \left(\frac{1}{c^2}\frac{\partial^3}{\partial r \partial t^2} + \frac{1}{c^3}\frac{\partial^3}{\partial t^3} - \frac{1}{2R^2 c}\frac{\partial^3}{\partial t \partial \theta^2} + \frac{1}{2R^2 c}\frac{\partial^2}{\partial t^2} + \frac{1}{2R^3}\frac{\partial^2}{\partial \theta^2} \right) u = 0 \tag{2.10}$$

Outside of Engquist and Majda's work, similar ideas have been in use in devising one way wave equations (paraxial approximations), especially in geophysics (Tappert [1977], Clarebout [1985]). Lindman [1975] had also suggested that one way wave equations can also be applied as NRBC's. In chapter 1, this viewpoint on NRBC's has already been dealt with.

2.2.3 Trefethen and Halpern's Studies

While studying one way wave equations, Trefethen and Halpern [1986] and Halpern and Trefethen [1988] approximated the factor $\sqrt{1-s^2}$ using not only Pade's approximations as Engquist and Majda had done, but several other rational functions like Chebyshev, Chebyshev - Pade, Newman, L^2 and L^α approximants as well. They carried out a number of numerical experiments to determine the efficacy of the various approximants as one way wave equations (i.e., NRBC's). They conclude that Pade approximations are best suited for nearly normal incidence on the truncation boundary, the results for larger angles of incidence are not so good.

Well Posedness Analysis of NRBC's

One important aspect as mentioned in the list of requirements for NRBC's (section 2.1.2) is that the mathematical model consisting of the governing differential equation on the given domain and the boundary conditions proposed for the truncation boundary should result in a well posed problem. Trefethen and Halpern [1986] have also studied the well posedness of various paraxial approximations (NRBC's) resulting from rational approximations to the term $\sqrt{1-s^2}$. In order to carry out this analysis, they make use of the theory developed by Kreiss [1970] for ascertaining well posedness of Initial Boundary Value Problems (IBVP) involving hyperbolic systems of equations.

Analysis of well posedness of the Engquist and Majda NRBC is available in Kolakowski [1985, 1986], in the context of linearized shallow water wave equations.

2.2.4 NRBC's based on discretized equations

The material above pertains to NRBC's derived for the continuous problem. Another approach that has been investigated is that of first discretizing the differential equations, and then obtaining NRBC's for difference equations. This has been carried out by Lindman [1975] and Randall [1988]. They use finite differences to discretize the continuum problem. Engquist and Majda [1979] conclude that this approach is not

preferable. The theory to analyze well posedness also has to be modified to suit the requirements of discrete equations.

2.2.5 Applications of Engquist and Majda NRBC's to particular situations

Use of the NRBC's devised by Engquist and Majda (equations 2.7 and 2.8) have been reported in the literature for situations other than what Engquist and Majda reported, too. They have been adapted for the time independent reduced wave equation, and also for three space dimensions as in Hariharan and Bayliss [1985]. Hariharan and Bayliss [1985] solve for sound radiation into the atmosphere from a cylindrical pipe.

2.2.6 Free parameter NRBC's

Wagatha [1983] enhanced the method employed by Engquist and Majda for deriving NRBC's by introducing a free parameter β during the approximation stage. The local NRBC's thus obtained reduce to Engquist and Majda NRBC's for specific values of β. The additional flexibility afforded by the free parameter can help in reducing spurious reflections if β is chosen optimally; Wagatha shows that for non normal angles of incidence it is possible to get better performance compared to the straightforward Engquist and Majda NRBC's. Another work of similar nature where a set of NRBC's with adjustable (user chosen) free parameters has been proposed is of Clayton and Engquist [1980]. A well posedness analysis of these has been carried out by Howell and Trefethen [1988] for certain values of the free parameters. Free parameter NRBC's have also been devised and used for governing differential equations other than the linear wave equation, for example compressible Navier Stokes equations. They will be discussed in the material that follows. Indeed, a part of the work reported in this dissertation deals with new free parameter NRBC's for compressible Navier Stokes equations.

2.2.7 Work of Bayliss and Turkel

Expanding the solutions of wave equations with axial and spherical symmetry asymptotically at large distances, Bayliss and Turkel [1980] obtained a sequence of NRBC's.

For the wave equation in three space dimensions, the m^{th} NRBC is

$$B_m u \equiv \left(\prod_{j=1}^{m} \left(\frac{1}{c}\frac{\partial}{\partial t} + \frac{\partial}{\partial r} + \frac{2j-1}{R} \right) \right) u = 0, \ on \ B \tag{2.11}$$

For the reduced wave equation, the corresponding NRBC is

$$B_m u \equiv \left(\prod_{j=1}^{m} \left(-ik + \frac{\partial}{\partial r} + \frac{4j-3}{2R} \right) \right) u = 0, \ on \ B \tag{2.12}$$

They have also provided a measure of accuracy for the above NRBC's. They show that for the placement of the truncation boundary far enough from the interior domain, the (analytical) solution of the wave equation with the NRBC specified by equation 2.11 applied on a sphere of radius R differs from the solution of the original problem (with a radiation condition applied at infinity) by $O(R^{-m-\frac{1}{2}})$ in the appropriately defined norm.

Bayliss and Turkel [1982] have also extended these ideas to the *linearized* Euler equations of gas dynamics. They have also used NRBC's for obtaining steady state solutions to these equations using a time marching technique. This will be considered in a later section.

2.2.8 Feng's Approach

The approach used by Feng [1983] is especially suitable for the reduced wave equation. He considers the reduced wave equation in two dimensions, and obtains an expression on the truncation boundary using the Green function method. This expression is *exact, nonlocal and integral.* In order to be able to use this expression as an NRBC, he uses asymptotic approximation valid at large distances to get an expression which is local, and can be used as a boundary condition. The geometry he considers for the artificial boundary is a circle with radius R; indeed, to obtain an exact expression, one is restricted to the choice of easily solvable boundaries. This situation arises in the work of Keller and Givoli [1989, 1990] also. Feng's sequence of NRBC's for an artificial boundary that is a circle of radius R are

$$F_0 u \equiv (-\frac{\partial}{\partial r} + ik)u = 0 \tag{2.13}$$

$$F_1 u \equiv \left(-\frac{\partial}{\partial r} - (-ik + \frac{1}{2R}) \right) \; u = 0 \tag{2.14}$$

$$F_2 u \equiv \left(-\frac{\partial}{\partial r} - (-ik + \frac{1}{2R} - \frac{i}{8kR^2}) + \frac{i}{2kR^2}\frac{\partial^2}{\partial \theta^2} \right) \; u = 0 \tag{2.15}$$

$$F_3 u \equiv \left(-\frac{\partial}{\partial r} - (-ik + \frac{1}{2R} - \frac{i}{8kR^2} - \frac{1}{8k^2R^3}) + (\frac{i}{2kR^2} + \frac{1}{2k^2R^3})\frac{\partial^2}{\partial \theta^2} \right) \; u = 0 \tag{2.16}$$

Use of the FEM over the spatial domain delimited by the artificial truncation boundary from the exterior is a very good option in solving the reduced wave equation in conjunction with the above NRBC's. However, NRBC's of order greater than three can not be used with the standard FEM. NRBC's derived in Keller and Givoli [1989, 1990] are also amenable to FEM solutions.

2.2.9 Higdon's Generalization:

Higdon [1986] has derived the following sequence of NRBC's for the two dimensional time dependent wave equation 2.1. The method he uses to do this is to first discretize the equation 2.1 using finite differences, develop discrete boundary conditions for the truncation boundary, and then show that the continuous counterparts of the discrete boundary conditions are of the form

$$H_m u \equiv \left(\prod_{j=1}^{m} \left(\cos \alpha_j \frac{\partial}{\partial t} - c\frac{\partial}{\partial x} \right) \right) \; u = 0, \; on \; B \tag{2.17}$$

In the above, m is the order of the NRBC. This is perfectly non-reflecting for a plane wave striking B, where B is perpendicular to the x-axis, at angles $\pm\alpha_j$, $j = 1..m$. Even a reasonably small value of m gives rise to low spurious reflection for a wide range of angles of incidence.

Further, he proves that by appropriate choice of α_j in equation 2.17, one can derive any stable and optimal NRBC that has been alternatively obtained by means of a symmetric rational approximation from the scalar wave equation 2.1. The word optimal here means that the coefficients of the NRBC have been tuned to minimize the reflection coefficients of the various Fourier modes. *Reflection coefficient* is the fractional amount of reflected wave with respect to the incident wave. That is to say, a stable NRBC derived using symmetric rational approximations such that it contains

coefficients that perform optimally with respect to their absorption characteristics has associated with it α_j, it's angles of perfect absorption, that completely characterize it. In the above, by optimal performance one means that reflection can not be decreased by modifying the coefficients in the NRBC. The NRBC so derived may *not* have explicit appearance of the parameters α_j, but this choice has implicitly been made. Higdon [1986] also demonstrates this result for the NRBC's developed by Engquist and Majda [1977], Wagatha [1983] and Trefethen and Halpern [1986].

Keys [1985] had also obtained similar NRBC's in his earlier work.

2.3 NRBC's for other equations governing wave propagation

2.3.1 NRBC's in fluid structure interaction problems

Problems of fluid structure interaction can be categorized into two classes– underwater acoustics where waves are reflected from a submerged body, and (water) waves getting scattered by an offshore structure. The fluid medium in most of these situations is very large, and is considered to be extending to infinity, while the solid model can be considered either finite or infinite depending on the situation. An example of this situation is that of water waves generated due to some seismic activity, and there is an interaction with a structure/ ground. Sharan [1987] has considered such a configuration in two dimensions, he assumes the ground to move horizontally. For the fluid region the reduced wave equation is applied, whereas in the solid, time-harmonic (no explicit time dependence in the governing differential equations) *linear* elastodynamic equations are assumed. An NRBC is derived based on a Fourier series solution which works well if the artificial truncation boundary is chosen far enough from interior scatterers. FEM is used to discretize the domain. Zienkiewicz and Newton [1969], Bando et. al. [1984] and Sharan [1988] also consider fluid structure interaction problems of various kinds where similar concepts have been applied. Singh et. al. [1990] have discussed various schemes for solutions of such problems and applied them to certain benchmark problems, but the boundary conditions they have used at the finite truncation boundary of the fluid is not an NRBC. Similar situation exists in Singh et. al. [1991 b].

2.3.2 NRBC's for dispersive wave equation

For the dispersive wave equation, Engquist and Halpern [1988] have proposed the NRBC of the form

$$\frac{\partial u}{\partial t} + \frac{\partial u}{\partial n} + Ku = 0, \ on \ B \tag{2.18}$$

In the above, K is an operator that does not contain time. The same operator appears in the corresponding NRBC for the steady state, namely, $\partial u/\partial n + Ku = 0$. This operator can be either non-local or local in space. The authors have discussed this aspect, and also proved well posedness and convergence to steady state in the limit $t \to \infty$. The extension of the NRBC from the dispersive g.d.e. to the hyperbolic case is also covered by them.

2.3.3 NRBC's for a particular class of time dependent equation

Time dependent equations of the form

$$(Qu)_t = \nabla^2 u + k^2 u, \tag{2.19}$$

where Q is an operator, support waves in the domain where they are applicable. Kriegsmann and Morawetz [1980] consider Q of the form where the solutions to equation 2.19 consist of a plane wave plus an outgoing scattered wave. Examples where this form of Q occur are mentioned below. Further, the solutions tend to a steady state as time goes to infinity. For a circular truncation boundary of radius R, the NRBC for equation 2.19 (with the above form of Q assumed) is

$$2kR^2(i - \frac{1}{kR})(u_r + \frac{1}{c}u_t) = (\frac{\partial^2}{\partial\theta^2} + \frac{1}{4})\ u \ on \ B \tag{2.20}$$

This NRBC has been derived by using the asymptotic solution to equation 2.19 for the above form of Q for large distances. The authors have used finite differences to discretize the problem, and applied the method to solve problems in a number of fields, including one in plasma physics. In order to obtain steady state solution, a time marching scheme has been employed. Kriegsmann [1982] has also applied a similar technique for the problem of two dimensional wave guides.

2.3.4 NRBC's for problems in gas dynamics, hydrodynamics and meteorology

Incompressible Navier Stokes equations

Pearson [1974], while considering two dimensional *incompressible* Navier Stokes equations with a finite difference scheme applied to solve them, used a boundary condition on a truncated domain which is similar to the Sommerfeld radiation condition. It has the form

$$u_t + cu_n = 0, \quad on\ B \tag{2.21}$$

In the above equation, u_n is the normal derivative on the truncation boundary B. u is the appropriate field variable. The phase velocity c has to be evaluated on the truncation boundary B using a *linearized* dispersion relation.

Orlanski [1976] also uses equation 2.21 as a boundary condition; in addition, he calculates the propagation velocity at each grid point on the boundary from the data on the neighbouring grid points.

Other work of similar kind, where variations of above procedure are investigated for different problems in meteorology, includes that of Raymond and Kuo [1984], Carpenter [1982], Miller and Thorpe [1981], Klemp and Lilly [1978], and Wurtele et. al. [1971].

Jim and Braza [1993] have developed boundary conditions for *incompressible* Navier Stokes equations which apply to *velocity* components such that *vortices* leave the domain without reflection from the artificial boundary. Persillon and Braza [1998] apply this to investigate the transition to turbulence in the wake of a circular cylinder.

Small disturbance equation for time dependent transonic flow

An equation from gas dynamics which is also amenable to the technique of rational approximations for pseudo-differential operators (in addition to the wave equation for $infinitesimal$ field fluctuations in the gas) is the equation governing small disturbances in a transonic, unsteady flow. Engquist and Majda [1981] have used the technique to devise NRBC's for this equation. The governing equation is *nonlinear*, Engquist

and Majda handle this by *freezing* the nonlinearity, the NRBC is devised as if the equation was linear. Also, the wave propagation speed on the truncation boundary B is arbitrarily large, this requires the use of special approximations to the square root function rather than those used in their work on scalar wave equation by Engquist and Majda [1977, 1979].

Jiang and Wong [1990] treat the problem by using rational approximations of the absolute value function rather than approximations to the square root function that Engquist and Majda used.

Compressible flow of inviscid and viscous fluids

For problems in this class, analytical techniques (for devising the NRBC as well as checking well posedness, etc.) generally are applied to the governing system of equations only after a linearization has been performed on them. The work in this field is not as systemized as that for the (linear) scalar wave equation or the (nonlinear) small disturbance transonic flow equation. There are no general results available either. Literature has examples of work both for inviscid, compressible (Euler) equations of gas dynamics, and of compressible viscous flow (compressible Navier Stokes equations). The usefulness of NRBC's for solving the time dependent equations as well as for obtaining a steady state solution for unbounded geometries, is evident. In the latter case, the efficacy of the NRBC can be measured by the reduction in the number of iterations required to compute the steady state solution. This aspect is dealt with in greater detail in chapter 4 where new NRBC's are proposed and investigated for these equations.

Hedstrom [1979] considered a class of nonlinear hyperbolic systems in one space dimension. He obtained an NRBC which performs well for transonic flow (no strong outgoing shocks). The boundary condition is equivalent to:

$$\frac{\partial p}{\partial t} - \rho c \frac{\partial u}{\partial t} = 0 \tag{2.22}$$

In the above, ρ is the density, c is the speed of sound, p is the pressure and u is the x-component of velocity. This b.c. requires no *a priori* knowledge of the steady

state values of the variables, hence a steady state solution calculated with their use is dependent on the initial data. In particular, if the steady state values of the variables are prescribed, this NRBC is not suitable for use in a time marching solution.

Thompson [1987] extended this work to two space dimensions. In this and a later paper, Thompson [1990], he considered the homologous expansion of an adiabatic gas.

Rudy and Strikwerda [1980, 1981], starting from the NRBC developed by Hedstrom [1979], formulated another one which includes a *free parameter*. The NRBC is of the form:

$$\frac{\partial p}{\partial t} - \rho c \frac{\partial u}{\partial t} + \alpha(p - p_\infty) = 0 \tag{2.23}$$

The governing equations form a nonlinear system, the NRBC is linear. The term containing the free parameter α ensures that the complete data specified for a compressible Navier Stokes flow field (for the transonic regime) is made use of. Hence, independent of the initial data, the steady state value of outflow pressure is guaranteed to be equal to the specified value of p_∞. This can be seen as follows. At steay state, the terms containing partial derivatives with respect to time in equation 2.23 can be dropped off, the result thus obtained is $p = p_\infty$ (on the outflow boundary where this NRBC is applied), $\alpha \neq 0$.

Rudy and Strtikwerda [1981] apply this NRBC to compute the steady state solution for a flat plate placed in a uniform stream by means of time marching, and provide data on the convergence speed and also on pressure fluctuations near the boundary when various boundary conditions (including NRBC's) are used at the downstream subsonic outflow boundary. In Rudy and Strikwerda [1980], an analysis is provided for the optimum value of the free parameter for the *linearized* set of governing equations, where the optimum is defined in terms of the time (iterations) required to reach the steady state. However, the optimum value based on the linear analysis and that obtained from numerical experimentation are quite different as seen in Rudy and Strikwerda [1981]. This discussion is relevant to the new NRBC's proposed and studied in chapter 4.

Wilson [1982] has obtained a discrete boundary condition for this set of equations. He first formulates an NRBC that is non local in time, and then localizes it.

In section 2.2.7, the work of Bayliss and Turkel [1982] which extends their ideas for the scalar wave equation has already been mentioned. Bayliss and Turkel [1982] consider *linearized* Euler equations of gas dynamics. They have also used NRBC's for obtaining steady state solutions to these equations using a time marching technique.

Hagstrom and Hariharan [1988] also obtain an NRBC for the nonlinear Euler equations for a spherically symmetrical spatial domain by using an asymptotic solution of the far field equations. They compare their results to those of Thompson [1987].

Dispersive tsunami waves

Kim et. al. [1988] deal with the two dimensional Boussinesq equation (a nonlinear fourth order partial differential equation) for water level anomaly that governs weakly dispersive tsunami waves. They derive an NRBC for a rectangular computational domain by using order of magnitude arguments for the various terms in the governing equation. They then subject this NRBC to numerical experiments, using a finite difference approximation with a ray-following scheme.

Free surface flows

Free surface flows can be modeled either by linear hydrodynamic analysis or by nonlinear equations for free surface flows. In the former, non linearities can be introduced only through the boundary conditions. In the latter, the governing differential equations themselves are non linear. Jagannathan [1992] has devised an NRBC for nonlinear free surface flows in two dimensions (horizontal-vertical plane). The method used by him can be described as *energy flux equalization.* He poses the problem in terms of the amount of energy that should leave the computational domain through the non reflecting (open) boundary. Even when an NRBC is not formulated by the use of energy arguments, such an assumption is implicitly made– an improper NRBC leads to improper accumulation of energy in the domain through spurious reflections, a proper one implicitly defines the energy flux out of the boundary at just the right

level. Under the condition of steady state, the average rate of energy input should equal the average rate of energy flux from the truncated domain. It must be noted though that the occurence of the steady state does not necessarily imply that the solution is correct, an incorrect steady state can be obtained due to the application of wrong boundary conditions. Using these arguments, Jagannathan [1985] has formulated NRBC's through two approaches– that of energy flux maximization and of energy flux equalization (at the truncation boundary).

2.3.5 NRBC's for elastic waves

The exact one dimensional NRBC mentioned above (equation 2.6) has been studied in the context of a semi-infinite longitudinally vibrating rod by Kuhlemeyer and Lysmer [1973] in conjunction with the Finite Element Method (FEM). Lysmer and Kuhlemeyer [1969] also provide a set of NRBC's for the two dimensional case for elastic waves. This boundary condition has been called the *classical viscous boundary condition* in the literature. It is expressed as

$$\alpha \rho c_n \frac{\partial u_n}{\partial t} = T_n \tag{2.24}$$

$$\beta \rho c_t \frac{\partial u_t}{\partial t} = T_t \tag{2.25}$$

where u denotes the displacement. Subscripts n and t denote coordinate directions normal and tangential to the truncation boundary B. c_n denotes the longitudinal wave (P wave) speed and c_t the transverse wave (S wave) speed. ρ is the mass density, and α and β are dimensionless parameters. These parameters can be chosen to minimize reflections for a wave striking the truncation boundary B at a given angle of incidence. Lysmer and Kuhlemeyer [1969] have suggested $\alpha = \beta = 1$ as a good choice for these parameters based on their consideration of incident longitudinal, transverse and surface waves *separately*. FEM is applied to discretize the problem on the computational domain. However, the boundary conditions given in equations 2.24 and 2.25 give rise to large spurious reflections in certain situations (for example, large angles of incidence). Castellani [1974] has discussed these errors.

White et. al. [1977] use a different procedure to obtain better values of the parameters α and β in the classical viscous NRBC (equations 2.24 and 2.25), rather than choosing them equal to 1. They do this by using relationships between *velocities* and *stresses* on the truncation boundary B for the *discretized model*. Discretization has been carried out using FEM.

Clayton and Engquist [1977] have used the rational approximations and pseudodifferential operators technique (used by Enguist and Majda for the scalar wave equation) to obtain NRBC's for elastic waves, too. Detailed analysis of these has been carried out by Engquist and Majda [1979] also. The simpler of these NRBC's are

$$(\frac{\partial}{\partial t} - c_n \frac{\partial}{\partial x_n}) u_n = 0 \tag{2.26}$$

$$(\frac{\partial}{\partial t} - c_t \frac{\partial}{\partial x_t}) u_t = 0 \tag{2.27}$$

They perform perfectly for plane waves at normal incidence. Higher order NRBC's contain linear combination of second order partial differential operators involving x_n, x_t and t. They also consider the situation where instabilities may occur at corners of the boundary delimiting the computational domain (that is, 'edges' on the boundary on the two sides of which two different boundary conditions apply), and suggest a special procedure for corners.

A number of workers have used the NRBC's suggested by Clayton and Engquist [1977]. Emerman and Stephen [1983] and Mahrer [1986] have carried out numerical experiments with these NRBC's. Emerman and Stephen [1983] discovered that these NRBC's are unstable for $c_n/c_t < 0.46$. They suggested alternative discrete NRBC's.

Sochacki [1988] started by considering cases where only P plane waves and only S plane waves are present separately. He derived conditions for each of these cases and then combined them to generate an NRBC applicable to the general case.

Scandrett et. al. [1986] solved the time dependent elastodynamic equations and obtained the time harmonic solutions to them. They then derived an approximate time dependent NRBC for two and three dimensions.

Higdon [1990] suggests NRBC's of a form which are a generalization of his NRBC's for the scalar wave equation (equation 2.17).

$$\left(\prod_{j=1}^{m}\left(\beta_j^i\frac{\partial}{\partial t}-c_i\frac{\partial}{\partial x_i}\right)\right)\ u_i=0,\ i=1,2 \tag{2.28}$$

The parameters β_j^i can be chosen to render the NRBC perfectly non reflecting for incident plane waves at particular angles of incidence. For $m=1$, NRBC in equation 2.28 reduces to the NRBC's given by equations 2.26 and 2.27. Higdon discusses the stability of these NRBC's, and also carries out an analysis of them for their behaviour at the corners (corners have been defined above). Surface waves are not treated.

Cohen and Jennings [1983] have also derived NRBC's for elastodynamics in two dimensions, which are modified versions of Clayton and Engquist NRBC's. The procedure they use for doing this involves certain ad-hoc approximations, and allows them to obtain a simple NRBC for three dimensions, too. They also carry out a stability analysis for the two dimensional case. The result of this analysis is presented in the form of a map of stability regions; the presentation is in terms of the Poisson ratio and the angle of incidence. In the regions of instability, a different boundary condition is proposed. Their calculations are based on FEM using upwind elements.

Bamberger et. al. [1988] have carried this work forward for time dependent elastodynamics. They propose a modification to Cohen and Jennings NRBC's to take into account Rayleigh surface waves as well. The resulting NRBC contains the operator $((\partial/\partial t)-c_R(\partial/\partial x_n))$ analogous to equations 2.26 and 2.27. In the above, c_R is the Rayleigh wave speed. The Rayleigh wave speed is obtained as the solution to a transcendental equation. It is shown that this NRBC is perfectly non reflecting for normal incidence of P, S and Rayleigh waves.

Robinson [1976] has obtained an NRBC by considering time harmonic elastic waves in two dimensions using elastic potentials associated with the Helmholtz decomposition. Barry et. al. [1988] derive an NRBC by carrying out an analysis of one dimensional time dependent problem in the Laplace transform domain and then modify it to make it satisfy an energy stability criterion.

2.3.6 NRBC's for electromagnetic waves

Moore et. al. [1988] have reviewed such boundary conditions for electromagnetic waves.

Kriegsmann et. al. [1987] deal with electromagnetic waves scattered from a perfectly conducting cylinder. The NRBC they devise is a local one, they call it an 'On Surface Radiation Condition'. The derivation is based on a far field approximation of an exact integral relation involving the Green's function. The condition is applied on the surface of the cylinder itself.

For time dependent Maxwell equations in a vacuum, Mur [1981] has used the Engquist and Majda NRBC's for each component of the electric field separately. Umashankar and Taflove [1982] consider the use of the same NRBC's for various applications.

Tajima [1981] deals with electromagnetic plasma governed by two dimensional steady state Maxwell equations. He uses a masking algorithm to derive an NRBC.

Blaschak and Kriegsmann [1988] have compared the NRBC's of Halpern and Trefethen (section 2.2.3) and those of Higdon (section 2.2.9) in the context of electromagnetic waves. They test a number of situations, including a *propagating pulse*, that is, a non-smooth wave form, and a time harmonic wave.

2.3.7 Schrödinger equation

Kosloff and Kosloff [1986] apply what is known as an absorbing layer (or a filtering scheme) to the Schrödinger equation. In such schemes, the solution is artificially damped in the region near the truncation boundary, and the usual Dirichlet or Neumann boundary condition is used on the boundary. In this sense, though the objective of the method is the same (i.e., to reduce the size of the computational domain), the method can not strictly be classified as an NRBC technique.

A number of nonlocal NRBC's have been developed for the Schrödinger equation. These are covered later in the section on nonlocal NRBC's.

2.4 Methods other than the use of NRBC's

2.4.1 Method of characteristics (MoC)

Characteristic based methods can be utilized to solve hyperbolic partial differential equations specified over infinite/ semi-infinite spatial domains. Godunov type schemes have been widely used in gas dynamics.

Lin and Ballman [1993 b, 1993 c, 1995 a] have extended the Godunov type characteristic based finite difference methods of gasdynamics to stress waves in elastodynamics. They solve many plane problems where no source term is present in the g.d.e. In Lin and Ballman [1995 b], they have also developed explicit finite difference schemes for systems with a source term, which they apply to axisymmetric problems of elastic wave propagation in half space. In Lin and Ballman [1993 a] they solve the problem due to Chen [1975] by applying finite difference methods originally developed in the context of gas dynamics. Niethammer, Kim and Ballman [1995] extend the method to rectangular plates with curvilinear boundaries– the problem they solve is that of an infinite plate with a hole, subjected to sudden in-plate impact. A notable feature of their solution is that they have been able to employ the limiting value of the Courant Friedrichs Lewy (CFL) number = 1, Lin and Ballman [1995 a].

2.4.2 Domain transformation

Goldstein [1980] deals with various methods to solve the reduced wave equation (no time dependence, an elliptic partial differential equation) in an unbounded domain.

Analytical techniques of mapping the infinite domain to a finite domain can be used in certain situations. Grosch and Orszag [1977] use algebraic and exponential mappings to transform the infinite domain into a finite one. Depending on the condition at infinity, this technique may fail in some situations. The method works better for solutions that vanish rapidly or tend to a constant at infinity, it is not so good for solutions that oscillate at infinity. Cases where the method works well, which includes the one dimensional wave equation and Burger's equation, are discussed in detail by them. They find that algebraic transformations are better than exponential ones.

2.4.3 Addition of solutions

Smith [1974] deals with a method where reflections are eliminated by adding together the solutions (they can be numerical solutions) of several problems. In each of these problems a certain combination of Dirichlet and Neumann boundary conditions is used on the truncation boundary. The boundary is assumed to be planar and piecewise continuous; if reflections from n plane surfaces have to be eliminated, 2^n such solutions must be added together. For elastodynamics, this procedure has to be applied separately for dilatational and surface waves.

2.4.4 Artificially Absorbing Layers/ Filtering schemes

In filtering schemes, the solution is artificially damped in the region near the truncation boundary. The amplitude is gradually reduced in a strip of nodes near the boundary (a sudden reduction would be akin to an inhomogenity in the medium, and will cause reflections), and the usual Dirichlet or Neumann boundary condition is used on the boundary. A filtering scheme thus implies a modification of the *governing differential equation* itself in the region adjacent to the boundary. Damping can be applied either at the level of the continuous model or explicitly introduced in the discretized equations. Literature also refers to this approach as the use of Perfectly Matched Layers (PML).

Some papers that deal with filtering schemes are Cerjan et. al. [1985], Sochacki et. al. [1987], and Hanson and Petschek [1976]. Kosloff and Kosloff [1986] apply a filtering scheme to the Schrödinger equation. Thus, the potential function itself is modified in the exterior domain in a manner that backward diffraction from the absorbing layer thus obtained is minimized over a prescribed spectral range. The method is simple to implement for two and three dimensions.

Zhang and Ballman [1994] have used this approach to solve for the wave field in an elastic solid. In the transition layer, they apply absorption techniques such that the material properties of this region match perfectly with the kernel region where the original g.d.e. applies. They have used two techniques– one reduces the amplitude of the waves in the transition layer before the wave strikes the truncation boundary, the other slows down the wave speeds in the transition layer. They solve for a geometry

where a crack is present in the solid, a characteristic based finite difference discretization is carried out in the spatial domain.

Other examples of the use of this method are provided in Yevick et. al. [1995], Macias et. al. [1995] and Vibók and Balint-Kurti [1992]. Kurihara and Bender [1983] use it for a model in weather prediction.

Simultaneous use of an NRBC and a filtering scheme

Instead of using NRBC's and filtering schemes in isolation, they can be used simultaneously. Israeli and Orszag [1981] take this approach and show that the results are better than the isolated use of either. They consider two types of filtering for the scalar wave equation and the Klein Gordon equation.

Filtering schemes for Euler equations of gas dynamics

Filtering schemes have been applied to two dimensional, nonlinear Euler equations also. For gas flows governed by these equations, one may wish to truncate the domain to a small size. However, a peculiar situation may occur in this case. Two shock waves originating *inside* the domain which travel outwards (and which the boundary must allow to leave the domain without reflections) may collide outside the domain. This collision may result in generated waves to *reenter* the domain, these waves are *physical* and must be captured by the solution. The boundary treatment in this situation must anticipate the collision and allow for the solution to contain these physical waves. Filtering schemes designed to do this either *slow down* the waves approaching the boundary from the interior in a layer near the boundary, or reduce the amplitude of the waves as considered previously. For linearized Euler equations, Hu [1996] has used such a method. He considers the various types of waves supported by the linearized Euler equations (acoustic, vorticity and entropy waves).

2.4.5 Use of infinite elements in FEM discretization

In the context of the Finite Element Method, an option is the use of infinite elements for modeling the infinite spatial domain, Zienkiewicz [1977]. An infinite element is a semi

infinite element with some nodes at infinity. Shape functions for the infinite element are chosen so that the asymptotic behavior of the solution at infinity is captured by them. Hence one requires to calculate some integrals over infinite domains numerically. Chen [1990] has employed this method to solve for water wave radiation and scattering in one and two space dimensions. The corresponding equations are Webster's Horn equation (for the 1-d case) and Berkhoff's equation (for the 2-d case). Chaturvedi and Roy [1994] have used NRBC's to solve this problem.

2.4.6 Extrapolation formulae at the boundary

Many researchers have applied discrete equations on the artificial boundary which are equivalent to a variable being extrapolated at the boundary with respect to the neighbouring grid points. Chu and Sereny [1974] have used this procedure for invscid, compressible, one dimensional gas flow governed by the nonlinear Euler equations. The extrapolation formula is time dependent, and they solve for the steady state by marching in time. Elvius and Sundström [1973] carry out this procedure for nonlinear shallow water wave equations, Liao and Wong [1984] do this for problems in elastodynamics. The former paper uses a finite difference discretization, the latter uses FEM.

2.5 Nonlocal NRBC's

Nonlocality in time arises *naturally* in viscoelasticity where the medium possesses a memory. For two dimensional waves in a viscoelastic medium considered by Trautenberg et. al. [1982], the NRBC that has been derived depends on an ever increasing amount of past data with the passage of time. However, in order to carry out practical computations, the information required for the NRBC is limited to about twenty past steps in time to obtain results that are accurate.

However, for mediums that do *not* possess memory, an *exact* NRBC is still nonlocal in time. This situation is visible in the derivation by Engquist and Majda of their NRBC for scalar wave equation (section 2.2.2). Before arriving at the local NRBC mentioned in equations 2.7 and 2.8 by using rational approximations, the intermediate

step is an exact expression that is nonlocal in both space and time.

The ability to eliminate the exterior, indeed, is achieved at the cost of nonlocality. For time independent (time harmonic) problems, an NRBC has to be nonlocal in space so that the *entire exterior domain can be represented exactly.* For time dependent problems, an *exact* condition has to represent, in addition, the history of the exterior.

For time harmonic problems, a number of exact NRBC's have been proposed. Fix and Marin [1978], Keller and Givoli [1989], Givoli and Keller [1989, 1990] have proposed what is known as a Dirichlet to Neumann (DtN) NRBC, it involves a nonlocal operator M which is known as a DtN map because it relates the (Dirichlet) datum u (field variable) to the (Neumann) datum $\partial u/\partial n$, where n denotes the normal derivative at the boundary. The NRBC has the form

$$\frac{\partial u}{\partial n} = Mu, \ on \ B \tag{2.29}$$

Such an NRBC is very convenient to apply with the FEM. The NRBC involves the solution of an integral equation on the truncation boundary. MacCamy and Marin [1980] deal with the convergence of this NRBC with the FEM. Canuto et. al. [1985] have utilized NRBC of the form given by equation 2.29 with a spectral scheme of solution. Hariharan [1986] has summarized this method and reviewed other NRBC's, too. Givoli [1991] also reviews a number of schemes for obtaining NRBC's.

The nonlocal operator is, in general, complex to implement. In certain situations, however, this difficulty can be avoided. An example is Keller and Givoli [1989].

Nonlocal NRBC's for Schrödinger-type equations

Schrödinger-type equations are evolution partial differential equations of type:

$$\frac{\partial}{\partial t}u = \frac{-i}{c}(\frac{\partial^2}{\partial x^2}u + V(x,t)u) \tag{2.30}$$

$$u(x,0) = u_0(x) \tag{2.31}$$

where c is a real constant, and $V(x,t)$ is the potential.

The Schrödinger equation can be considered a prototype of the above equation, it is given by

$$i\hbar\frac{\partial}{\partial t}\Psi = -\frac{\hbar^2}{2m_0}\frac{\partial^2}{\partial x^2}\Psi \tag{2.32}$$

In the above (equations 2.30, 2.31 and 2.32), $\hbar$ is the Planck's constant, Ψ is the wave function which replaces u of equation 2.30, and m_0 is the rest mass of the particle. u_0 has support only in a finite interval, $\|u_0\|_{L^2}$ is bounded, and $u(x,t)$ must vanish as $x \to \pm\infty$ for $t > 0$.

Note that the techniques developed by Engquist and Majda are applicable to hyperbolic equations. Halpern [1991] has considered the case of mixed parabolic-hyperbolic equations. Hagstrom [1986] has dealt with parabolic equations. Unlike the case of hyperbolic equations where a radiation condition applies at infinity, equation 2.30 (a parabolic equation) satisfies

$$\lim_{s\to\infty} u(x) = 0 \tag{2.33}$$

For such equations, nonlocal NRBC's have been obtained for both the continuous and the discretized g.d.e. Examples of the former are Baskakov and Popov [1991]. For such schemes it has been found that stability occurs only for disjointed intervals of $\Delta t/\Delta x^2$. Schmidt and Yevick [1997] have developed a technique to obtain nonlocal NRBC's for the discretized Schrödinger-type equations.

2.6 Remarks on work reported in this dissertation

Most of the efforts for deriving NRBC's have been confined to simple geometries. Simple geometries also serve the purpose of benchmarking the calculations based on NRBC's. Quite often analytical solutions are available for such a geometry for the g.d.e. under consideration, at other times solution for such simpler geometries can be obtained by numerical means other than the application of an NRBC over a truncated domain. The results for such a situation allows one to proceed with greater confidence in applying the NRBC formulated by whatever means to geometries that are relatively

complex. An example of this is provided in Chaturvedi and Roy [1999] and in the work reported in chapter 3 of this dissertation.

An example of formulation and benchmarking of NRBC's for a simple geometry for compressible Navier Stokes equations is the work reported in chapter 4 of this dissertation.

Chapter 3

Application of NRBC's to a complex geometry

In this chapter, use of the procedure of NRBC's to delimit a large physical spatial domain to a smaller computational domain of interest to calculate the pressure field in the moderator of a Pressurized Heavy Water Reactor (PHWR) after a coolant channel has failed, is reported. Non Reflecting Boundary Conditions are applied to the moderator boundary while a perfectly reflecting boundary is assumed for the channels.

Analysis is required to show that the use of various boundary conditions (b.c.) to be used with the governing differential equation (time dependent scalar wave equation for pressure) does not render the problem ill posed, hence a well posedness analysis is presented for the various NRBC's that can be used. This analysis is also required for the 'corners' formed when two different b.c.'s are applied to contiguous portion of the spatial boundary, this has also been carried out for the relevant corners.

Before applying the method to the problem of the PHWR, it is validated for the problem of the pressure field in a homogeneous domain in which a sinusoidal source is placed arbitrarily. Analytical results are available for this situation. Agreement with the analytical result gives one confidence in going ahead with the application of the method to the much more complex geometry of the PHWR. Results for a 'hairline crack' and a 'fish mouth opening' are discussed in this context.

3.1 Introduction

This chapter reports the application of NRBC concept to a problem of great importance– to that of large heat exchangers in nuclear and process industries. The procedure of using NRBC's to delimit a large physical domain to a smaller computational domain of interest is applied to calculate the pressure field in the moderator of an Indian 500

MWe Pressurized Heavy Water Reactor (PHWR) after a single coolant channel has failed. The dimensions of the geometrical model of the PHWR have been obtained from Singh et. al. [1991 a] (Figures 3.6(a)- 3.6(h)).

When this happens a pressure shock propagates in the fluid domain (moderator) due to the release of high enthalpy coolant into the low pressure moderator. The effect of this pressure field on the channels in the *immediate* neighbourhood of the channel that fails needs to be investigated to determine their likelihood of failure in turn. However, the moderator domain itself is much *larger* compared to the *small* immediate neighbourhood of interest. This is an indication that the truncation of the domain to an interior region and application of NRBC at the truncation boundary may be fruitfully applied to realistically model the situation. NRBC's are applied to the moderator boundary while a perfectly reflecting boundary is assumed for the channels. In this connection, the work of Singh et. al. [1991 a] can be mentioned, where the domain has been truncated to a small size, but Sommerfeld radiation condition has been applied on the truncated moderator boundary, although this condition is applicable only at infinity. Radiation condition has also been used by Singh et. al. [1990] on truncation boundaries at a finite distance in space when they solve the problem of exterior shell-fluid interaction for a simpler geometry (a spherical shell immersed in an infinite fluid). A similar situation exists in Singh et. al. [1991 b].

In the previous chapter, a review of the relevant class of NRBC's for the scalar wave equation has been provided (section 2.2). This chapter picks up the theme from where that discussion ends.

3.2 Problem description

In a PHWR, fuel assembly (in channel form) surrounded by pressurized coolant heavy water (D_2O) is contained in a pressure tube. A Calandria tube separates this high pressure system from the outside low pressure moderator. The Calandria vessel contains many such assemblies immersed in unpressurized moderator water. The assembly is horizontal.

Combined failure of pressure tube and calandria tube is postulated as an im-

portant single failure event for the above system. Sequence of events that then take place are surmised to be crack tip propagation, decompression of high enthalpy coolant through the crack opening, shock wave propagation, phase change of fluid and fluid-structure interaction. Instead of tackling all of these events in a single study, we limit ourselves to computing the complex pressure field generated in the neighbourhood of a single coolant channel subsequent to its failure *based on acoustic assumption.* This will cover the *first few milli seconds* of highly transient phase. The computed pressure field in the fluid mesh can then be used to calculate the loading on the neighbouring channels to examine the likelihood of their failure. The effect of channel arrays and multiple wave reflection effects are taken into account in the formulation.

The nature of the openings after the crack can be modeled based on the criteria of 'fully open slit' (Hill et. al. [1985], Singh et. al. [1991 a]) as follows:

1. Line wave loading

   a) Axial hair line crack at the mid span of channel.

   b) Circumferential break of progressively increasing sizes, culminating in a complete circumferential break, at the mid span of channel.

2. Surface wave loading

   a) Axial slit with a circumferential opening of at least 1/3 times the circumference at the mid span of channel, (fish mouth opening).

   b) Complete circumferential double ended rupture at the mid span of channel.

Figures 3.6(a)-(h) show the proposed computational domains. Different types of failures described by appropriate source conditions can be assumed to occur at the channel that fails, and the resulting pressure field in the moderator computed. Results are presented here for the cases 1(a), 1(b) and 2(a) above.

In the proposed 2-dimensional model, failure is assumed to occur sufficiently far away from the tube sheet and the calandria wall. On the fluid boundary of the moderator, an appropriate Non Reflecting Boundary Condition is applied, because the disturbance that propagates out of this boundary decays as it travels outwards

in the large exterior domain. To solve the problem, Sommerfeld radiation condition (equation 2.4) has been used by Singh et. al. [1991 a] in the hope of eliminating spurious reflections from the mesh boundary of the fluid (moderator). As mentioned in connection with equation 2.4, this condition is valid only at infinite distance from the source, and should not be used at truncation boundaries introduced when delimiting the larger domain to a smaller domain of interest. The work reported in the following sections demonstrates the existence of spurious reflections if this b.c. is used. On the channels, a perfectly reflecting boundary condition can be assumed in order to simulate the wave reflection effects.

The shock pressure at the source (i.e., the channel that fails) is followed by a quasi steady pressure after flashing. For the conditions present in the actual situation, Singh et.al. [1991 a] have already calculated a shock pressure (p_{shock}) of $6.186MPa$ and a quasi steady pressure (p_{qs}) of $5.486MPa$. The duration of the initial shock is decided by the time of crack propagation and the relaxation time for nonequilibrium thermodynamic condition. Once p_{qs} is reached, other transients due to bubble growth take over; they are not under the scope of this study.

In the model one may have to assume that a number of sources are active simultaneously, depending on the nature of the crack opening. Thus, in the two dimensional model we intend to deal with, case 1(a) is equivalent to a point source acting on the channel boundary. Case 1(b) can be taken care of by incorporating a number of such point sources along the circumference of the channel, so that the entire angle of rupture is covered. One may, in the first instance, try applying the same approach for 2(a) as that for case 1(b). However, it must be noted that in the two dimensional model this situation would be exactly identical to case 1(b), and no new information will be obtained. Hence, cases 2(a) and 2(b) must not be modeled using the proposed two dimensional domain.

3.3 Problem formulation

The compressible Navier Stokes equations are linearized to the acoustic governing differential equation (g.d.e.) which is hyperbolic in time

$$\frac{\partial^2 p}{\partial t^2} = a_\infty^2 \nabla^2 p \tag{3.1}$$

where p is the perturbation in pressure, a_∞ the speed of sound in undisturbed medium, and t the time.

The explicit second order finite difference scheme for equation 3.1 is

$$\begin{aligned} p_{i,j}^{k+1} &= 2p_{i,j}^k - p_{i,j}^{k-1} + \lambda_x^2(p_{i+1,j}^k - 2p_{i,j}^k + p_{i-1,j}^k) \\ &+ \lambda_y^2(p_{i,j+1}^k - 2p_{i,j}^k + p_{i,j-1}^k) \end{aligned} \tag{3.2}$$

for points interior to the boundaries, with,

$$\lambda_x = \frac{a_\infty}{\Delta x \ / \Delta t} \ and \ \lambda_y = \frac{a_\infty}{\Delta y \ / \Delta t} \tag{3.3}$$

where,

i,j are the indices in x and y directions respectively,

k is the index for time,

Δx, Δy are equidistant steps in x and y directions,

Δt is the step in time.

Based on the Courant Friedrichs Lewy criteria for stability,

$$\Delta t \leq min\left(\frac{\Delta x}{a_\infty}, \ \frac{\Delta y}{a_\infty}\right) \tag{3.4}$$

The usual assumption in deriving the wave equation for pressure is that perturbations are small in magnitude, and the mean velocity is zero. However, the wave equation itself (mathematically) does not preclude discontinuous initial conditions. Thus, independent of the method of derivation, one can subject the wave equation to discontinuous initial conditions. However, the linear wave equation will not allow 'weak solutions'. Taking also into account the effect of the finite difference grid used, it must be remembered that the discontinuity in the intial condition will not be seen as a 'step'; as the initial condition propagates through the medium, it will smoothen out. In view of above, one can view the wave equation as the zeroth order approximation to the problem, which still brings out some interesting features of the physical

situation. Since the transient phase in the scope of this study lasts only for a few milli seconds, the actual flow of fluid out of the crack need not be considered and we can concentrate on just the effects of pressure wave propagation in the complex geometry under consideration. This is justified on the grounds that the speed of sound in the moderator fluid is much greater than the speed of the moderator fluid itself.

3.4 NRBC's for the domain

For the rectangular domain set forth for the problem, it is proposed to use NRBC's of the form in equation 2.17.

Consider the first order NRBC that absorbs incident waves at angle α with the unit normal $\hat{n}$ to the boundary B. Since $\hat{n}$ points outwards from the interior region, and the incident wave moves from the interior towards the exterior, this NRBC is

$$\left(\cos(\alpha)\frac{\partial p}{\partial t} + a_\infty \frac{\partial p}{\partial n}\right)_{on\ B} = 0 \tag{3.5}$$

In the above, α is the parameter of the NRBC, which can be chosen to minimize reflections. In order to quantify this, the concept of reflection coefficient is used. It can be defined as the fractional amount of the incident wave reflected after striking the boundary. By putting the incident wave in the b.c. (equation 3.5) the reflection coefficient, R_1, for this boundary condition can be shown to be

$$R_1 = -\frac{\cos\alpha - \cos\theta}{\cos\alpha + \cos\theta} \tag{3.6}$$

Note that for zero reflection $R_1 = 0$. θ is the actual angle of incidence of the wave striking B, where equation 3.5 is applicable. Also note that the choice of $\alpha = \pi/2$ results in perfect reflection, $R_1 = 1$, for $\theta \neq \pi/2$. $\theta = \pi/2$ is termed the "glancing regime". For the choice of $\alpha = \theta$ zero reflection is achieved, this indicates that it is possible to have different values of α for different locations on the boundary B depending on the most likely value of θ at that location, thus improving the performance of the NRBC.

Figure 3.1 shows the variation of R_1 with the angle of incidence θ for fixed values of the parameter α. The range of values of interest for θ (angle of incidence) is $(0, \pi/2)$.

As mentioned above, for each of the curves of constant α, the zero lies at the point $\theta = \alpha$. Choice of $\alpha = 0$ renders the NRBC useless- this corresponds to the glancing regime. For other values of α, it is seen that as long as θ is in the neighbourhood of α, the magnitude of the reflection coefficient is small. The neighbourhood in which $\mid R_1 \mid < 0.1$ is quite large for values of $\alpha < \pi/2$. As θ tends to $\pi/2$, R_1 increases in magnitude to 1.

Though the range of $\theta > \pi/2$ is not relevant, because the angle of incidence by definition is $\leq \pi/2$, R_1 has been plotted for the range $(0, \pi)$ in figure 3.2. When $\theta = \pi - \alpha$, where $\alpha \in (0, \pi/2)$, R_1 becomes infinite.

If the incident waves strike B from only one known direction, the first order NRBC, equation 3.5, is perfectly well suited for use because one can choose α to be equal to θ. However if there are reflecting surfaces present in the interior region of interest, causing multiple reflections from within the computational domain, waves may approach the truncation boundary from more than one direction. The direction(s) of approach is(are), in general, not known in advance. Thus a single choice of α, even if it matches with an angle of incidence, does not fully eliminate non physical reflection from the truncation boundary. In this context it should be noted that for a wide range of $(\alpha - \theta)$, R_1 still has a small value.

One can opt for higher order NRBC's in such a situation. To annihilate waves from m directions, an m^{th} order NRBC is introduced by applying the operator in equation 3.5 m times. This is demonstrated for the choice of m = 2 below :

$$\prod_{j=1}^{2} \left(\cos(\alpha_j) \frac{\partial}{\partial t} + a_\infty \frac{\partial}{\partial n} \right) p \Bigg]_{on\ B} = 0, \tag{3.7}$$

where a_∞ is assumed to be the same for the waves from the two directions. One now has at one's disposal more than one parameters α_j to tune the NRBC for better performance. R is now given by

$$R_2 = - \prod_{j=1}^{2} \frac{\cos \alpha_j - \cos \theta}{\cos \alpha_j + \cos \theta} \tag{3.8}$$

with subscript 2 denoting the reflection coefficient for the second order NRBC. Thus zero reflection is now possible for two different values of θ by appropriate choice of α_1

and α_2.

However, note that equation 3.7 involves the second normal derivative– for example, for the case of B perpendicular to the x-axis, $\partial^2 p/\partial x^2$ is involved. In order to allow the use of equation 3.7 as a boundary condition, this *second* normal derivative has to be expressed in terms of the field variable p itself, the *first* normal derivative, time derivatives and tangential derivatives (or any combination of them). This can be done by using the governing differential equation 3.1 itself. For the case when $\hat{n}$ points along the x-axis, we get

$$\left((\cos\alpha_1\cos\alpha_2+1)\frac{\partial^2}{\partial t^2}+a_\infty(\cos\alpha_1+\cos\alpha_2)\frac{\partial^2}{\partial t\partial x}-a_\infty^2\frac{\partial^2}{\partial y^2}\right)p\Bigg]_{B\perp x-axis}=0 \quad (3.9)$$

As can be seen from equations 3.5 and 3.9, discretization of the second order NRBC is more involved than that for the first order NRBC. As the order of the NRBC is increased, this complexity increases, too.

3.4.1 Well posedness of boundary conditions

As is obvious, for the physical problem under discussion one condition per boundary is required; hence also one condition on each non-reflecting (artificial) boundary. For hyperbolic systems of governing differential equations, choice and number of boundary conditions should be such that the Initial Boundary Value Problem (IBVP) is not rendered ill-posed. Thus we now investigate the well posedness of the proposed NRBC's with the IBVP formulated above. For this purpose, the domain will be considered to be a half space, $x \leq 0$, with B perpendicular to x-axis at $x = 0$.

In context of the domains on which we carry out our computations, the analysis of a 'corner' formed by the application of two different boundary conditions on two intersecting segments of the boundary is also of interest. We present a well posedness analysis of this situation also.

For the case of greater than one dimension, the 'normal mode analysis' of Kreiss [1970] gives necessary and sufficient conditions to be imposed on a boundary (for a hyperbolic system) such that the problem is well posed. Here, the first and second order

NRBC's, equations 3.5 and 3.9 respectively, are subjected to normal mode analysis to check well posedness.

The following requirement, which has been termed the Uniform Kreiss Condition (UKC) in literature (Kreiss [1970]), has to be satisfied:

For a hyperbolic problem on a half space $x \leq 0$, i.e., $\partial/\partial n = \partial/\partial x$, let

$$L\left(\frac{\partial}{\partial x}, \frac{\partial}{\partial y}, \frac{\partial}{\partial t}\right) p \Big]_{x=0} = 0 \tag{3.10}$$

be the homogeneous b.c. For the normal mode analysis, consider solutions of the form

$$p = \exp(\xi x + i\eta y + \tau t) \tag{3.11}$$

where, for the parameters ξ, η and τ, $\mathrm{Re}(\xi) \geq 0$, $\mathrm{Im}(\eta) = 0$ and $\mathrm{Re}(\tau) \geq 0$ have been assumed. Then UKC demands that, for well posedness,

$$L(\xi(\eta, \tau),\ i\eta,\ \tau) \neq 0 \tag{3.12}$$

Here ξ is related to η and τ through the dispersion relation.

First order NRBC:

For the first order NRBC given by equation 3.5,

$$L(\eta,\ \tau) = \cos(\alpha)\tau + a_\infty \xi \tag{3.13}$$

since, for the half space $x \leq 0$ used as the domain for well posedness analysis, $\hat{n}$ is the x axis.

The dispersion relation is obtained from the g.d.e.,

$$\tau^2 \ = \ a_\infty^2(\xi^2 - \eta^2)\ ,$$

from which follows

$$\xi = \left(\eta^2 + \frac{\tau^2}{a_\infty^2}\right)^{\frac{1}{2}}\ . \tag{3.14}$$

Here the root with non negative real part is chosen. Note that η^2 and a_∞^2 are both real and non-negative.

Therefore, in equation 3.13,

$$L(\eta,\ \tau) = \cos(\alpha)\tau + a_\infty \left(\eta^2 + \frac{\tau^2}{a_\infty^2}\right)^{\frac{1}{2}} \tag{3.15}$$

The expression in equation 3.15 can never be zero for $-\pi/2 < \alpha < \pi/2$, hence this NRBC renders the problem well posed for $\mid \alpha \mid < \pi/2$– i.e., non-grazing incidence on B.

However, for $\mid \alpha \mid = \pi/2$, i.e., for grazing incidence on the boundary, $L = 0$ for $\tau = \pm\sqrt{(-1)}a_\infty\eta$. Now, if the UKC is violated only for a value of τ with $\mathrm{Re}(\tau) = 0$, the problem is weakly ill posed– disturbances will neither grow nor decay in time.

Thus, the first order NRBC– equation 3.5– is weakly ill posed only for $\mid \alpha \mid = \pi/2$.

Second order NRBC:

For the second order NRBC given by equation 3.9,

$$\begin{aligned} L(\eta,\ \tau) &= (\cos\alpha_1 \cos\alpha_2 + 1)\tau^2 + a_\infty^2(\cos\alpha_1 \\ &+ \cos\alpha_2)\xi\tau + a_\infty^2\eta^2 \\ \Rightarrow L(\eta,\ \tau) &= (\cos\alpha_1 \cos\alpha_2 + 1)\tau^2 + a_\infty^2(\cos\alpha_1 \\ &+ \cos\alpha_2)\tau(\eta^2 + \frac{\tau^2}{a_\infty^2})^{\frac{1}{2}} + a_\infty^2\eta^2 \end{aligned} \tag{3.16}$$

The above quantity is zero for $\alpha_j = \pm\pi/2$, $j = 1, 2$, and $\tau = \pm\sqrt{(-1)}a_\infty\eta$. Thus the second order NRBC– equation 3.9– renders the problem well posed if $\mid \alpha_j \mid < \pi/2$ $(j = 1, 2)$. If either of α_1 or α_2 or both $= \pm\pi/2$, the problem is weakly ill-posed.

$L(\eta,\ \tau)$ is zero also if $\cos\alpha_1 = \cos\alpha_2$ and $\tau = \pm\sqrt{(-1)}(a_\infty\eta)/\sin\alpha_1$. However, $\cos\alpha_1 = \cos\alpha_2$ means that α_1 and α_2 have been chosen on the opposite sides of the boundary, that is, on the interior and the exterior sides. The one chosen in the exterior domain corresponds to the incoming waves, not the outgoing ones which are under

consideration. This situation would lead to weak ill-posedness, but such a choice is never made.

Since the weak ill posedness in case of both first and second order NRBC arises only for waves of tangential incidence ($\xi = 0$), in which case, too, the disturbances are confined to the boundary and will not propagate into the interior, use of the two NRBC's considered is justified. In the problem of PHWR considered here, $\alpha = \pi/2$ is never chosen since the actual angle of incidence θ does not equal $\pi/2$ at the non reflecting boundary B for *known* directions of waves (i.e., the angle formed by joining the source S directly to a point on the non reflecting boundary B with a straight line). One can not a-priori be sure of the situation after multiple reflections in one of the more complex domains with many channels.

But there may be another situation where a problem may arise. In order to describe this problem, we define the following term. A 'corner' in the 2-d spatial domain is defined as a point on the piecewise continuous curvilinear boundary where two such piecewise curves intersect. In general, the b.c.'s on the two sides of the corner can be different.

Now a corner can be looked upon as the boundary of the boundary of the full domain. In the half space domain in connection with which the well posedness analysis was done above, there are no corners. Since the introduction of the truncation point of the boundary (i.e., a corner) can cause unstable solutions within the subspace of the boundary, we still have to investigate when unstable solutions may be generated at the corner. Appropriate conditions will then have to be applied at the corner in such a case.

Treatment of corners

For this purpose, consider the quarter space of the third quadrant in the x-y plane, and call it Ω. Then $\partial\Omega_j$ $(j = 1, 2)$ denotes the boundaries (which can be considered the subspaces of Ω) formed by the negative x and y axes respectively. The origin, O, is the corner, $\partial(\partial\Omega_j)$, $j = 1, 2$. An IBVP is given on Ω.

We can define four associated IBVP's, one each on the half spaces $x \leq 0$ and

$y \leq 0$, and one each on the subspaces $\partial\Omega_1$ and $\partial\Omega_2$. For the latter two, the boundary under investigation is their point of intersection O.

In the absence of any less severe known conditions, the following sufficient condition for the quarter space problem has been used by Romate [1992].

> The quarter space problem is well posed if the associated half space problems, as well as the subspace problems, are all well posed.

Based on this criteria, the corners formed by the following combinations have been examined using the UKC. The half space problems have already been examined above for the two NRBC's, in the following we consider the quarter space problems.

(i) First order NRBC and a perfectly reflecting wall

On the negative x–axis, we have

$$\cos\alpha \frac{\partial p}{\partial t} + a_\infty \frac{\partial p}{\partial y} = 0, \tag{3.17}$$

and at the origin

$$\frac{\partial p}{\partial x} = 0. \tag{3.18}$$

On the subdomain $\partial\Omega_1$, i.e., the negative X-axis, equation 3.17 reduces to an ordinary differential equation (o.d.e.) in time, and *no* b.c. is required at the corner O. This is further evident in the discretization of the quarter space problem, wherein the field value at the corner does not affect any grid point on the boundary. Indeed, for the mutually perpendicular orientation of the boundaries $\partial\Omega_1$ and $\partial\Omega_2$, and the use of Central Difference Approximation (CDA) for the governing equation over the domain Ω, the corner value does not affect any other grid point in the domain.

(ii) First order NRBC on both Ω_1 and Ω_2

$$\partial\Omega_1 : \quad \cos\alpha_1 \frac{\partial p}{\partial t} + a_\infty \frac{\partial p}{\partial y} = 0, \tag{3.19}$$

on negative x-axis, and,

$$\partial\Omega_2 : \quad \cos\alpha_2 \frac{\partial p}{\partial t} + a_\infty \frac{\partial p}{\partial x} = 0, \tag{3.20}$$

at the origin O.

Both reduce to o.d.e.'s in time on their respective subdomains and conclusions similar to those in case (i) above hold. Hence, no extra b.c.'s are needed at the origin, O.

(iii) Second order NRBC and a perfectly reflecting wall

On $\partial\Omega_1$, i.e. the x-axis :

$$\begin{aligned} a\frac{\partial^2 p}{\partial t^2} \quad &+ \quad b\frac{\partial^2 p}{\partial t \partial y} - a_\infty^2 \frac{\partial^2 p}{\partial x^2} = 0 \qquad (a) \\ where & \\ a \quad &= \quad (\cos\alpha_1 \cos\alpha_2 + 1), \\ b \quad &= \quad a_\infty(\cos\alpha_1 + \cos\alpha_2) \qquad (b) \end{aligned} \tag{3.21}$$

On $\partial\Omega_2$, the perfectly reflecting wall which is the y-axis:

$$\frac{\partial p}{\partial x} = 0 \tag{3.22}$$

Equation 3.21(a) can be considered as the g.d.e. for the subdomain of the negative x-axis, with the origin as the boundary, where the b.c. given by equation 3.22 is applicable. In equation 3.21(a), which we wish to consider on the domain of x-axis, normal derivative (dependence on y coordinate) can be factored out by assuming periodic solutions in the y direction of the form:

$$p = \exp(i\eta y)\psi(x,t) \tag{3.23}$$

Note that the solution assumed in equation 3.11 for normal mode analysis of the half space problem is but a special form of equation 3.23 being used here to factor out reference to the normal coordinate. Therefore we can directly continue the analysis of the well posedness of this configuration in a manner similar to that for the half

space problem, without really going ahead with the reduction of equation 3.21(a) to its one dimensional counterpart. Hence we assume solutions of the form given by equation 3.11, with $\mathrm{Re}(\xi) \geq 0$, $\mathrm{Im}(\eta) = 0$, and $\mathrm{Re}(\tau) \geq 0$. The dispersion relation is now obtained from the g.d.e., equation 3.21(a), for which the b.c. is equation 3.22. Thus the dispersion relation is

$$\xi = \pm\frac{1}{a_\infty}(a\tau^2 + ib\tau\eta)^{1/2}, \ where\ i = \sqrt{(-1)} \tag{3.24}$$

and

$$L(\eta, \tau) = \xi = \pm\frac{1}{a_\infty}(a\tau^2 + ib\tau\eta)^{1/2}. \tag{3.25}$$

The above is zero if $\tau = 0$ or $\tau = -i(b/a)\eta$. In both the cases $\mathrm{Re}(\tau) = 0$, and the problem is weakly ill posed. Further, this situation implies $\xi = 0$ (equation 3.25). The disturbances at the corner neither grow nor decay with time, but are reflected faithfully along the negative x-axis, which exactly is what a perfectly reflecting b.c. is expected to do. Thus we can apply the perfectly reflecting b.c., equation 3.22, at the corner being considered.

(iv) Second order NRBC on both Ω_1 and Ω_2

On Ω_1 : (i.e., x–axis),

$$a\frac{\partial^2 p}{\partial t^2} + b\frac{\partial^2 p}{\partial t \partial y} - a_\infty^2\frac{\partial^2 p}{\partial x^2} = 0 \tag{3.26}$$

and

On Ω_2 : (i.e., y–axis),

$$a\frac{\partial^2 p}{\partial t^2} + b\frac{\partial^2 p}{\partial t \partial x} - a_\infty^2\frac{\partial^2 p}{\partial y^2} = 0 \tag{3.27}$$

a and b have been defined in equations 3.21(b), in which α_1 and α_2 can be chosen differently for equations 3.26 and 3.27.

We need a b.c. at O for both the equations. The condition on the other boundary can not be used when considering a particular boundary because of the presence of tangential derivatives.

A completely different, symmetric NRBC for such a case, to be applied at O (the corner), has been proposed by Engquist and Majda [1979], namely

$$\sqrt{2}\,\frac{\partial p}{\partial t} + a_\infty \left(\frac{\partial p}{\partial x} + \frac{\partial p}{\partial y}\right) = 0, \tag{3.28}$$

at O.

Thus we have to consider here equation 3.26 on the negative x-axis, and equation 3.28 at the origin O. Symmetry will guarantee similar results for equation 3.27.

The dispersion relation is therefore,

$$\xi = \pm \left(\frac{(a\tau^2 + i\ b\ \tau\eta)^{1/2}}{a_\infty}\right), \quad with \quad i = \sqrt{(-1)}, \tag{3.29}$$

and

$$L(\eta,\ \tau) = \sqrt{2}\tau \pm (a\tau^2 + i\ b\tau\eta)^{\frac{1}{2}} + i\ a_\infty \eta, \tag{3.30}$$

which is never zero. Thus a well posed problem results.

Note that the use of second order NRBC results in the requirement of special treatment of corners formed by the intersection of two boundary segments where the second order NRBC has been applied on both the segments.

3.5 Present work

From the discussion in the preceding sections, the following may be noted. Equations 3.5 and 3.9, imply that the discretization of the second order NRBC is more involved than that for the first order NRBC. For a large range of $(\alpha - \theta)$, the reflection coefficient R_1 (equation 3.6) is small. Further, the use of second order NRBC results in the requirement of special treatment of corners formed by the intersection of two boundary segments where the second order NRBC, equation 3.9, has been applied on both the segments. In such a situation, for example, a completely different, symmetric NRBC, can be applied at the corner, namely equation 3.28. In view of this discussion, the first order NRBC, equation 3.5, has been used in our calculations at the non

reflecting boundaries (B) of the moderator fluid obtained from the truncation of the computational domain, while a perfectly reflecting boundary condition

$$\left.\frac{\partial p}{\partial n}\right]_{channel\ boundary} = 0 \tag{3.31}$$

has been used at the channel boundaries (Γ) in the present work.

The combinations described in (i) and (ii) in section 3.4.1 are thus applicable in this context.

α has been chosen for the non-reflecting boundary's nodes by calculating the angle of the boundary node with respect to the source node (S), except when it is more or less clear from the node's location that the primary wave from the source does not reach the node in question directly, but may reach it only after unknown reflections from the channels. In the latter case α is arbitrarily chosen to keep R_1 low.

The source history is (section 3.2)

$$\begin{aligned} p &= 0\ for\ t < 0\ ms \\ &= 6.186\ MPa,\ 0 \leq t \leq 0.5\ ms \\ &= 5.486\ MPa,\ t > 0.5\ ms. \end{aligned} \tag{3.32}$$

The initial conditions are

$$p(x,\ y)]_{t=0} = 0\ \forall\ (x,y) \in \Omega,\quad except\quad (x,y)_{source} \tag{3.33}$$

and

$$\left.\frac{\partial p}{\partial t}\right]_{t=0} = 0\ \ \forall\ \ (x,y)\ \in\ \Omega \tag{3.34}$$

3.6 Results and discussion

3.6.1 Validation of the method

In order to validate the procedure, test runs were conducted with a homogeneous square domain (i.e., one without any channels in it) with a sinusoidal point source placed arbitrarily in it. The domain used for this purpose, the location of the sinusoidal

source S in it along with the locations A, B and C where pressure histories were recorded is shown in figure 3.3. The sinusoidal source used is given by

$$p_{sinusoidal\ source} = 1MPa\ sin(2\pi(t/0.5ms)) \tag{3.35}$$

At any other point in the domain, a sinusoidal response with the same period but an attenuated amplitude, and a time lag corresponding to that point's distance from the source, was expected. The magnitude of the attenuated amplitude was expected to satisfy the inverse square law based on energy conservation (exact solution for the cylindrically symmetrical 2 dimensional problem), if the boundary conditions were to perform satisfactorily.

In the validation runs, common data was the input for the two sets of boundary conditions, namely

1. First order NRBC, equation 3.5, and
2. Sommerfeld radiation boundary condition used by Singh et. al. [1991 a], equation 2.4 written for pressure.

By comparing the results for the two, we intend to show that the use of latter results in spurious reflections, thus justifying our use of NRBC's.

Now, for this configuration, the law of energy conservation for wave equation over the 2-dimensional homogeneous domain (exact solution) implies

$$\frac{(Amplitude\ at\ A)^2}{(Amplitude\ at\ C)^2} = \frac{(Distance\ SC)}{(Distance\ SA)} = 2.0 \tag{3.36}$$

From the plots shown in figure 3.4 (for node A) and figure 3.5 (for node C), the corresponding ratios of the square of the amplitudes are

$$\frac{(Amplitude\ at\ A)^2}{(Amplitude\ at\ C)^2} = \frac{0.088^2}{0.063^2} = 1.95\ , \quad for\ first\ order\ NRBC. \tag{3.37}$$

while,

$$\frac{(Amplitude\ at\ A)^2}{(Amplitude\ at\ C)^2} = \frac{0.085^2}{0.053^2} \approx 2.4\ , \quad for\ Sommerfeld\ b.c.'s. \tag{3.38}$$

The pressure histories at locations A and B are expected to be identical since these two locations are symmetrical with respect to the source S in all respects. This should be the case even with the set of boundary conditions which fail to suppress reflections, as long as the above symmetry is maintained, and it did happen.

Further, for boundary conditions that fail to suppress reflection, the following can be argued. For the simple case of waves in one space dimension, for example a string, if a wave incident on a boundary was partially reflected and partially transmitted, a reflected wave which has a smaller amplitude, same frequency and opposite phase will travel back into the domain and interfere with the outgoing wave field. The net effect of this interference will be smaller amplitude of the waves in the domain than would have been if the outgoing wave had been fully transmitted. For a 2-dimensional case there will be reflections from many boundaries. The amplitude and phase of the reflected waves reaching the point being considered will depend on how far this point is from the various boundaries. For points in space near to a particular boundary, for example the node C in the domain under consideration (figure 3.3), the effect of the nearest boundary will dominate, and one would expect results similar to that described for the 1-dimensional case. Such indeed is the case, the amplitude for node C calculated with Sommerfeld boundary conditions as used by Singh et. al. [1991 a] is less than that obtained with NRBC's (figures 3.4 and 3.5). Here, it may be remarked that these comparisons are based on the code developed by the author, Singh et. al.'s [1991 a] code is not available to us. However, results presented by Singh et. al.[1991 a] for shock loading (equation 3.32) are lower than our estimates, even in the approach to steady state of quasi-static pressure after the shock has subsided, which further confirms these observations.

The very good numerical agreement for the NRBC with theory increases the confidence in using them with the complex geometry of the PHWR model.

3.6.2 Results for PHWR

For the 2-dimensional PHWR model described in section 3.2 (figures 3.6(a)-(h)), simulations were carried out for domains with progressively increasing sizes, with more

and more channels placed in it. Different types of failures can be implemented as appropriate source conditions at the channel that fails, and the resulting pressure field in the moderator computed. Results are presented here for the cases 1(a) and 2(a) enumerated above.

The smallest domain used (figure 3.6(a)) had two rows of three channels each, with the source (failed) channel placed as shown. Figures 3.6(b) and 3.6(c) both have four rows of four channels each, but the placement of the source channel in them differs. In the latter case (figure 3.6(c)), it is surrounded by a greater number of reflecting channels. Similarly, figures 3.6(d) and 3.6(e) both have six rows of six channels each, in figure 3.6(e) the placement of source channel is such that it is surrounded by a greater number of reflecting channels as compared to figure 3.6(d). In figure 3.6(f), there are seven rows of seven channels each, the source channel is located in the middle of this matrix. In figure 3.6(g), the number of channels is further increased to 8X8. Figure 3.6(h) is the largest of the domains considered, with nine rows of nine channels each, with the source channel placed in the center of the matrix of channels. We intend to show that as more and more channels with larger domains are considered, the results tend towards domain independence, especially in the transient response, because the neighbourhood of the failing channel no longer sees (in an approximate sense) any new channels that may be introduced farther off from this neighbourhood.

Results for hairline fracture

The case of hairline fracture is modeled in the 2 dimensional domains of the figure 3.6 as a point source. The source channel fails at a location that is at an angle of 45 degrees with the horizontal. Point S in the various domains denotes the source, it is the point where that channel fails.

Points A, B, C, D, E and F shown in each of the eight domains considered, have the same relative location with respect to the source channel S. Of these, points A to D are on channels other than the source channel, and F is on the same channel that fails. Point E is the nearest point from the point S that lies on a channel *different* from the failed channel. Note that points on the source channel itself, for example the point

F, will be much nearer to the point S compared to the point E. From the point of view of loading of the channels point F may not be of much interest as it lies on the channel that has already failed, but from the point of view of waves reflected from these points and the interference pattern resulting at other channels due to them, these points are of interest. We discuss this issue in the following paragraphs. Pressure histories at some of these points (A, B, C, D, E) are presented for each domain (described in figures 3.6 (a) to 3.6 (h)) in figures 3.7 to 3.14. Figures 3.15 to 3.21 show the exploded view for the first millisecond of the pressure evolution for each of the domains. Mesh size used for the plots shown is $\Delta x = \Delta y = 1.43\ mm$. Based on the results presented in figures 3.7 to 3.21 we make the following observations.

We observe that the steady state pressures calculated here are closer to what equation 3.32 indicates compared to Singh et. al.'s [1991 a] results which are lower. An explanation of why it should be so has been proposed in section 3.6.1. When we consider the domains shown in figures 3.6(b) to (h), which consider multiple reflections from a large number of channels, approach to steady state gets delayed. As the number of reflecting channels surrounding the source is increased, pressure values at the same time (for the same node) are seen to be lower– an effect analogous to that of spurious reflections, but here the reflections arise due to reflecting surfaces (channels) in the domain and are real. Note further, in the domain of figure 3.6(a), the oscillations superimposed on the main trend are less pronounced compared to the other domains because there are very few channels to reflect and thus to create a complex pressure field for this case. Another effect of lesser channels in the smaller domain is that the pressure history at a given point, say A, portrays the step like nature of the source condition (equation 3.32) to a larger extent. This effect is visible from the fact that steady state is reached much faster for smaller domains as compared to domains with larger number of channels.

The nature of the pressure history curves can be explained as follows. The source pressure consists of two pressure 'steps', the first one of $6.186 MPa$, lasting for $0.5 ms$, followed by a second step of $5.486 MPa$. If one considers just the propagation of a pressure 'impulse' (that is, one modeled by the Dirac delta function) rather than

a 'step', one would expect the following behaviours for one and two space dimensions. In the 1-d case, the pulse would propagate with it's magnitude unchanged (except for the smoothening out as the pulse propagates, in view of the g.d.e. used), while in two or more dimensions, the magnitude of the pulse will decrease as it moves farther off from the source (in view of energy conservation for cylindrical symmetry). However, if instead of a pulse we have a step, only the corner of the step will exhibit above behaviour. For our case, the first wave that reaches a point in the 2-d domain will have a magnitude lower than the source peak of $6.186MPa$, depending on the distance of that point from the source. The second step of $5.486MPa$ is visible in the plot, for example, for point F, where $0.5ms$ after the first wave reaches it there is a drop in pressure. For the kind of b.c.'s used for the moderator (NRBC's)- i.e., where the pressure value is not a fixed value but adjusts with time, solution at any point in the domain will show 'asymptotic pressure escalation' as finally the pressure at the point reaches the constant value of the step. Note that for the problem under consideration this 'constant' value is the value of the second step equal to $5.486MPa$.

The constant value of $5.486MPa$ of the second pressure step is a 'quasi- static' value and not a 'static' value, and after this phenomenon is over, other phenomena occur as mentioned in section 3.2. Hence, of main interest from the practical point of view is the transient response in the pressure histories shown.

Figures 3.15 to 3.21 show the exploded view of the pressure history for the first millisecond for domains in figures 3.6(a) to 3.6(h) respectively. It is seen, especially from figures 3.16 to 3.21, that the plots for points E and A are almost similar; this is so because point A is placed almost at a similar distance and orientation as point E with respect to the source point S. As far as the neighbourhood of points A and E is concerned, for domains in figures 3.6(c) to 3.6(h) each of these two points sees a similar number and orientation of reflecting channels around it. For the domains in figures 3.6(a) and 3.6(b) the neighbourhoods of these two points vis a vis the reflecting channels around them are not so similar. Results presented in figure 3.15 (for the domain in figure 3.6(a)) similarly show a lesser similarity in the pressure history of points A and E as compared to that seen in figures 3.16 to 3.21 for the domains with

a greater number of channels. E or A can therefore be considered candidates for the most severely affected channels due to the failure at S.

Results for increasing number of channels, figures 3.6(b)-(h), show secondary and tertiary oscillations superimposed on the main trend. These secondary frequencies of lower value and tertiary frequencies of higher value are visible clearly in figure 3.17 which shows an exploded view of the pressure history for the first millisecond, for the domain in figure 3.6(e). The secondary frequency is approximately 5 *per* ms, tertiary frequency is of an order of magnitude higher. One would expect oscillations corresponding to waves reflected from channels at varying distances from a particular node to be present in the solution. Based on this interpretation, oscillations corresponding to reflections from channels that are nearest will have higher frequencies compared to reflections from channels that are farther off. Considering the minimum channel to channel distance of $177mm$ and the sound speed of $1481.4mm/ms$, one obtains the highest value of frequency of the order of 4 *per* ms due to this effect. But, in addition, waves reach a point, say A, not only from the source point S and reflections from channels *other* than the source channel, but *also* from reflections from points on the source channel *itself*, for example from point F. These points can be infinitesimally close to the point S in the exact analysis; in the numerical solution this distance will be of the *order* of the grid spacing. Similar observations can be made for the points on any given channel. The resultant wave pattern produced at any point in the solution domain thus also exhibits interference of waves due to reflections from various points on the *same* channel. Depending on constructive and destructive interference of these waves, frequencies higher than that based on reflections only from *different* channels (as calculated above from channel to channel distance and wave speed) will be exhibited. Waves of various wavelengths are present in the solution, each wavelength will have a different interference characteristic depending on (a) the path differences of the interfering waves and (b) their phase differences. To this situation, there will be the added complexity of having two pressure steps, which will produce an even more complicated pattern of interfering waves in the solution domain. These high frequencies are seen in the results we present.

During the initial period of time immediately after the failure, this interference pattern is much more marked with a relatively higher amplitude about the mean trend. This is because initially there are only a few waves arising directly from the source and due to one or two reflection(s) from channels. Their interference pattern at a point in the computational domain is relatively well marked. With time, a criss cross pattern of waves due to multiple reflections in the domain is set up. If we follow an infinitesimal part of a wave front, after many reflections within the domain it will exit out through the non reflecting boundary, albeit with a much smaller amplitude. The effect of this criss cross pattern of multiply reflected waves on the interference pattern is thus likely to be small, interference due to them will result in small amplitudes about the mean trend and the interference pattern will be less marked at larger time. This does occur to a certain extent, but superimposed oscillations are still discernable at large times. The main cause that secondary and tertiary oscillations persist for a long period of time right upto the steady state can thus be attributed to the existence of the continued source of pressure impulse at the failed channel (as can be seen from the source conditions, equation 3.32). Continued generation of pressure pulses from the failed channel and their reflection from the points on the same channel as well as from different channels, thus results in both the trend and the superimposed oscillations in pressure history at a point in the computational domain.

It may also be noted that once domain independence has been achieved this effect does not grow.

As we consider larger domains containing more channels in our quest for domain independence, we find that peaks, nature and periods of oscillatory behaviour superimposed on the main trend, and approach to steady state value show similar behaviour when this computational phenomenon is encountered. Domains in figures 3.6 (e) and 3.6 (f), or higher, can be considered appropriate for 2-dimensional modeling of the failure event postulated in the PHWR, especially from the point of view of capturing the transient phenomena and the continued oscillatory loading of the tubes. They are small enough for computational purposes, and illustrate well the application of NRBC's in truncating large domains to small ones. This aspect will be reinforced

further when the results for fish mouth failure are considered below.

Results for fish mouth failure

For this type of failure, results are presented for the domains in figures 3.6 (a), 3.6 (c) and 3.6 (e). Three sizes of fish mouth are considered, namely:

- 29 deg, where the fish mouth starts at 23 deg with respect to the x axis on the source channel S, and ends at 52 deg (0.4 radians to 0.9 radians), measured counter clockwise. The results for this case are presented in figures 3.22 and 3.23 for nodes A and B for the three domains mentioned above.

- 60 deg, where the fish mouth starts at 30 deg with respect to the x axis on the source channel S, and ends at 90 deg, measured counter clockwise. The results for this case are presented in figures 3.24, 3.25 and 3.26 for nodes A, B and C.

- 360 deg, that is, *complete circumferential break* of the source channel. The results for this case are presented in figures 3.27, 3.28 and 3.29 for nodes A, B and C.

The first and most striking difference that can be observed from the results for the hair line case is that the steady state is reached much earlier now. In fact, the larger the size of the 'fish mouth', the faster the steady state is reached. That is to say, as the fish mouth size of failed channel increases, the pressure response at any point in the domain shows more and more of a step like character. One also sees clearly that the steady state value of the solution is equal to the quasi static pressure of D_2O (equal to 5.48 MPa) as mentioned in equation 3.32. The much faster approach to this pressure is as expected. The larger the fish mouth opening, more is the moderator exposed to the pressure inside the pressure tube, resulting in faster approach to steady state.

Fish mouth failure is modeled by the use of multiple source points (points with the pressure history given by equation 3.32) on the source channel. Waves that reach a given point in the computational domain from such successive neighbouring points are successively slightly out of phase with each other, but are of exactly the same magnitude. Upon reaching a point in the computational domain they are likely to result

in an interference pattern that is strongly marked due to large amplitude oscillations about the mean trend, as compared to that obtained for the hairline fracture, especially during the intial period after the failure. In this connection, the theory proposed in the previous section dealing with the results for hairline fracture should be recalled. Results for fish mouth openings corroborate this theory. It is seen that the tertiary oscillations of higher frequency also are more discernable compared to the results for hairline fracture, as they now have larger oscillations about the mean trend. Recalling that these oscillations were attributed to *reflections from points lying on the same channel* for the case of hairline fracture, and from the fact that in the case of fish mouth opening *there actually are a number of sources lying next to each other on the same channel*, these results corroborate the assertion that tertiary oscillations actually arise due to waves arising/reflecting from points on the same channel, i.e., points in closer proximity of each other as compared to the minimum channel to channel distance. It should be noted that these effects become stronger as the fish mouth size grows larger, this is expected in view of the above explanation.

The peak value reached in these cases is also much higher, with the value increasing with the size of the fish mouth opening, as compared to the case of hairline fracture. Peak pressure for the case of failure with a big fish mouth is quite high; for the smaller computational domain of figure 3.6(a) (which considers the smallest number of channels in the model) it is substantially higher than the steady state value. This happens because a number of impulses reaching a particular point in the domain from the points of failure on the source channel reinforce each other. Such a failure is thus seen to be more dangerous than a hairline fracture. The result which was witnessed in the case of the hairline fracture is seen here too: the value of pressure at a given point in space and at a given instant is highest for the smallest computational domain (figure 3.6 (a)), and decreases as the domain size grows to that in figure 3.6 (e). The effect of reflection from multiple channels in the arrangement shown, for example, in figure 3.6 (e), is to suppress the peaks. In general, whether the reflections reinforce or suppress the crests will depend, for the particular geometrical arrangement, on whether the waves interfere constructively or destructively.

The loading in both these types of failures, as far as the steady state value of pressure is concerned, is in accordance with equation 3.32. This can result in the collapse of the calandria tube whose theoretical collapse pressure is 0.366 MPa (Singh et. al. [1991 a]), but not of the pressure tube as they are pressurized from the inside and have a theoretical collapse pressure of 9.18 MPa.

However, an oscillatory loading of the channels is also visible, which persists for a long time. These oscillatory loads inevitably will set up vibrations in the tubes– lengthwise vibrations in the tubes can result depending on the length of the tube between stiffeners and the point along its length where this load is applied. In addition, there can be oscillations of the cross sectional area. The minor oscillatory loading persists for long, and can sustain the vibrations of the tube for a long period of time. This problem is three dimensional and a complete analysis requires a fluid-structure interaction code.

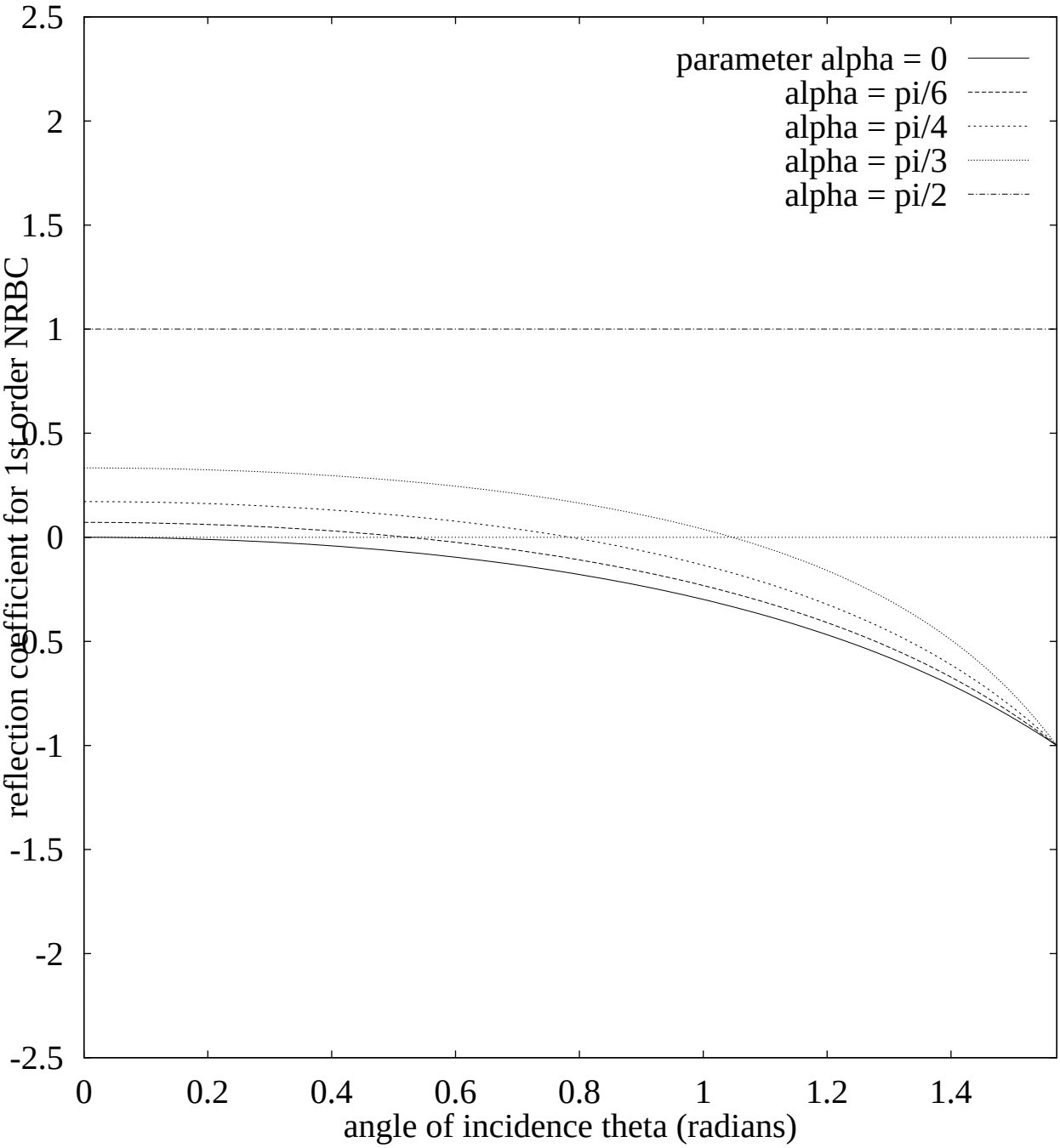

Figure 3.1: Reflection coefficient R_1 vs. angle of incidence $\theta \in (0, \pi/2)$ for various values of α

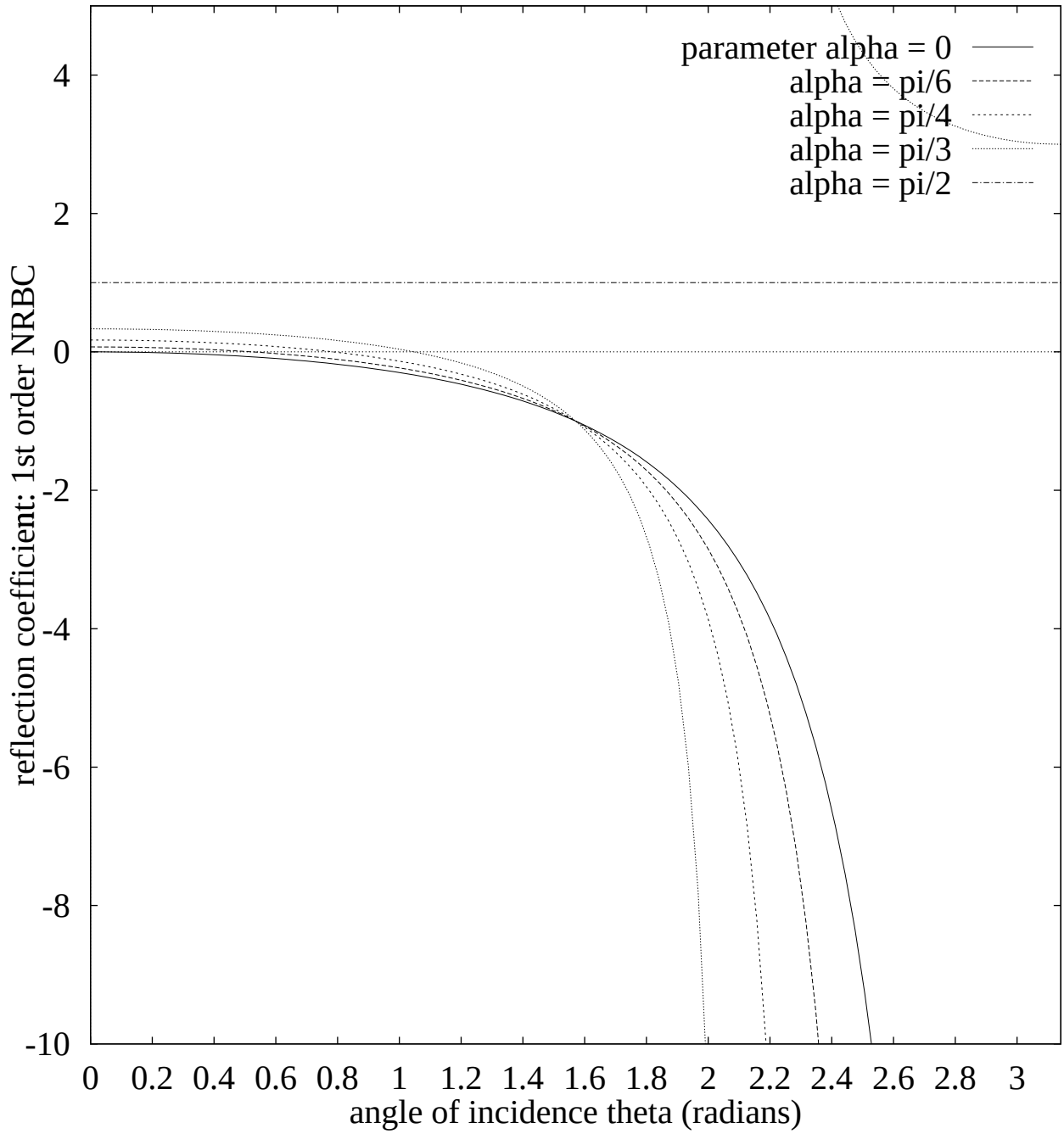

Figure 3.2: Reflection coefficient R_1 vs. angle of incidence $\theta \in (0, \pi)$ for various values of α

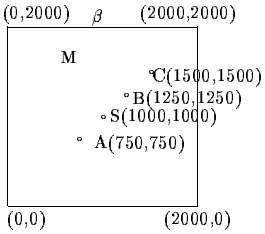

S: Source; A,B,C: nodes where pressure history is recorded. M: Moderator; β: Non Reflecting Boundary

Figure 2.1: Homogeneous domain (i.e., devoid of reflecting channels), with NRBC's applied at its sides.

Figure 3.3: Homogeneous domain, i.e., devoid of reflecting channels, with NRBC's applied at its sides.

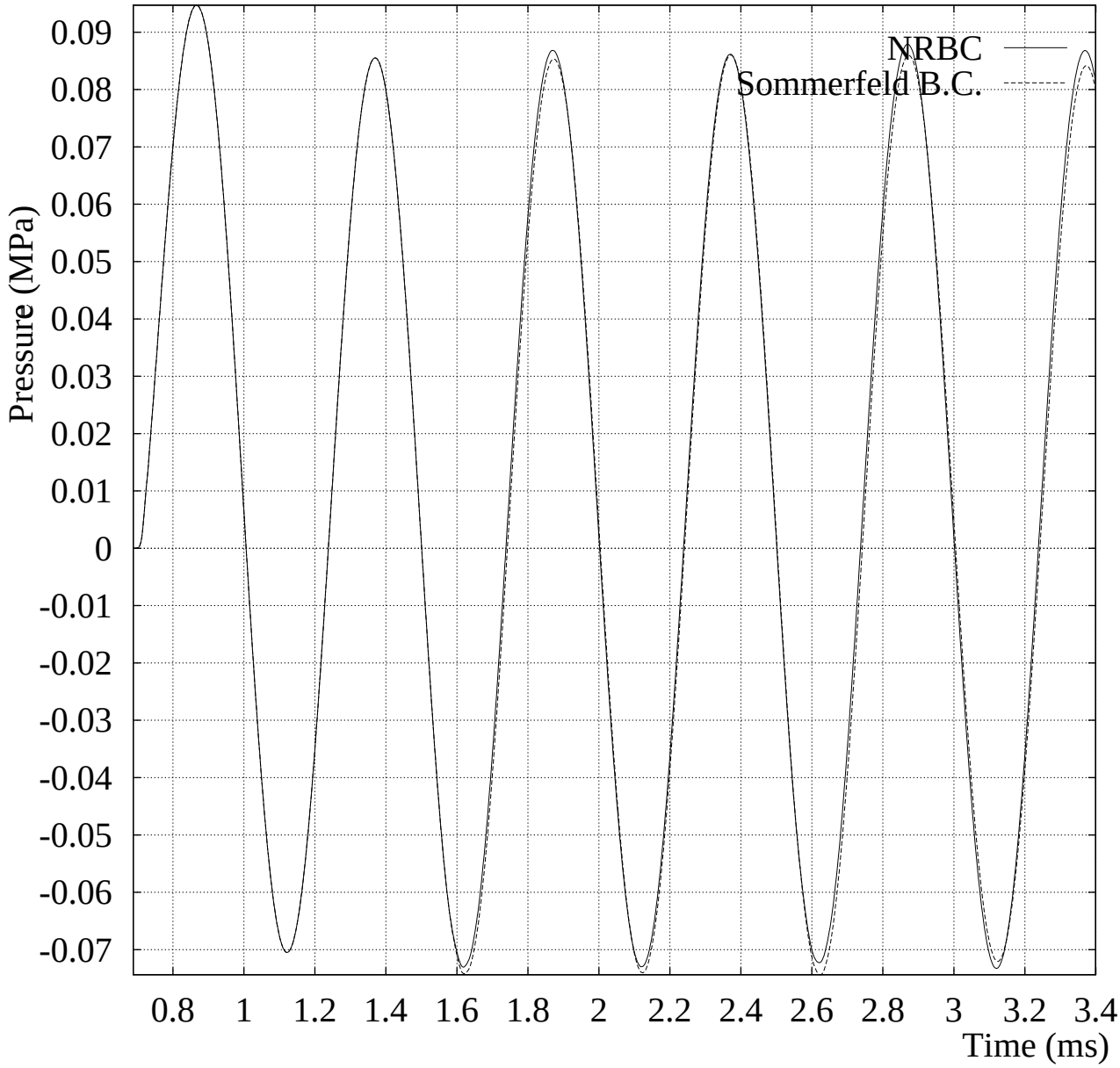

Figure 3.4: NRBC vs. Sommerfeld's radiation b.c. at node A for homogeneous domain with sine source

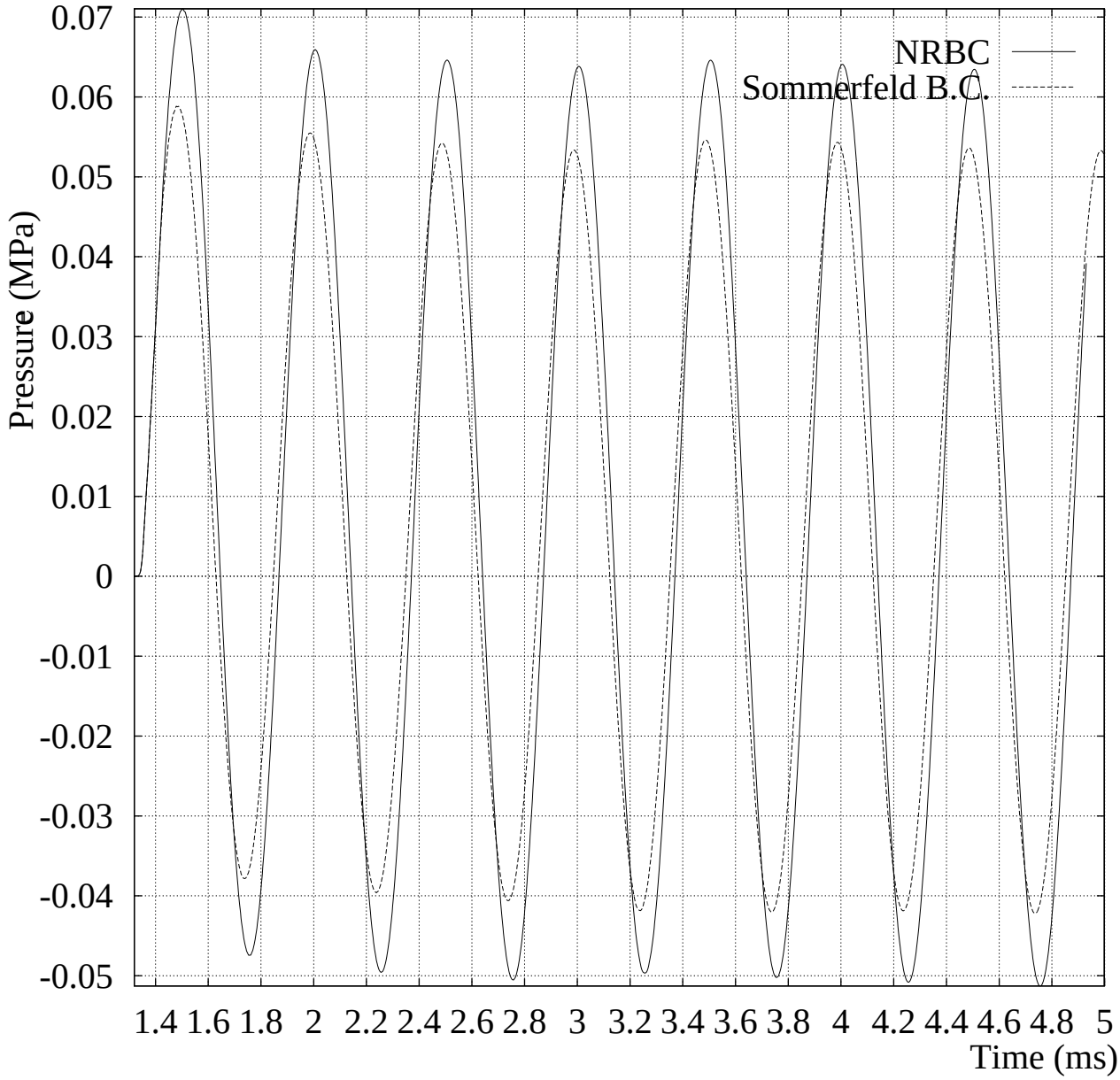

Figure 3.5: NRBC vs. Sommerfeld's radiation b.c. at node C for homogeneous domain with sine source

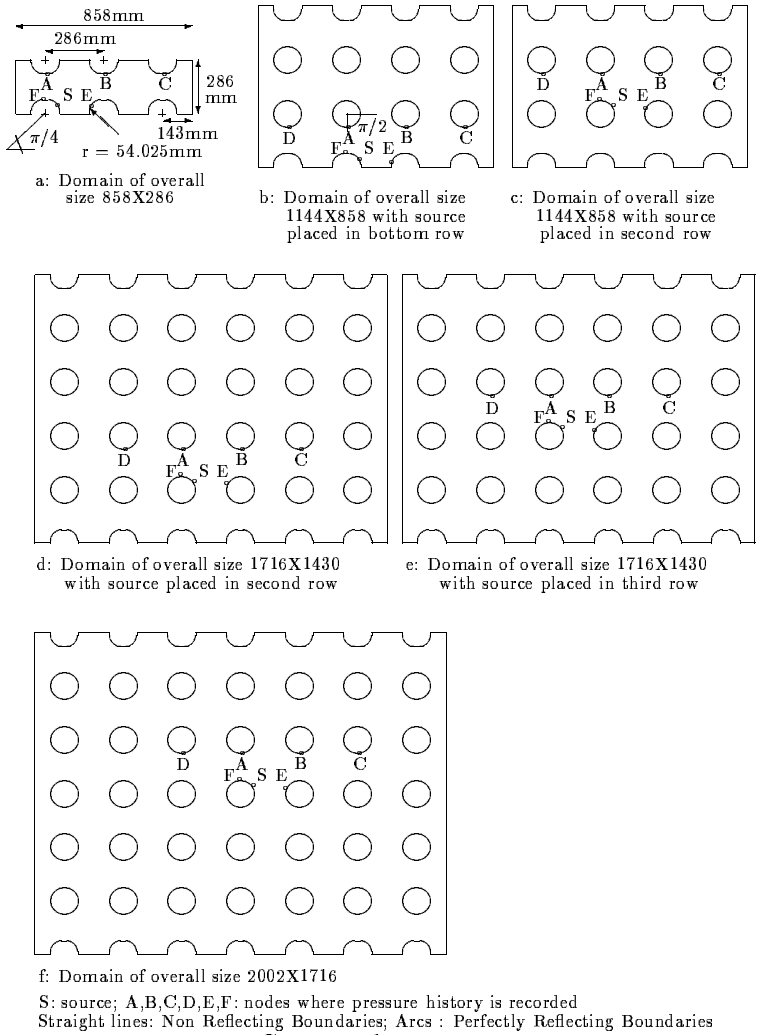

Figure 2.4: Continued on next page ...

1

Figure 3.6: (a) to (e). Progressively expanding domains used for computation. Relative locations of nodes A,B,C,D,E and F with respect to source S remains the same.

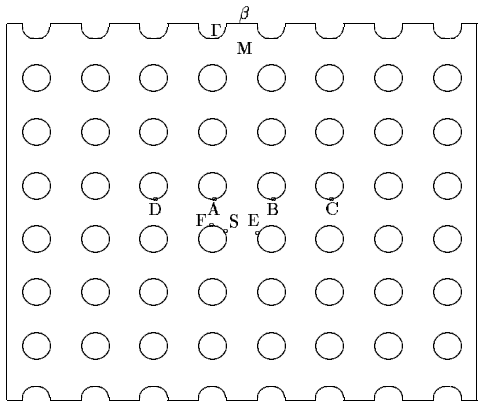

g: Domain of overall size 2288X2002

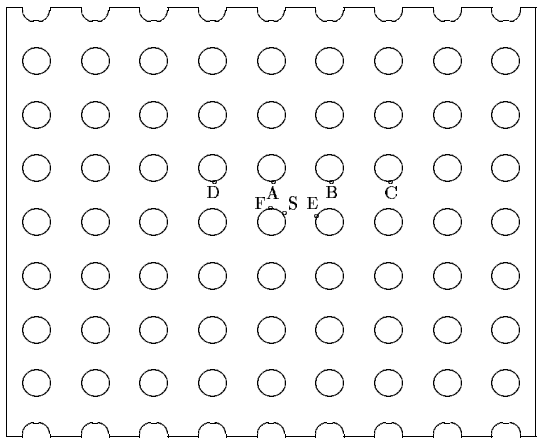

h: Domain of overall size 2574X2288

S: source; A,B,C,D,E,F: nodes where pressure history is recorded; M: Moderator
β: Non Reflecting (Moderator) Boundary; Γ : Perfectly Reflecting (Tube) Boundary

Figure 2.4 : Progressively expanding domains used for computation. Relative locations of nodes A,B,C,D,E and F with respect to source S remains the same.

1

Figure 3.6: (g) to (h). Progressively expanding domains used for computation. Relative locations of nodes A,B,C,D,E and F with respect to source S remains the same.

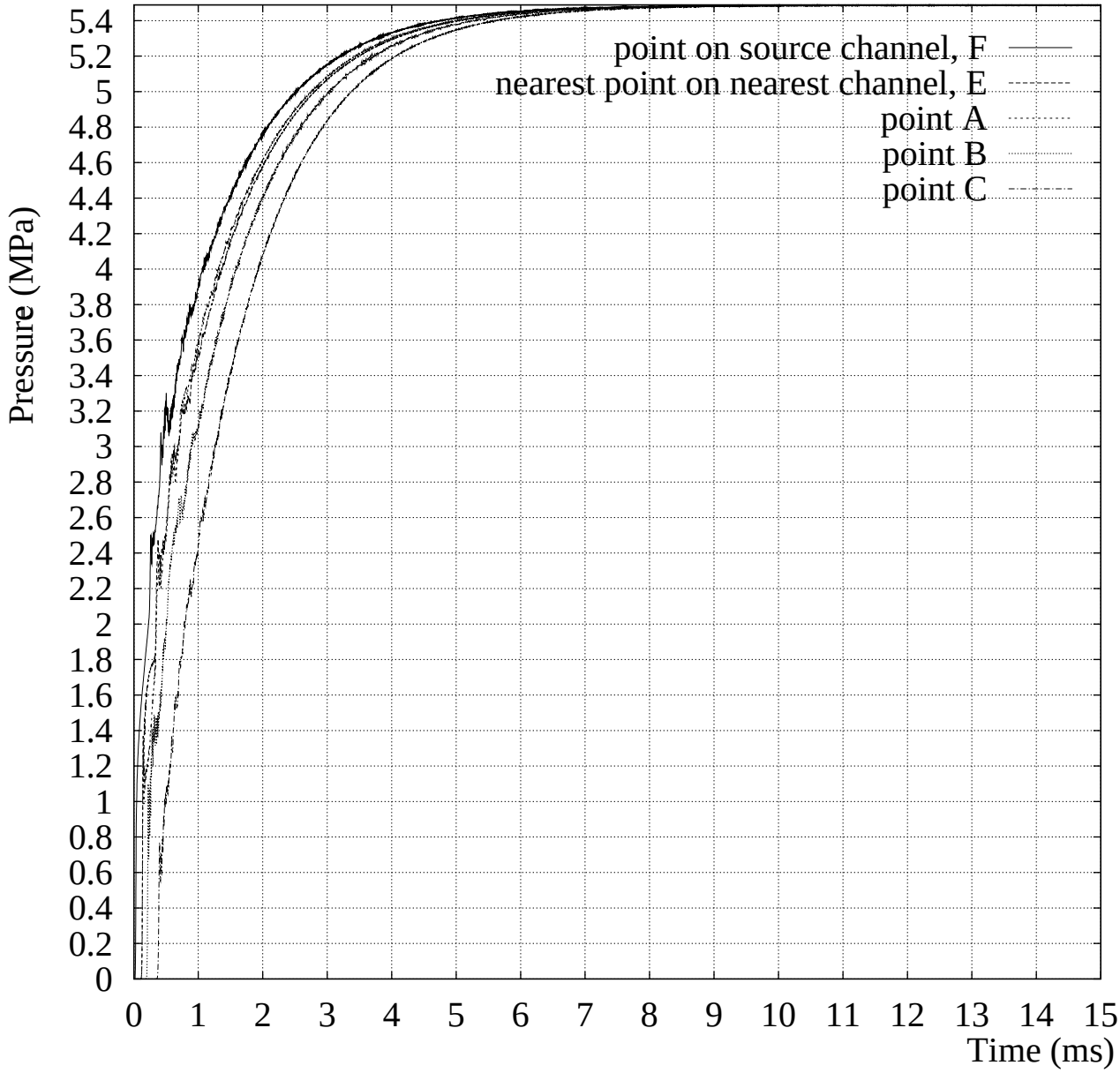

Figure 3.7: Pressure for domain in figure 3.6(a), hair line failure

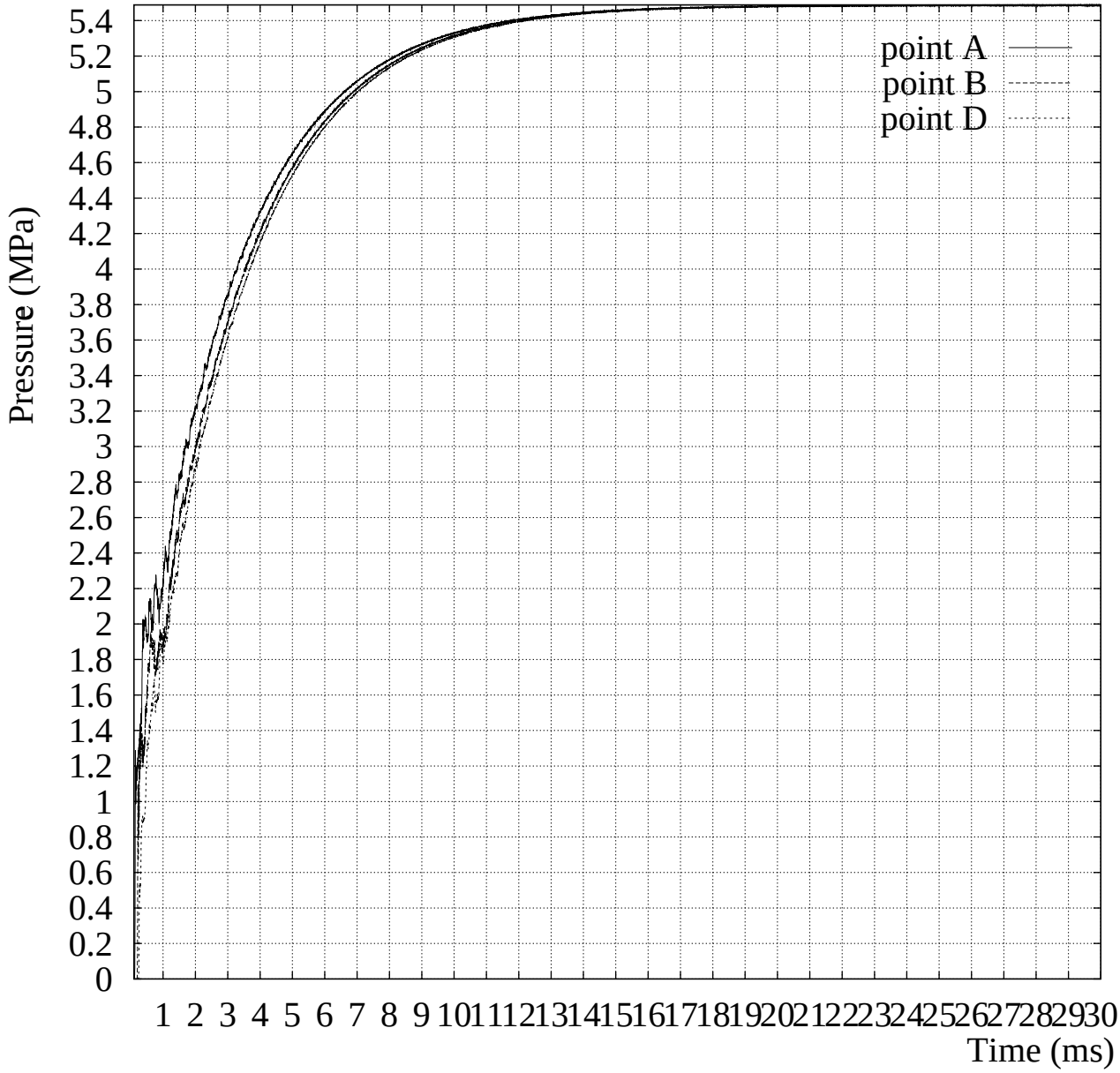

Figure 3.8: Pressure for domain in figure 3.6(b), hair line failure

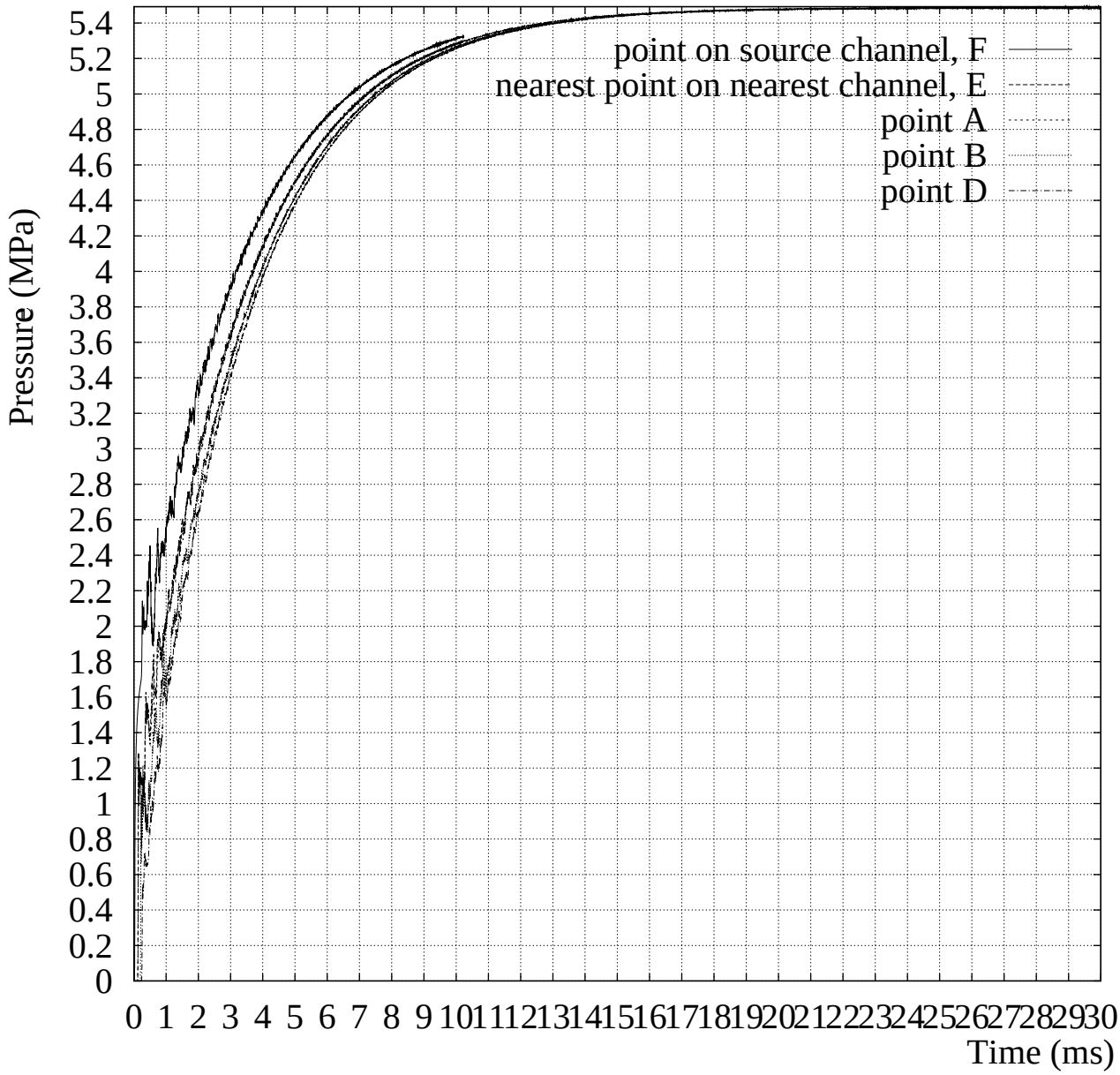

Figure 3.9: Pressure for domain in figure 3.6(c), hair line failure

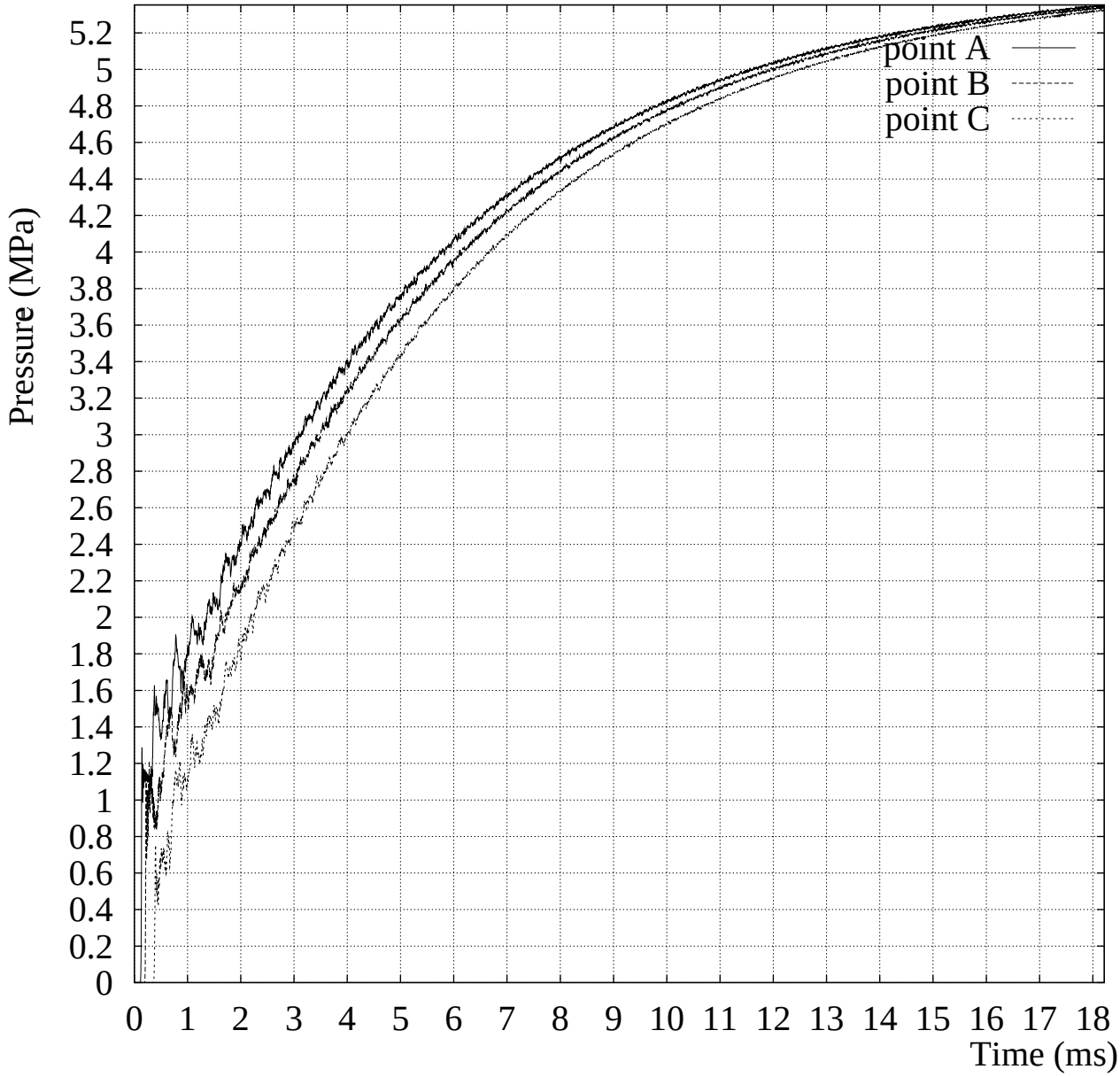

Figure 3.10: Pressure for domain in figure 3.6(d), hair line failure

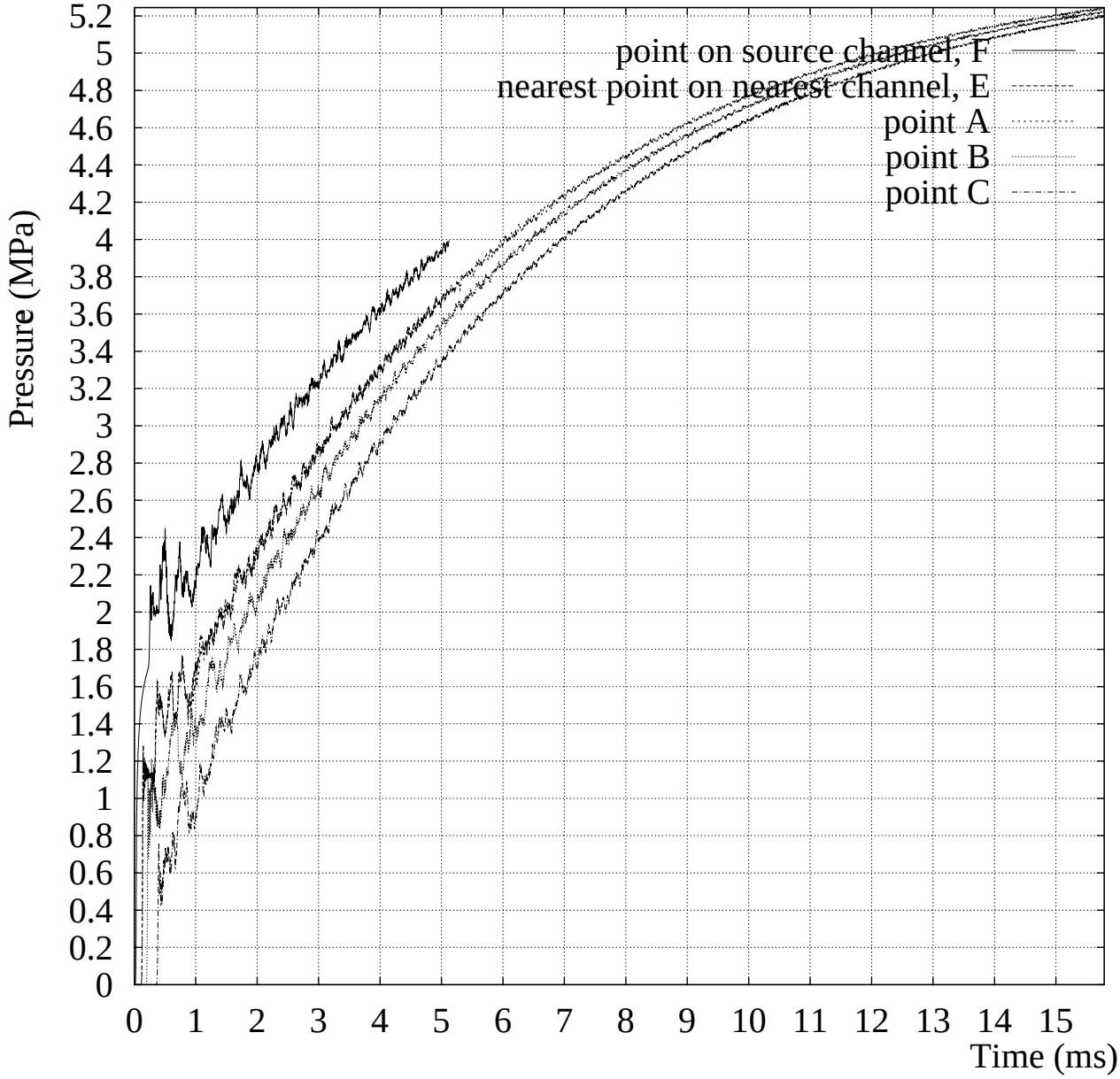

Figure 3.11: Pressure for domain in figure 3.6(e), hair line failure

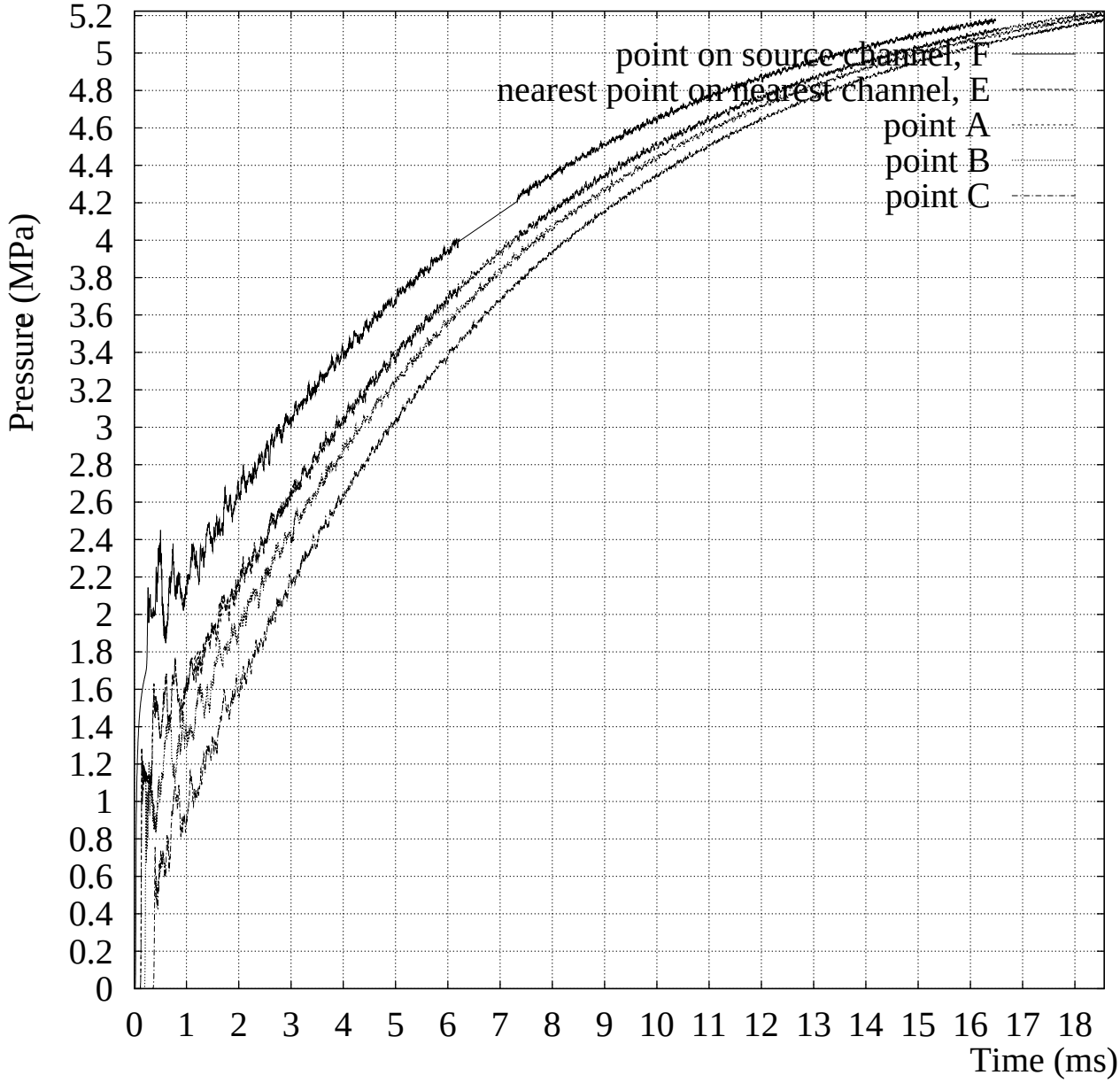

Figure 3.12: Pressure for domain in figure 3.6(f), hair line failure

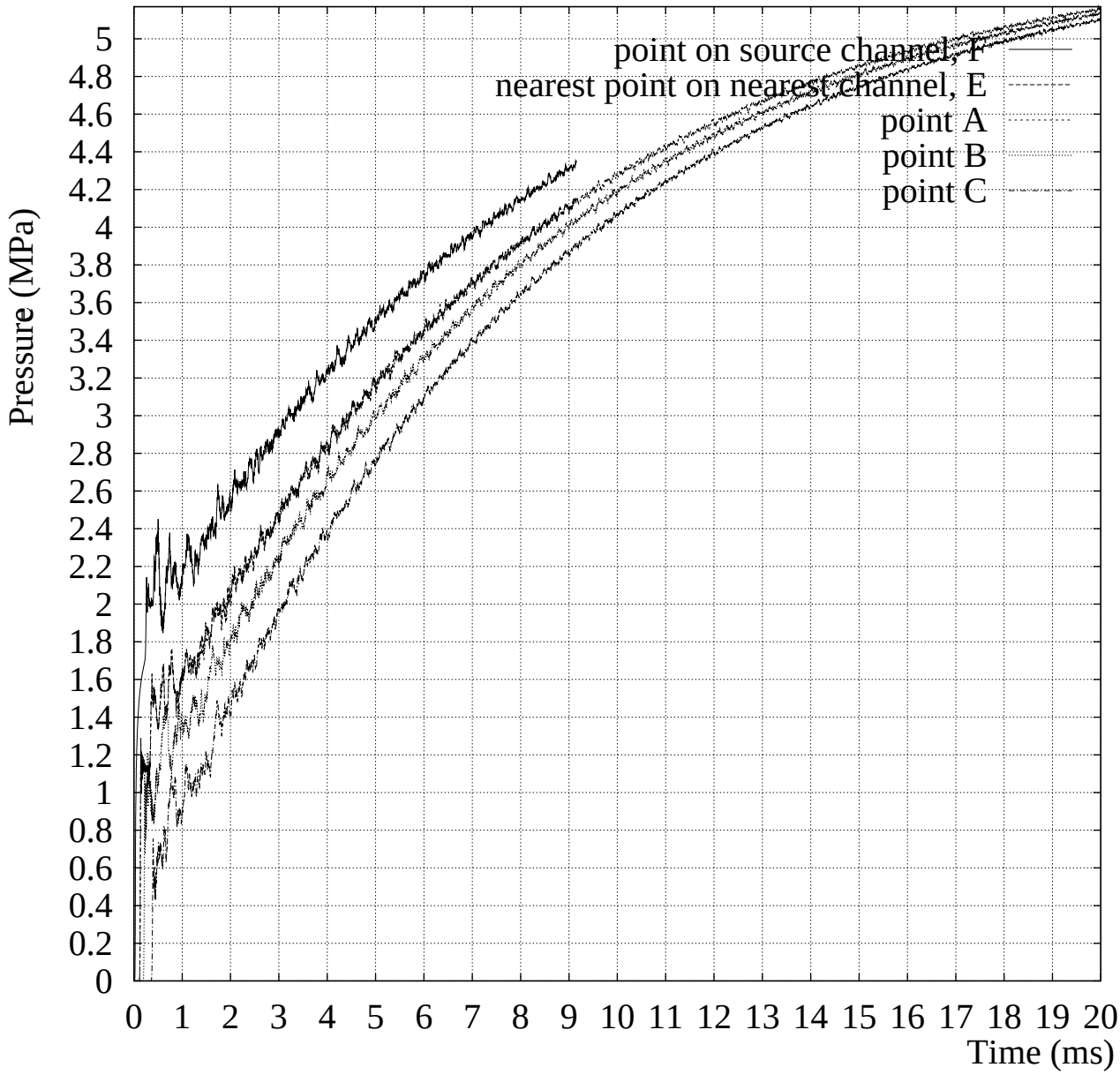

Figure 3.13: Pressure for domain in figure 3.6(g), hair line failure

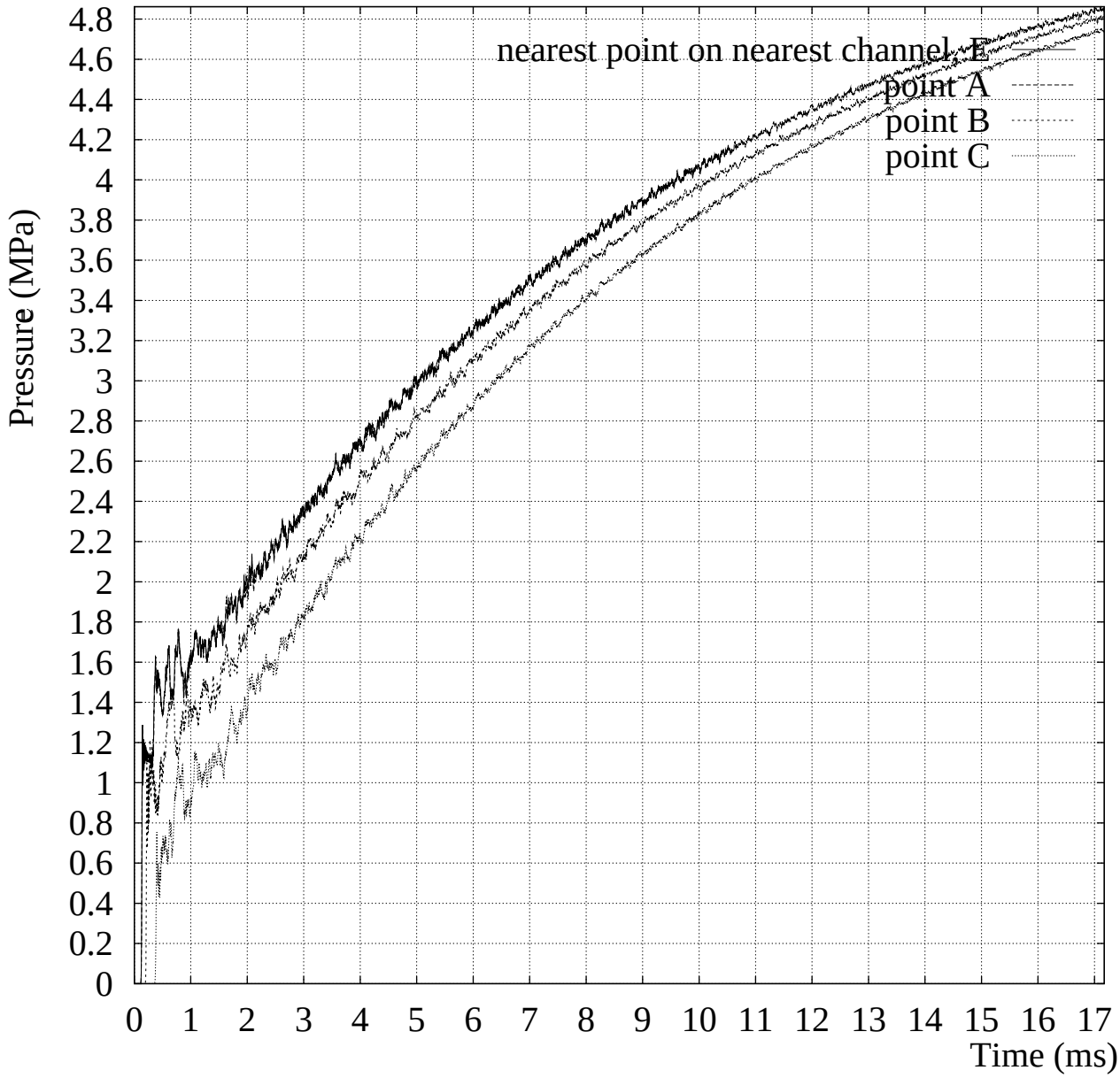

Figure 3.14: Pressure for domain in figure 3.6(h), hair line failure

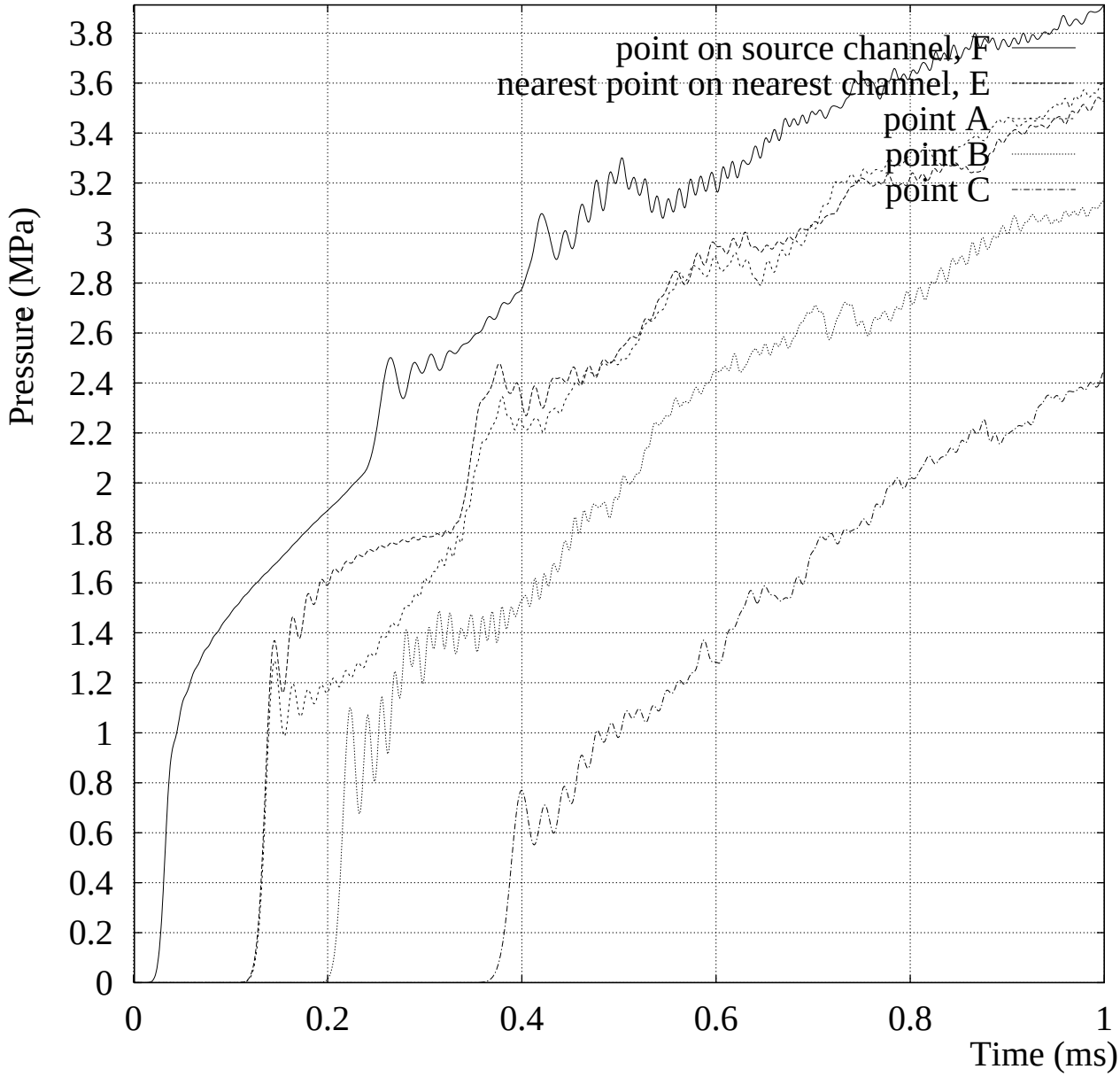

Figure 3.15: Early transition pressure for domain in figure 3.6(a), hair line failure

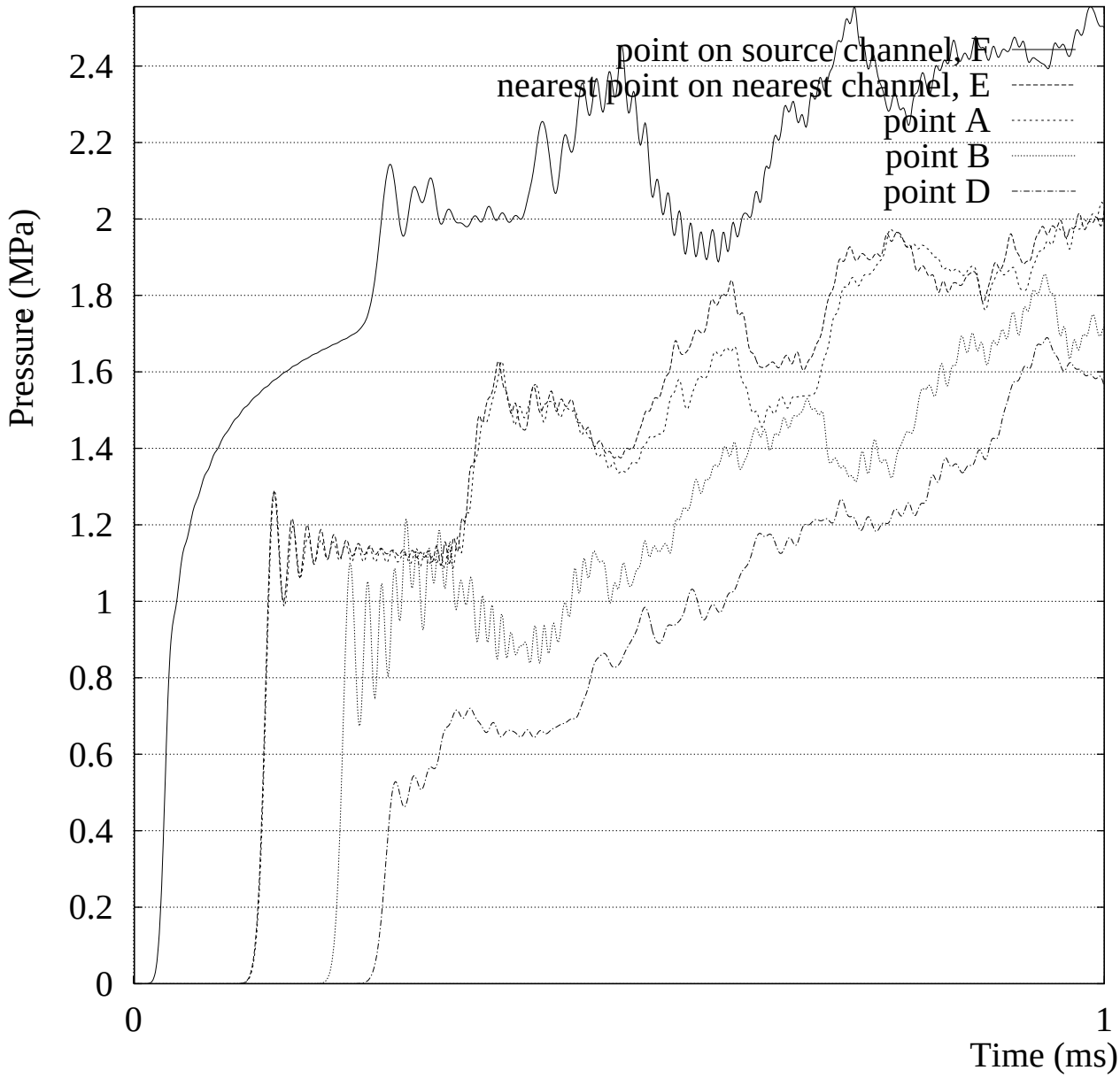

Figure 3.16: Early transition pressure for domain in figure 3.6(c), hair line failure

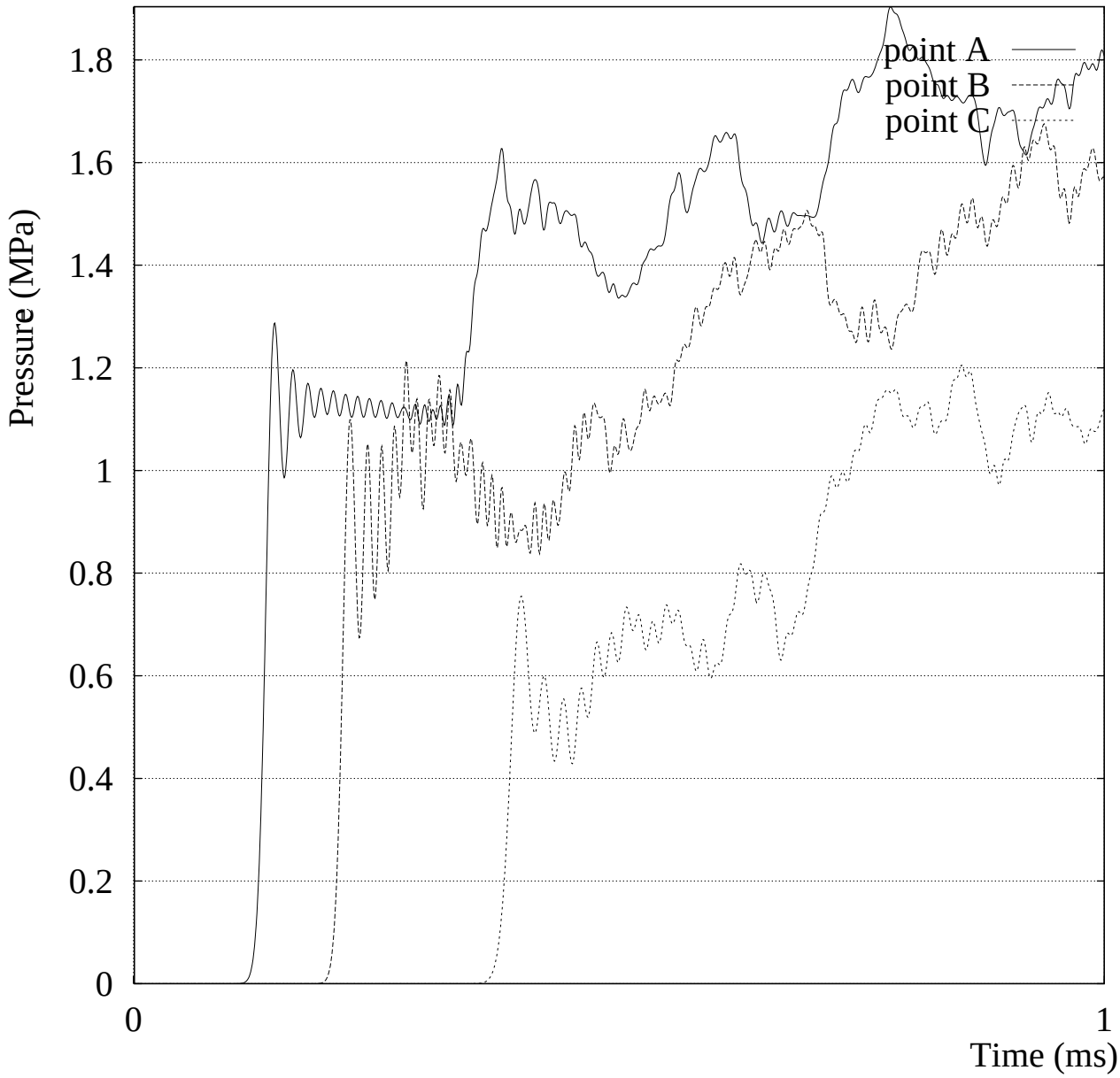

Figure 3.17: Early transition pressure for domain in figure 3.6(d), hair line failure

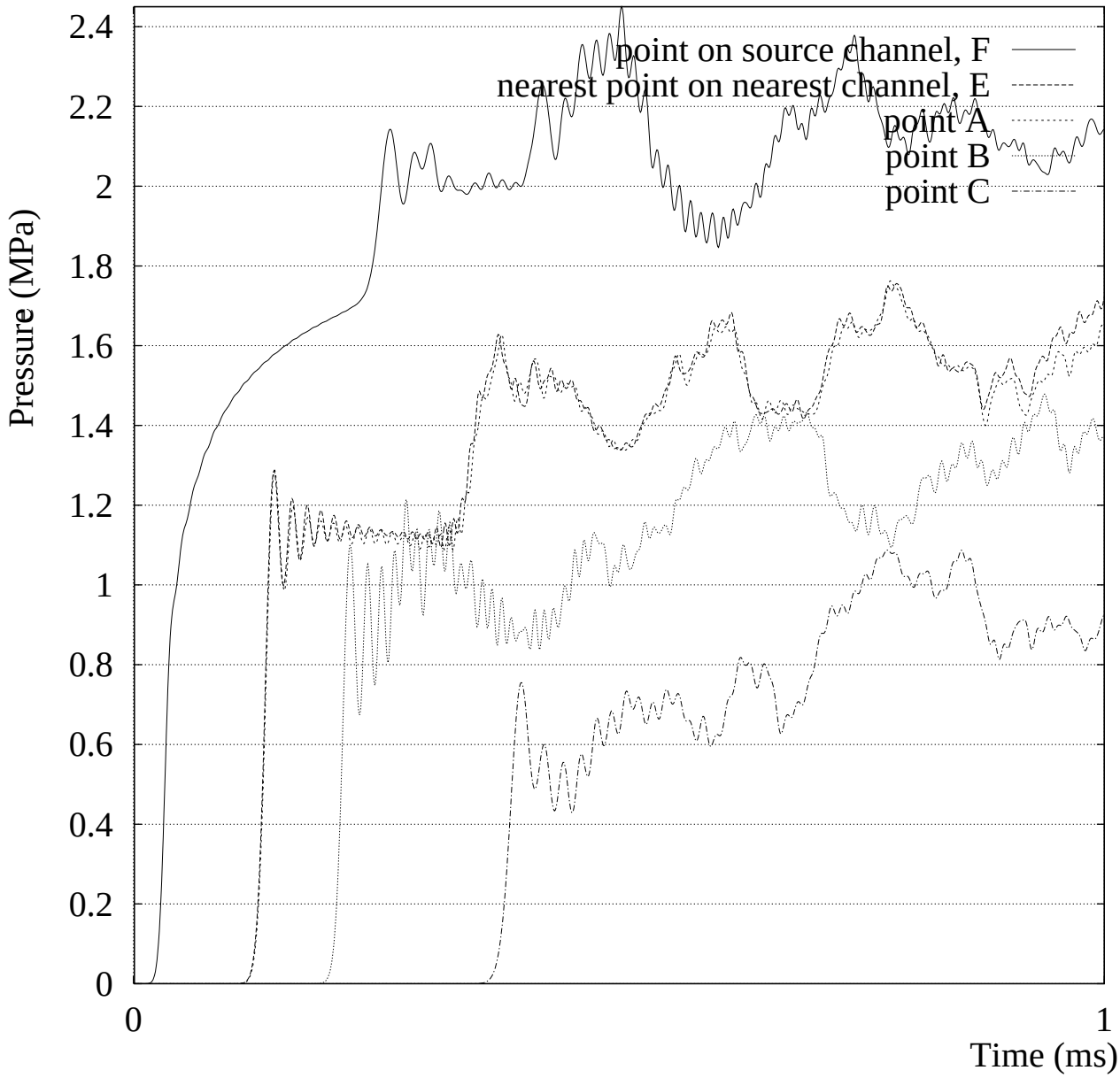

Figure 3.18: Early transition pressure for domain in figure 3.6(e), hair line failure

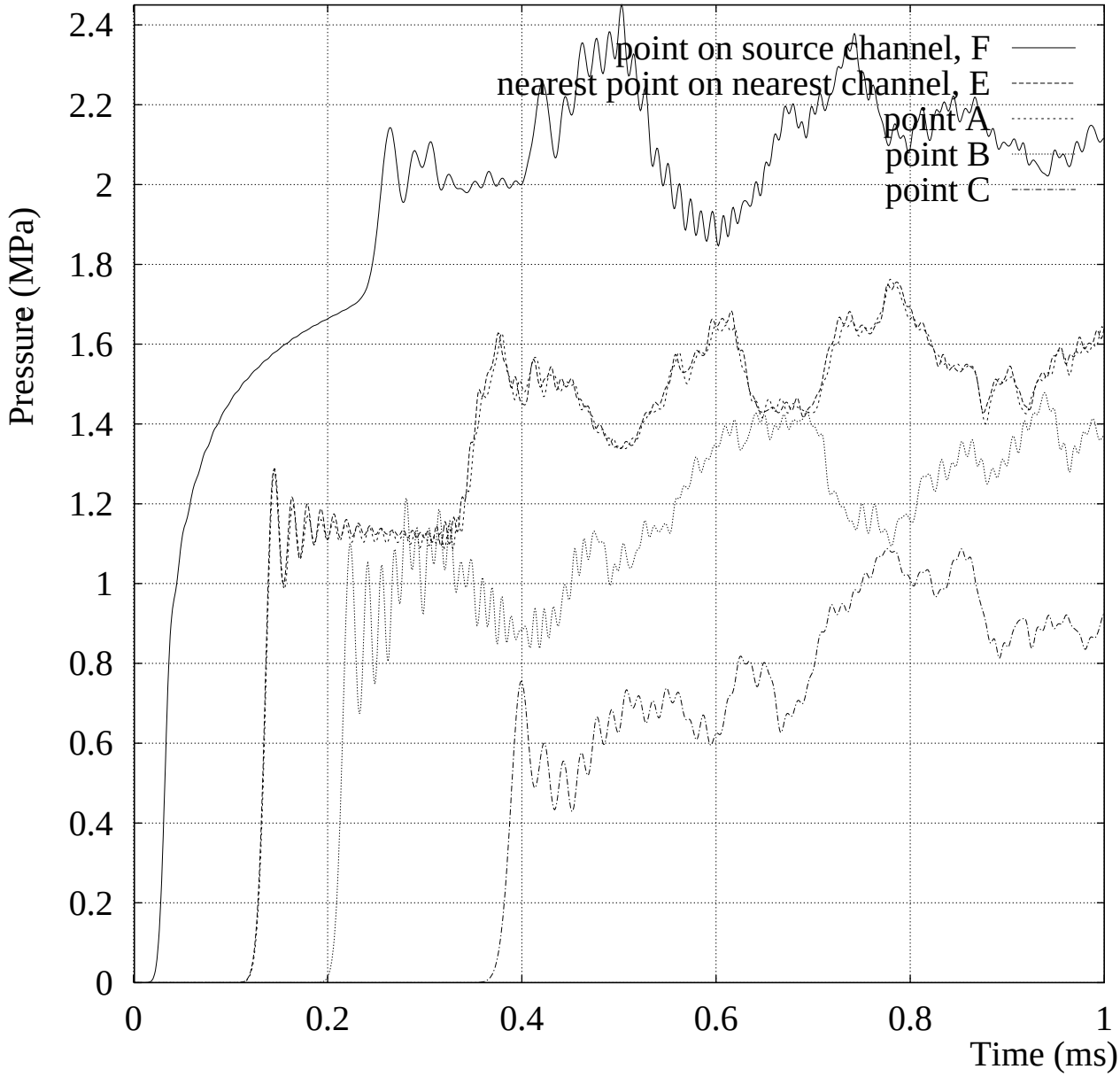

Figure 3.19: Early transition pressure for domain in figure 3.6(f), hair line failure

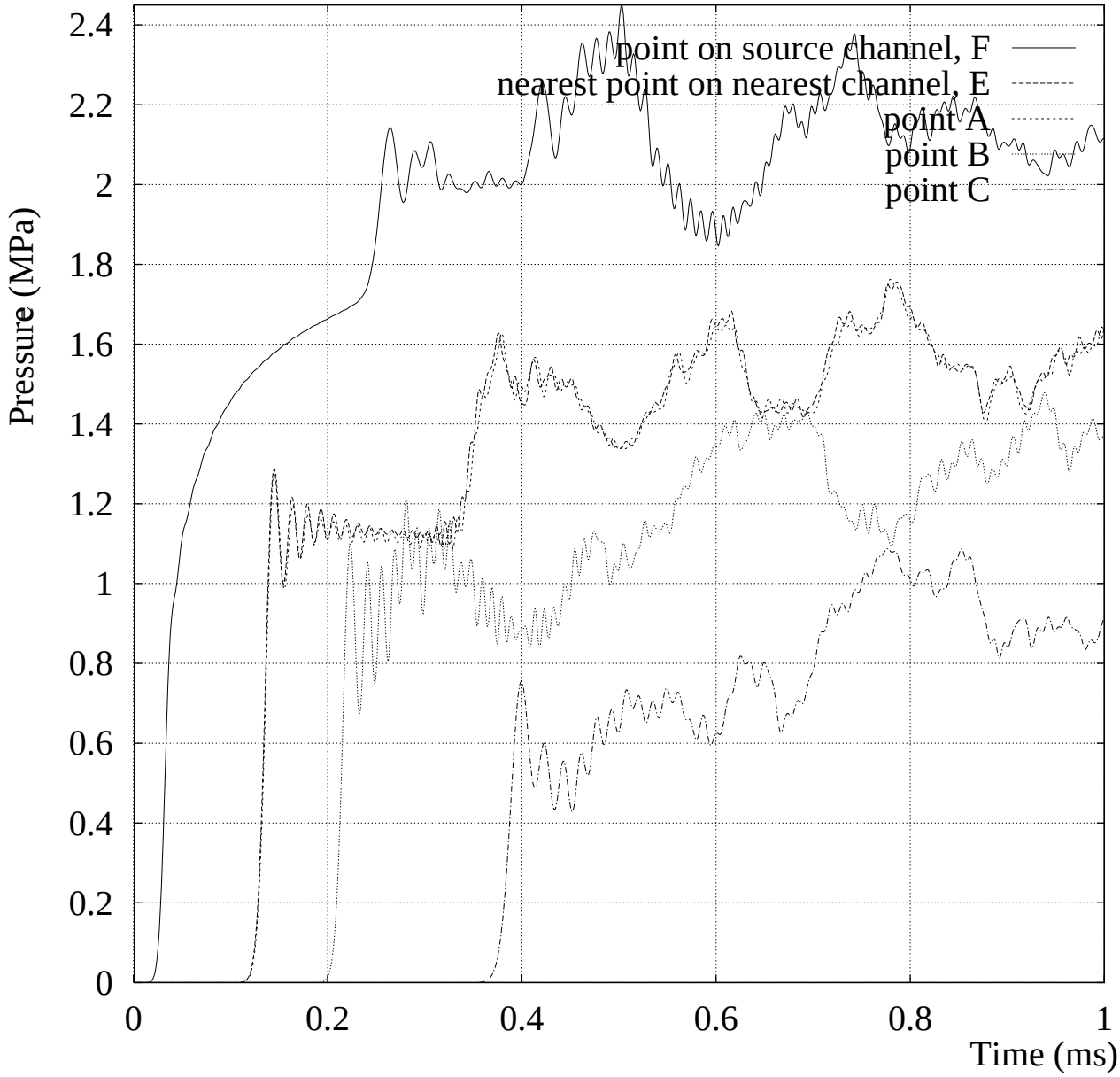

Figure 3.20: Early transition pressure for domain in figure 3.6(g), hair line failure

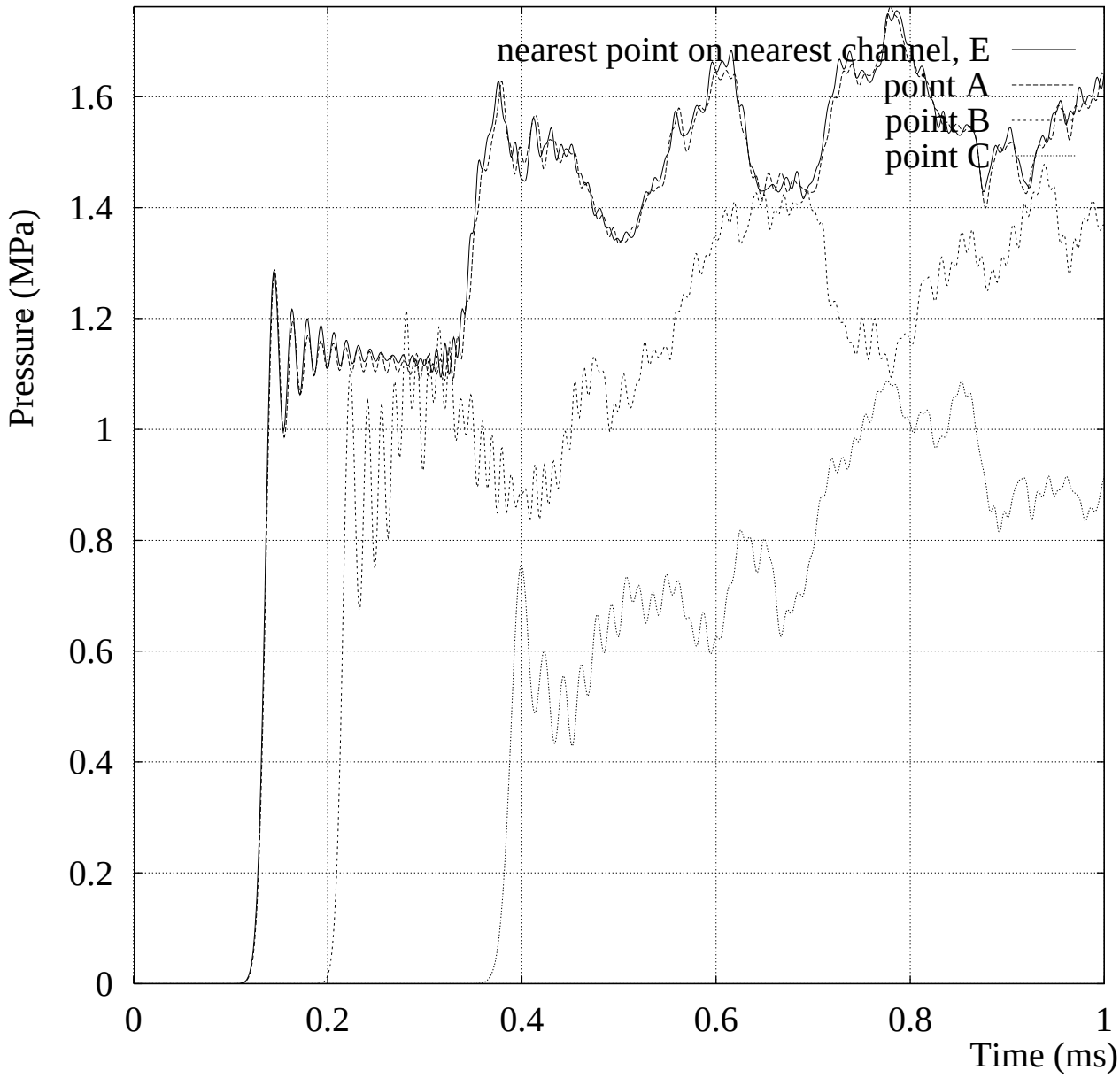

Figure 3.21: Early transition pressure for domain in figure 3.6(h), hair line failure

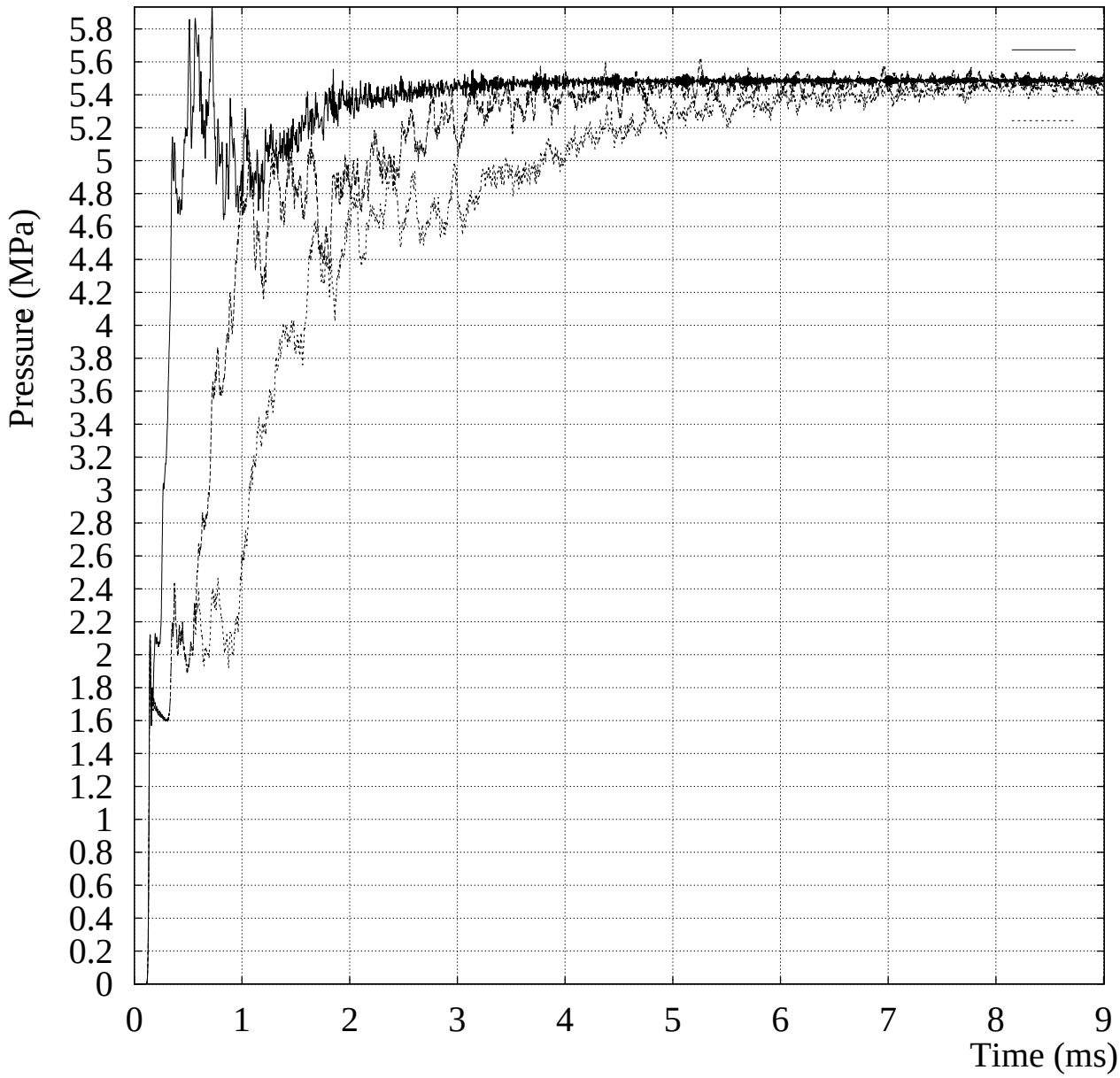

Figure 3.22: Pressure history at node A for domains in fig. 3.6(a,c and e): Fish mouth failure. The fish mouth is of size 29 degrees, and extends from 23 degrees to 52 degrees with respect to the x axis.

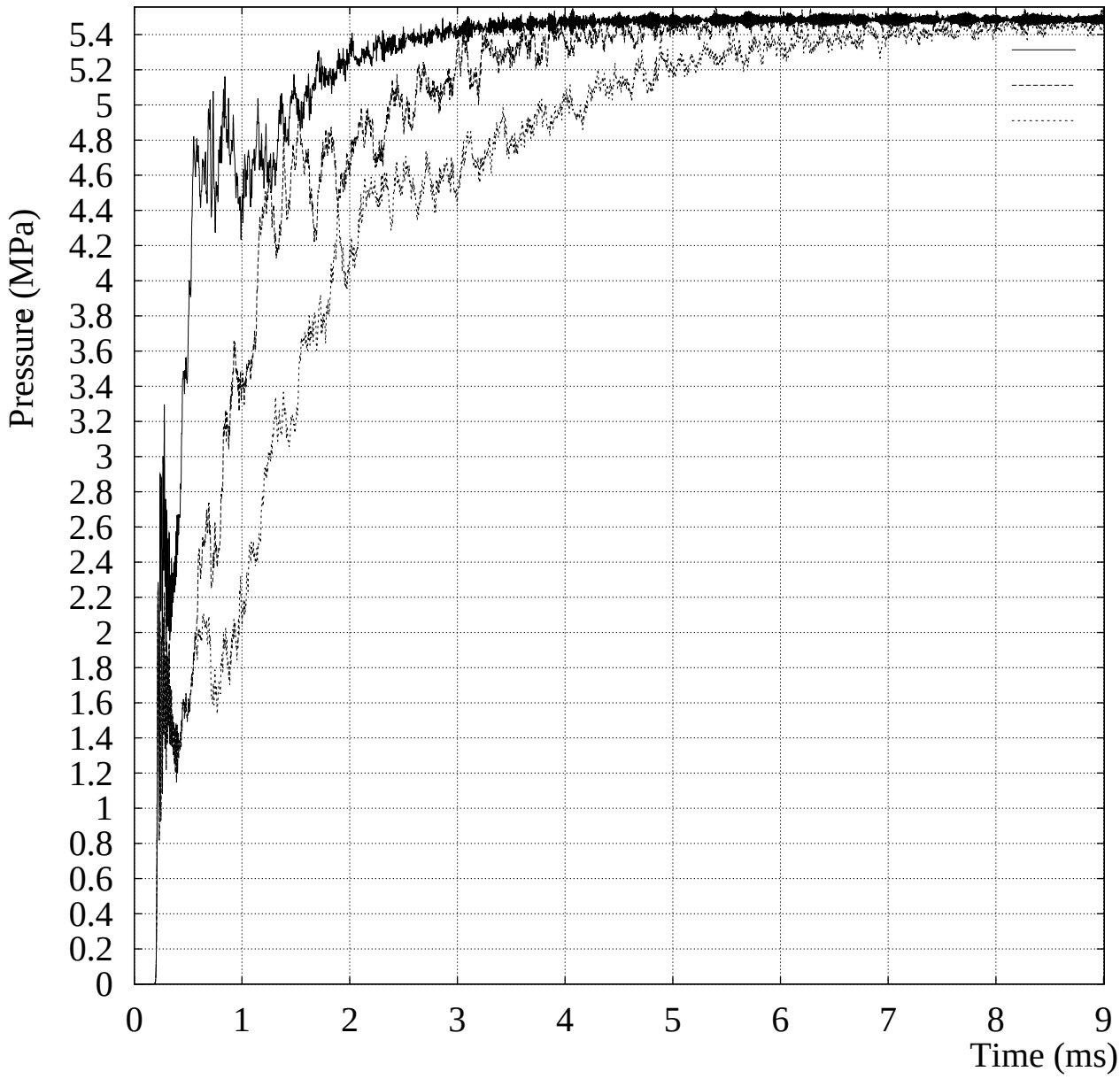

Figure 3.23: Pressure history at node B for domains in fig. 3.6(a,c and e): Fish mouth failure. The fish mouth is of size 29 degrees, and extends from 23 degrees to 52 degrees with respect to the x axis.

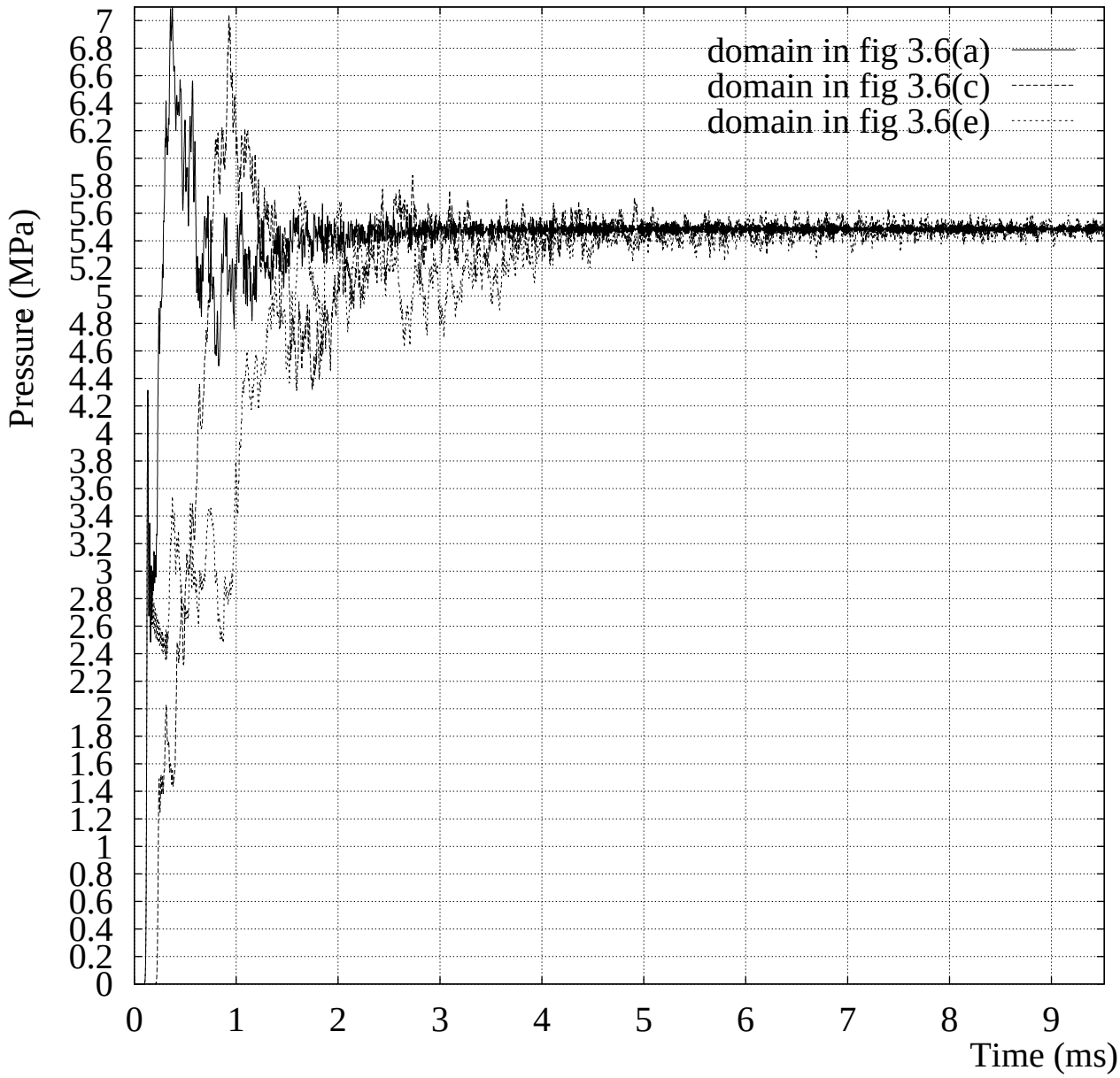

Figure 3.24: Pressure history at node A for domains in fig. 3.6(a,c and e): Fish mouth failure. The fish mouth is of size 60 degrees, and extends from 30 degrees to 90 degrees with respect to the x axis.

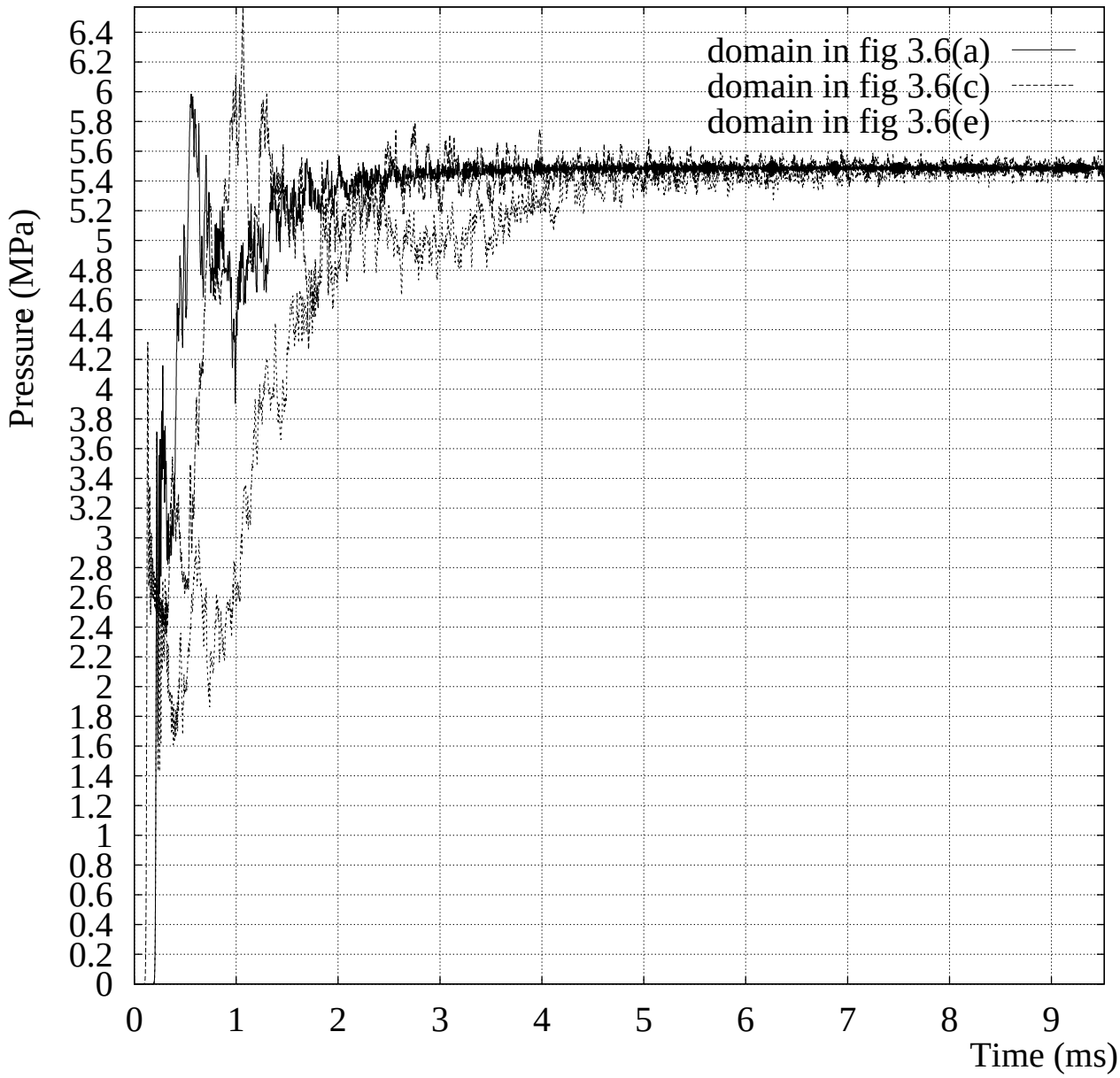

Figure 3.25: Pressure history at node B for domains in fig. 3.6(a,c and e): Fish mouth failure. The fish mouth is of size 60 degrees, and extends from 30 degrees to 90 degrees with respect to the x axis.

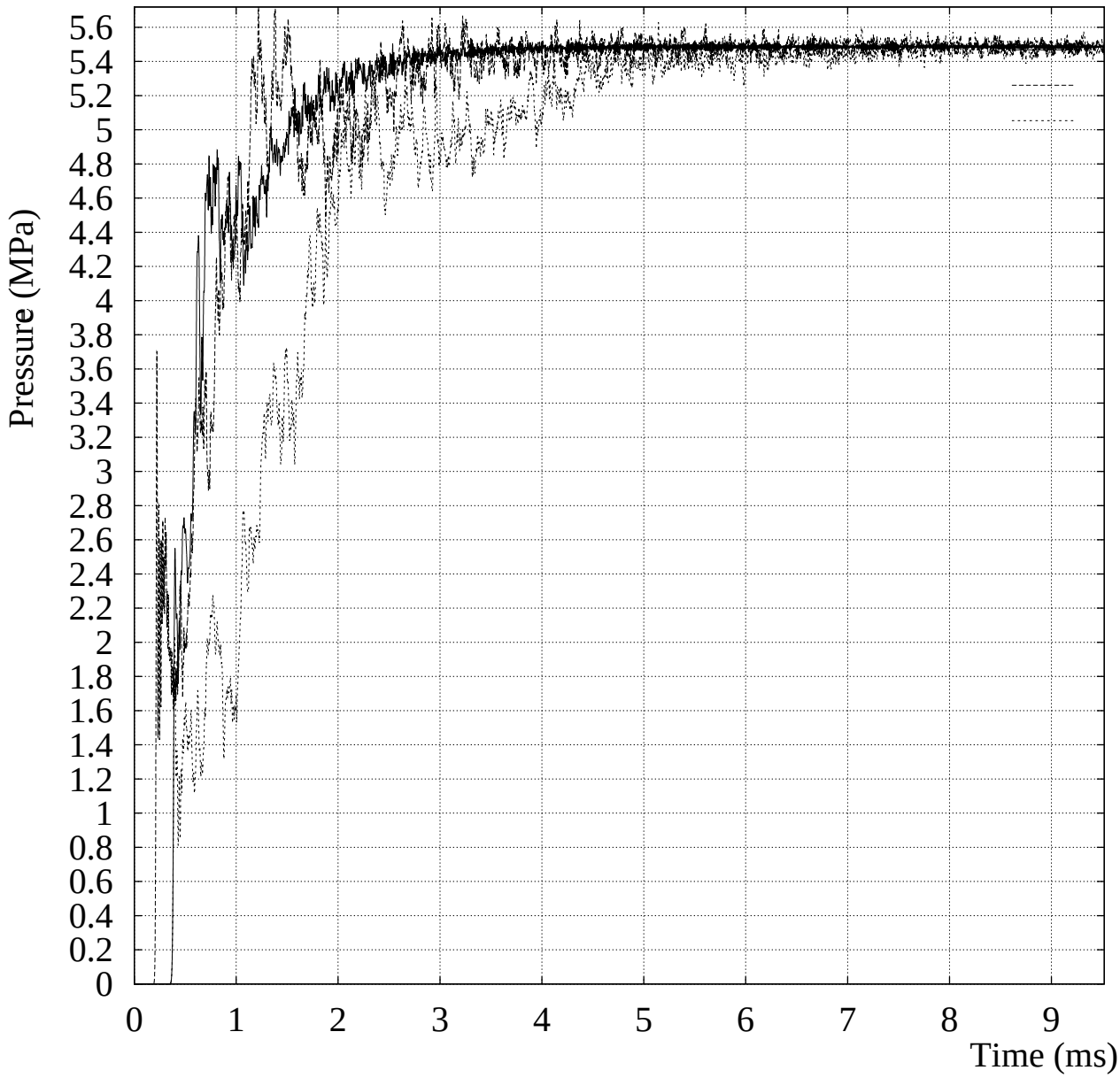

Figure 3.26: Pressure history at node C for domains in fig. 3.6(a,c and e): Fish mouth failure. The fish mouth is of size 60 degrees, and extends from 30 degrees to 90 degrees with respect to the x axis.

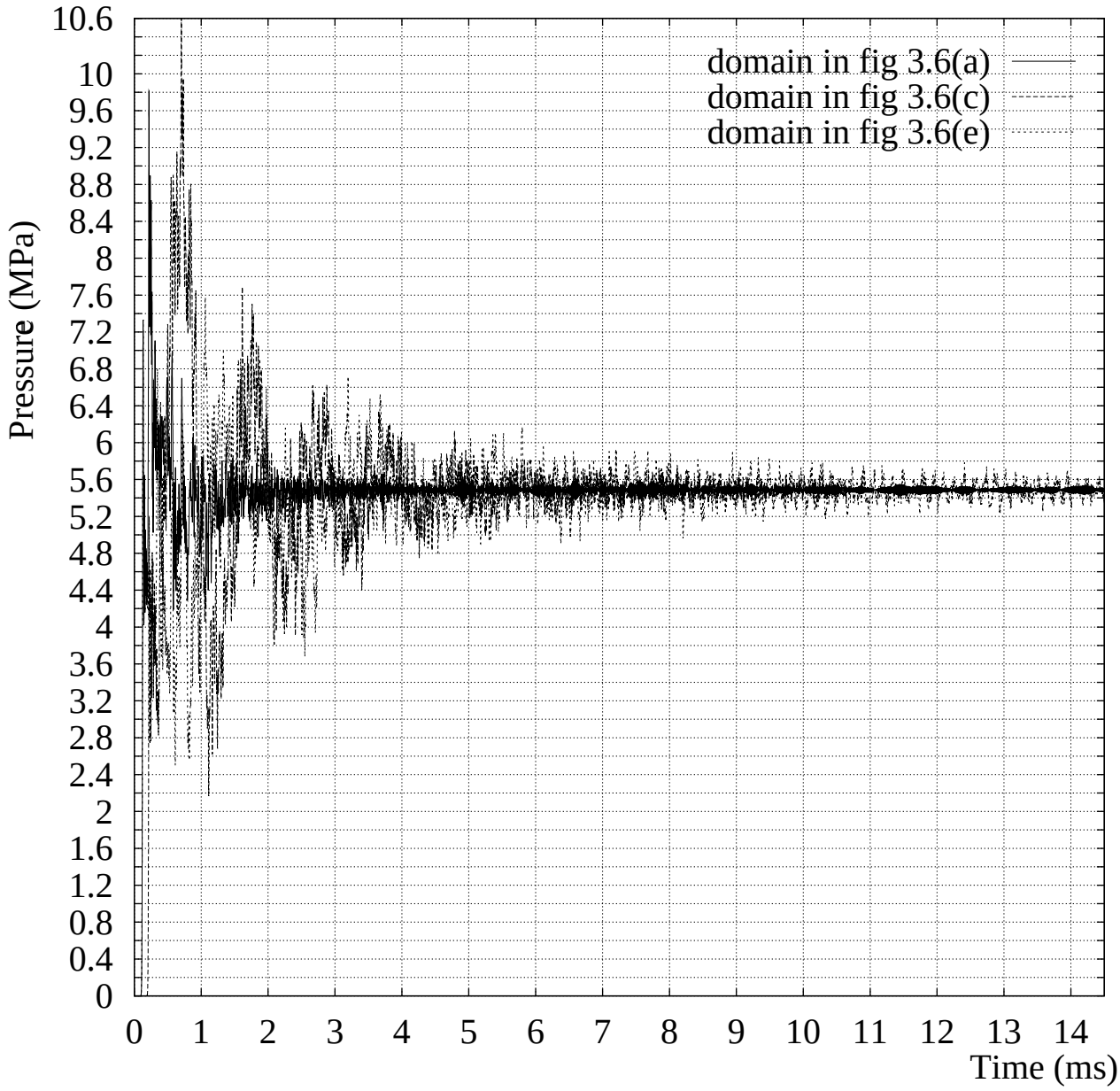

Figure 3.27: Pressure history at node A for domains in fig. 3.6(a,c and e): Complete circumferential break, i.e., a 'fish mouth' of size 360 degrees.

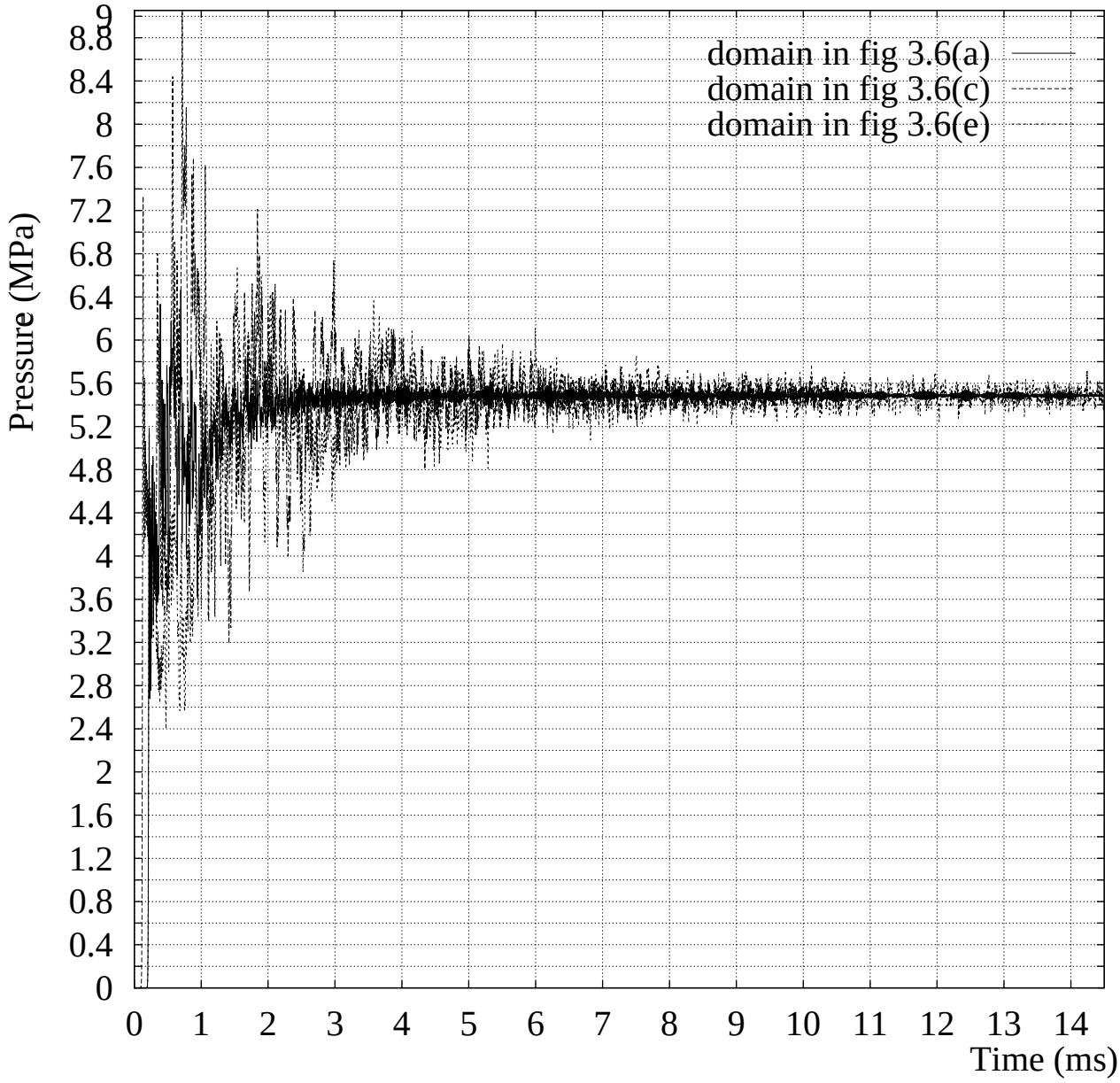

Figure 3.28: Pressure history at node B for domains in fig. 3.6(a,c and e): Complete circumferential break, i.e., a 'fish mouth' of size 360 degrees.

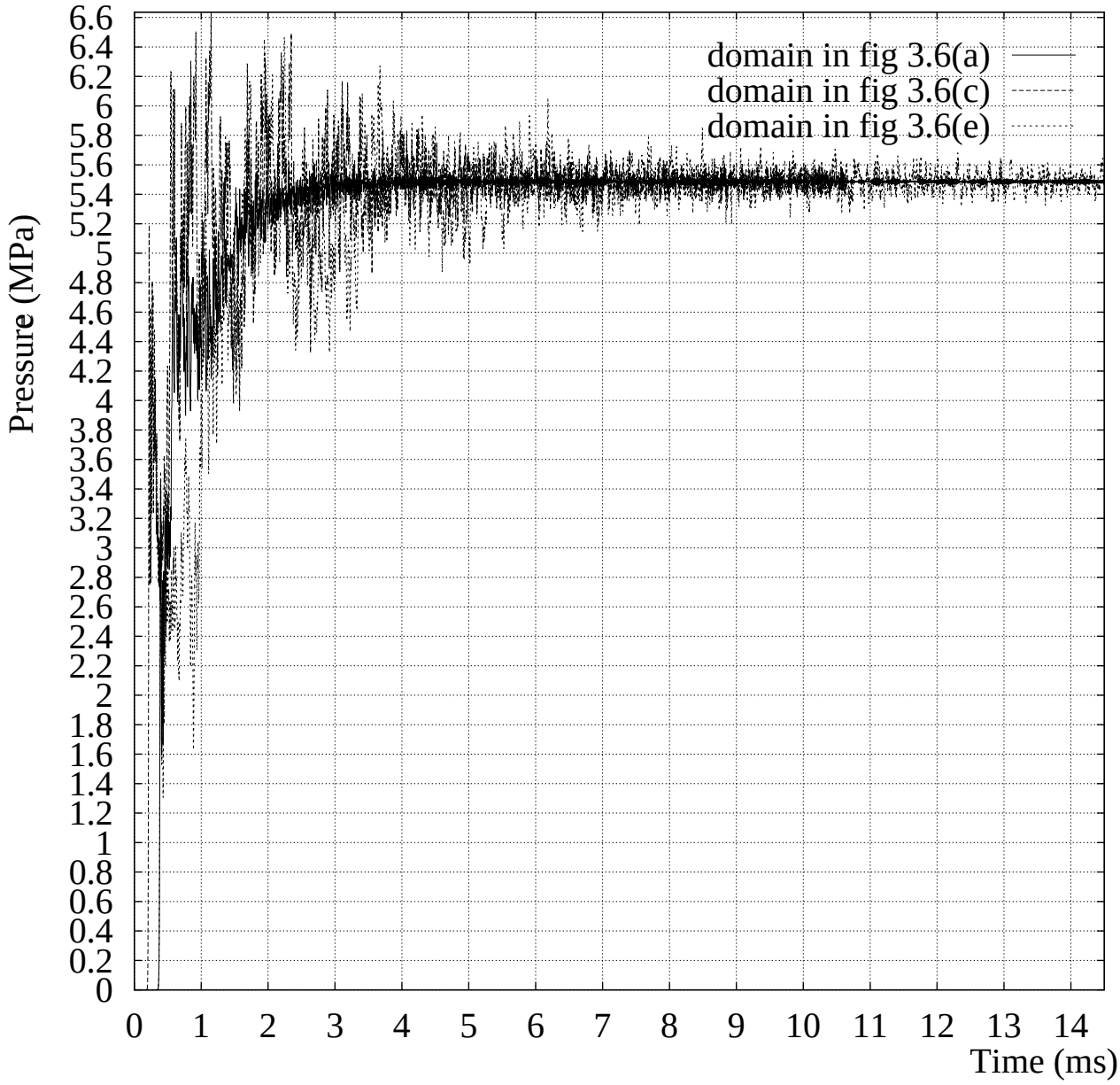

Figure 3.29: Pressure history at node C for domains in fig. 3.6(a,c and e): Complete circumferential break, i.e., a 'fish mouth' of size 360 degrees.

Chapter 4

New Two Parameters Non Reflecting Boundary Conditions for Compressible Navier Stokes Equations

In this part of the work, three *new* NRBC's for use with *compressible* Navier Stokes (NS) equations are presented. The proposed NRBC's are utilized in obtaining the steady state solution for a model problem of subsonic flow over a flat plate in an infinite uniform stream using a time marching approach. The domain is truncated to a finite region of computation, while maintaining the physics of the problem by applying the NRBC's at the boundary created at the outflow by the truncation process.

The aim of this work is to study the performance of the new NRBC's, where one measure of performance is the number of steps required for convergence. In contrast to the work carried out for the PHWR, where NRBC's were applied to relatively simpler wave equation, equations (as well as the boundary conditions) handled here are non linear. In the previous chapter, the geometry handled was complex, here it is simple. This, however, does not imply that one can not use the procedure when *both* the equations and the geometry are complex– this situation is not taken up in this report mainly to restrict the scope of study. Thus, the versatility of the procedure of using NRBC's for computational purposes is demonstrated.

4.1 Introduction

A general theory of boundary conditions (b.c.) for the full NS equations (that is, the effect of compressibility is included), with the boundaries ranging from rigid wall to an open boundary, is incomplete. The form and the number of the b.c.'s that are required

for a numerical solution depend on (a) the g.d.e.'s themselves, as well as (b) on the way they have been discretized. Mathematical results of well posedness analyses of various simplified and approximated situations are scattered in literature (for example, Oliger and Sundström [1978]); this and physically reasonable intuition can be used as a guide to proceed in such studies.

As a typical situation, the problem of uniform flow over an unbounded flat plate in two space dimensions as shown in figure 4.1 is considered. The domain is truncated so that an *inflow*, an *outflow* and an *upper* boundary are introduced in addition to the *no-slip* (wall) boundary of the unbounded flat plate at the bottom. Steady state solution is obtained on this rectangular spatial domain numerically, for which use is made of the time marching technique of MacCormack [1969].

Following general remarks can be made regarding the boundary conditions applicable to this problem.

1. As compared to the Euler equations of gas dynamics (inviscid compressible flow), the number of b.c.'s at inflow and outflow boundaries for the full NS equations (viscous and compressible flow) is larger.

2. The additional b.c.'s required for the full NS equations should be first order derivative conditions, where the derivative is taken in the flow direction. Otherwise, non physical boundary layers may result. In the case of Euler equations (zero viscosity), appropriate modifications in these conditions have to be introduced.

4.1.1 Time dependent two dimensional compressible NS equations

Subsonic flow in two dimensions is assumed, with x, y, and t denoting the two space and the time coordinates. The equations in the dimensionless conservative form are:

$$\frac{\partial U}{\partial t} + \frac{\partial F}{\partial x} + \frac{\partial G}{\partial y} = 0 \tag{4.1}$$

where,

$$U = [\rho \quad \rho u \quad \rho v \quad E]^T \tag{4.2}$$

are the (non dimensional) conserved quantities per unit volume, and,

$$F = \begin{bmatrix} \rho u \\ \rho u^2 + p - \tau_{xx} \\ \rho uv - \tau_{xy} \\ (E + p - \tau_{xx})u - \tau_{yx}v - \frac{\gamma}{Pr}\frac{k}{Re}\frac{\partial T}{\partial y} \end{bmatrix}, \tag{4.3}$$

$$G = \begin{bmatrix} \rho v \\ \rho uv - \tau_{yx} \\ \rho v^2 + p - \tau_{yy} \\ (E + p - \tau_{yy})v - \tau_{xy}u - \frac{\gamma}{Pr}\frac{k}{Re}\frac{\partial T}{\partial y} \end{bmatrix}, \tag{4.4}$$

are the flux vectors.

A non polar, Newtonian fluid is assumed. The constitutive equations for such a fluid are:

$$\tau_{xx} = \frac{\mu}{Re}(\frac{4}{3}\frac{\partial u}{\partial x} - \frac{2}{3}\frac{\partial v}{\partial y}) \tag{4.5}$$

$$\tau_{yy} = \frac{\mu}{Re}(\frac{4}{3}\frac{\partial v}{\partial y} - \frac{2}{3}\frac{\partial u}{\partial x}) \tag{4.6}$$

$$\tau_{xy} = \frac{\mu}{Re}(\frac{\partial u}{\partial x} + \frac{\partial v}{\partial y}) \tag{4.7}$$

In the above, u and v are the x and y components of the flow velocity, p is the pressure, ρ is the density and T the temperature of the fluid. E is the specific total energy, $\mu = \mu(T)$ is the coefficient of viscosity which depends on the temperature T of the fluid, k is the coefficient of heat conductivity, $\gamma = c_p/c_v$ where c_p and c_v are the specific heats at constant pressure and volume respectively, Pr is the Prandtl number and Re the Reynolds number.

It is further assumed that the fluid is a non reacting perfect gas, in this case, air. Therefore the equation of state (e.o.s.) is

$$\frac{p}{\rho} = (\gamma - 1)T \tag{4.8}$$

Viscosity is related to temperature by the Sutherland law. For air at $T = 288.2K$ $\mu = 1.789X10^{-5}\ kg/(ms)$, thus one gets

$$\mu = 2.5576426\ \ X\ 10^{-7}\ T^{0.75} \tag{4.9}$$

where μ is in $kg/(ms)$ and T is in Kelvin.

Non dimensionalization has been carried out using the following reference quantities:

$u_{ref} = u_\infty,\ L_{ref} = 1\ m,\ T_{ref} = u_\infty^2/c_v,\ \mu_{ref} = \mu(T_{ref}),\ \rho_{ref} = \rho_\infty,\ p_{ref} = \rho_\infty u_\infty^2,$

where the subscript ∞ denotes the free stream quantities.

4.1.2 Inflow b.c.'s for full NS equations

The system of partial differential equations (p.d.e.) for the full NS equations requires three b.c.'s at the subsonic inflow boundary. Direct specification of the physical variables themselves seems to be the most reasonable set of conditions for a wide range of problems, especially for a body placed in a free stream. Thus, u, v and either of ρ or T can be specified. Well posedness study for this set of b.c.'s has been carried out for the *linearized* system of equations obtained from the full NS equations by Oliger and Sundström [1978].

Requirements for the numerical solution:

However, while solving numerically, an additional fourth b.c. is required, too. Chu and Sereny [1974] have studied this aspect of inflow b.c.'s for time dependent, inviscid, compressible gas dynamics equations in one space dimension. Zeroth order extrapolation of the characteristic variable (Riemann invariant) for the linearized system of equations can be applied at the inflow boundary for obtaining numerical solutions. Symbolically, this is

$$\Delta p - \rho c \Delta u = 0 \tag{4.10}$$

where c the speed of sound in the fluid. This b.c. can be used to calculate p at the inflow boundary, then the unspecified variable can be determined using the e.o.s. of the fluid. For more references on such extrapolation boundary conditions for discretized equations, section 2.4.6 may be referred to.

4.1.3 Outflow b.c.'s for full NS equations

The system of p.d.e.'s at a *subsonic* outflow boundary requires one b.c. It seems reasonable to assume that sufficiently far away downstream, static pressure p_∞ is the one known physical quantity. This is so in many physical situations, for example, flow through a nozzle, flow over an aerofoil, etc. When computing, for instance, the steady state solution numerically in such a case, it must be remembered that the flow is subsonic. Hence any disturbances in the flow can be transmitted upstream, unlike the situation that arises in the case of supersonic flow. The above b.c. naively applied is physically equivalent to introducing such a disturbance in the flow. The non physical disturbances arising from reflections at the outflow boundary will be transmitted upstream. Transient calculations with such a b.c. on the truncated domain can be quite wrong. For a time marching procedure for calculating a steady state solution, undue delay in convergence is the least one is likely to encounter.

NRBC for the outflow boundary

The right approach would then be that p at the outflow should not be assumed equal to p_∞ itself, but calculated using an NRBC for pressure for the given p_∞.

In section 2.3.4, a review of the work on NRBC's for fluid flow problems, including that for compressible Navier Stokes equations has been provided. A few general remarks will be in order, and will put the work reported in this chapter in perspective. For problems in this class, analytical techniques for devising and checking well posedness generally are applied to the governing system of equations only after linearizing the equations. Examples of inviscid, compressible (Euler) equations of gas dynamics, and of compressible viscous flow (compressible Navier Stokes equations) are available in literature. NRBC's have been used for solving the time dependent equations, as well as for obtaining a steady state solution. In the latter case, the efficacy of the NRBC can be measured by the reduction in the number of iterations required to compute the steady state solution.

In section 2.2.7, the work of Bayliss and Turkel [1982] to extend their ideas for the scalar wave equation has already been mentioned. Bayliss and Turkel [1982]

consider *linearized* Euler equations of gas dynamics. They have also used NRBC's for obtaining steady state solutions to these equations using a time marching technique.

Hagstrom and Hariharan [1988] have obtained an NRBC for the nonlinear Euler equations for a spherically symmetrical spatial domain by using an asymptotic solution of the far field equations.

Hedstrom [1979] considered a class of nonlinear hyperbolic systems in one space dimension. He obtained an NRBC which performs well for transonic flow (no strong outgoing shocks). The boundary condition is equivalent to:

$$\frac{\partial p}{\partial t} - \rho c \frac{\partial u}{\partial t} = 0 \tag{4.11}$$

This b.c. requires no *a priori* knowledge of the steady state values of the variables at the outflow, in particular, p, which is the one data required at the subsonic outflow boundary for a well posed problem. Hence a steady state solution calculated with their use is *dependent on the initial data.* In particular, if the steady state value of the variable at the outflow is prescribed in the problem formulation, as it is in the examples mentioned at the beginning of this section (section 4.1.3), this NRBC is not suitable for use in a time marching solution to steady state.

Rudy and Strikwerda [1980, 1981], starting from the NRBC developed by Hedstrom [1979] (equation 4.11), formulated another one which includes a *free parameter.* It can be considered a generalization of the Hedstrom NRBC given in equation 4.11. Rudy and Strikwerda NRBC is of the form:

$$\frac{\partial p}{\partial t} - \rho c \frac{\partial u}{\partial t} + \alpha(p - p_\infty) = 0 \tag{4.12}$$

where the single parameter α is determined by trial and error to suit the situation, namely, whether one intends to use this b.c. to obtain the transient solution or to calculate the steady state solution.

Use of NRBC's of this form is indicated for subsonic flow which requires the specification of a boundary condition at the outflow (which in many cases is the specification of pressure), and is especially useful in computing the steady state solution by a time marching technique. The term containing the free parameter α ensures that the

complete data specified for a compressible Navier Stokes flow field (for the transonic regime) is made use of. Hence, independent of the initial data, the steady state value of outflow pressure is guaranteed to be equal to the specified steady state value of p_∞. This can be seen as follows. At steady state, the terms containing partial derivatives with respect to time in equation 4.12 can be dropped, the result thus obtained is $p = p_\infty$ (on the outflow boundary where this NRBC is applied), $\alpha \neq 0$.

Rudy and Strtikwerda [1981] apply this NRBC to compute the steady state solution for a flat plate placed in a uniform stream by means of time marching, and provide data on the convergence speed and pressure fluctuations near the boundary. They do this for various boundary conditions, including the NRBC of equation 4.12 for different values of α, applied at the downstream subsonic outflow boundary. An analysis is provided in Rudy and Strikwerda [1980] for the optimum value of the free parameter for the *linearized* set of governing equations, where the optimum is defined in terms of the time (iterations) required to reach the steady state. The optimum value based on the linear analysis and that obtained from numerical experimentation are quite different, as can be seen from the results provided in Rudy and Strikwerda [1981]. Rudy and Strikwerda [1981] have suggested $\alpha = 0^+$ for transient calculations and $\alpha \in (0.3, 0.4)$ for steady state calculations. Note that the governing equations form a *nonlinear* system, but the NRBC is *linear*.

Requirements for the numerical solution:

The numerical method requires three b.c.'s in addition to the above. Zeroth order extrapolation, for example $\partial u/\partial x = 0$, has been used in literature for u and v and either of ρ or T. Equation of state can be used to calculate the remaining of ρ or T. References on extrapolation boundary conditions for discretized equations have been presented in section 2.4.6.

4.2 Numerical Scheme

The explicit (second order) time marching MacCormak scheme (MacCormak [1969]) is used to calculate steady state flow properties. It can be used to calculate transient

solution also if the exact initial conditions are known. For steady state calculations it is similar to iterative search for the solution. The advantage of the scheme for steady state calculations is that subsonic (elliptic) and supersonic (hyperbolic) regions of the flow need not be known *a priori* and do not require different treatments. Shocks appear as regions of steep gradient in the solution. In presence of shocks in the flow, an artificial viscosity term may be introduced when solving for the inviscid Euler equations (von Neumann and Richtmyer [1950]); for the NS equations this is not required. For the model problem of flow over a flat plate that is solved here, the complication of mixed hyperbolic and elliptic regions of flow over space does not arise, but the same mathematical model (p.d.e. and the b.c.'s) and the numerical scheme can be applied to more complicated geometries like an aerofoil without any change.

The algorithm is briefly described below:

do at every time step (until convergence)

- calculate $U^{previous}$ corresponding to the values of the primitive variables at previous time step.
- calculate F and G (equations 4.1 to 4.9)
- *Predictor step*:
  1. $[\partial U/\partial t]^{predictor} = -\partial F/\partial x - \partial G/\partial y$, from the g.d.e.
  2. $U^{predictor} = U^{previous} + \Delta t[\partial U/\partial t]^{predictor}$, where Δt satisfies the stability criteria
  3. Boundary conditions can be applied here, but since this is the predictor step, we may avoid unnecessary calculations
- *Corrector step*:
  1. Calculate $F^{corrector}$ and $G^{corrector}$ based on $U^{predictor}$ (equations 4.1 to 4.9)
  2. $[\partial U/\partial t]^{corrector} = [-\partial F/\partial x - \partial G/\partial y]^{corrector}$

3. $2[\partial U/\partial t]^{average} = \partial U/\partial t]^{predictor} + \partial U/\partial t]^{corrector}$ where $\partial U/\partial t]^{average}$ is second order accurate
4. $U^{current} = U^{previous} + \Delta t[\partial U/\partial t]^{average}$, where Δt satisfies the stability criteria

- Apply boundary conditions.
- Find primitive variables.

enddo.

Steady state was achieved when the following convergence criteria was satisfied

$$\left|\phi_{i,j}^{n+1} - \phi_{i,j}^{n}\right| \leq \epsilon \tag{4.13}$$

where the subscripts i and j are grid indices in the x and y directions respectively, while the superscript denotes the time step. ϕ denotes each of the dependent variables, (u, v, ρ, T). ϵ was chosen equal to 10^{-6}. Convergence was checked only after every fiftieth time step. The code that was developed has the capability of imposing a convergence criteria on the g.d.e., itself, too.

4.3 Computational domain

The computational domain is shown in figure 4.1. The horizontal flat plate divides the two dimensional space into two semi infinite halves, of interest is the upper half. The computational domain is formed by *truncating* this two dimensional semi infinite spatial domain into a finite rectangular region of interest. The corners of the computational domain are at $(0,0), (2,0), (2,1), (0,1)$. The flat plate extends upstream in the flow beyond the computational domain: the leading edge (LE) with respect to the computational domain is shown in figure 4.1. A fully developed laminar flow enters the computational domain at the Inflow Boundary on the left. At any point downstream the flow profile is expected to exhibit a similar fully developed nature.

The grid consists of uniform increments in the x-direction, while the grid in the y-direction is stretched using a simple transformation given by

$$y = \frac{\beta + 1 - (\beta - 1)\exp(\lambda(1 - y_c))}{1 + \exp(\lambda(1 - y_c))} \tag{4.14}$$

In the above, β is the stretching coefficient. y is the vertical coordinate in the physical plane, and y_c in the transformed plane in which the computations were carried out. β must be chosen to place a sufficiently large number of grid points in the boundary layer region near the wall, the recommended value is in the range $1.02 \leq \beta \leq 1.06$.

Calculations were carried out for free stream Mach numbers $M_\infty = 0.8$. The Reynolds number based on the reference quantities was $1.535\ X\ 10^5$. The temperature in the flow field was 21.283^oC (530 R) and the total pressure was 143.638 Pa (3 psf).

4.4 Boundary conditions for the computational domain

We will use the nomenclature 'wall boundary' for the lower boundary, 'inflow boundary' for the boundary introduced on the left (that is, in the upstream direction), 'subsonic outflow boundary' or simply 'outflow boundary' for the boundary introduced on the right (the downstream direction), and 'upper boundary' for the boundary introduced on the top, as shown in figure 4.1. The use of the word 'introduced' in the above sentence implies that we have truncated the fluid domain to limit ourselves to a computational domain of interest.

4.4.1 Wall boundary

At the wall ($y = y_c = 0$), the no slip b.c. applies: $u = v = 0$, $T = T_\infty$. Since it is a rigid wall, $\partial p/\partial y = 0$ is applicable, and density ρ can be calculated from the e.o.s. for the fluid.

4.4.2 Upper boundary

At the upper boundary, v is expected to have a small positive value and u is more or less equal to the free stream value u_∞; that is, the flow crosses this boundary outwards, though the value of the velocity perpendicular to boundary is much lower than would

be obtained at the right boundary. Thus this boundary is a subsonic outflow boundary, and theory (4.1.3) demands that some quantity must be specified on this boundary. However, zeroth order extrapolation of all the four dependent variables works better than specifying either of p, T, or v as can be seen from the results of Rudy and Strikwerda [1981]. The reason proposed is the small value of velocity v with which the fluid crosses this boundary, while most of the fluid flows tangentially to the boundary with $u \approx u_\infty$. The results reported in the following sections also tally with these comments. This happens inspite of the fact that such a zeroth order extrapolation is not well posed mathematically for the *linearized* set of equations.

Note that if one chooses to specify, say, v, on this boundary, one way of doing so is by using the results of the perturbation theory of *incompressible* flow over a flat plate (van Dyke [1964]); for obtaining the values of v in the free stream portion of the flow an outer expansion for v can be applied. The assumption of incompressibility in the free stream can be justified on the grounds that the density is nearly constant in this region of the flow which lies outside the boundary layer.

However, whatever approach one decides upon, one needs to be very sure that the upper boundary chosen lies in the free stream. In the work presented here, zeroth order extrapolation at this boundary has been used. For the geometry described, the upper boundary is located approximately 10 boundary layer thicknesses above the wall. For choice of this boundary too near the wall with zeroth order extrapolation applied to it the accuracy of the solution suffers, for any set of boundary conditions applied to the inflow (left) and outflow (right) boundaries.

4.4.3 Subsonic inflow boundary

At the inflow boundary, we specify the values of $u_{1,j}^{n+1}$, $v_{1,j}^{n+1}$, $\rho_{1,j}^{n+1}$.

Temperature is calculated from

$$T_{1,j}^{n+1} = p_{1,j}^{n+1}/[(\gamma - 1)\rho_{1,j}^{n+1}], \tag{4.15}$$

where the pressure is found by extrapolating the outgoing characteristic variable for the *linearized* system as described in section 4.1.2, i.e.:

$$p_{1,j}^{n+1} = p_{2,j}^{n+1} - \rho_{1,j}^{n+1} c_{1,j}^{n} (u_{2,j}^{n+1} - u_{1,j}^{n+1}) \tag{4.16}$$

Note that $c_{1,j}$ is calculated at the time step n, not $n+1$. The other options for the inflow boundary can be:

1. Specification of T instead of ρ in the above. Hence ρ is found from the e.o.s., and p from equation 4.16.

2. Specification of u, v and T with zeroth order extrapolation for ρ, $\rho_{1,j}^{n+1} = \rho_{2,j}^{n+1}$, and equation 4.16 for p.

3. Specification of u, v and ρ with zeroth order extrapolation for T, $T_{1,j}^{n+1} = T_{2,j}^{n+1}$, and equation 4.16 for p.

4. Overspecification, that is specification of u, v, ρ and T, with equation 4.16 for p.

The inflow profiles for u, v, and ρ (or T) need to be obtained. If a boundary layer code is available, it can be used to specify these inflow profiles, as has been done by Rudy and Strikwerda [1981]. For the *free stream portion* of the inflow profile, v can then be calculated using the perturbation theory of incompressible flow (van Dyke [1964]). The outer expansion of v is given by

$$\begin{aligned} v &= \frac{\beta_1}{\sqrt{2Re}} \mathbf{R}\left(\frac{1}{\sqrt{s+iy}}\right) + O\left(\frac{1}{Re}\right) \\ &\approx \frac{\beta_1}{\sqrt{2Re\ s}}\left(1 - \frac{3y^2}{8s^2}\right) \end{aligned} \tag{4.17}$$

where $\mathbf{R}$ denotes the real part of a complex quantity, $i = \sqrt{-1}$, $\beta_1 \approx 1.22$, and s is the x distance from the leading edge of the plate. In the geometry under consideration (figure 4.1), $s = 1$. Hence, if v_{edge}, the value of v at the edge of the boundary layer is available (say, from a boundary layer code), v in the *free stream* portion of the inflow can be approximated by

$$v = v_{edge}\left(1 - \frac{3}{8}y^2\right) \tag{4.18}$$

In the free stream ρ is nearly constant, hence the the incompressiblity assumption in the above equations is a good approximation.

Another option is to choose the inflow boundary far away from the leading edge, so that we can assume a uniform stream at the inflow.

For the situation considered in the test problem, the option used is different from the above two. The *exponential* u-velocity inflow profile shown in figure 4.2, which is an approximation to the boundary layer profile for u, has been used. It is given by

$$u = 1 - e^{-60y} \tag{4.19}$$

Its use is justified in the following paragraph.

Effect of approximate inflow data on the solution

Since the inflow data, equation 4.19, is inaccurate by a small amount compared to the use of values from a good boundary layer code, it is expected to affect the accuracy of the solution downstream. In view of this we can use either equation 4.18 for v at the inflow, or even a constant value of $v = 0$. Similarly, $\rho = \rho_\infty$ can be specified at the inflow, and either equation 4.15 or simply $T = T_\infty$ can be used for calculating T. The aim in this report being the study of the effect of the new NRBC's proposed below for the subsonic outflow boundary, with respect to their *ability to suppress spurious reflections and thus achieve quick convergence to steady state*, the use of approximate inflow data as a model is justified.

4.4.4 Outflow boundary: new two parameter NRBC's

At the subsonic outflow boundary, the set of governing partial differential equations requires one boundary condition (Oliger and Sundstrom [1978]). Three additional b.c.'s are required for the application of the numerical method. We assume that the physical quantity known at the outflow boundary at steady state is the static *pressure*. As already discussed, when introducing a truncation boundary to delimit the computational domain, one has to be careful about the choice of the boundary condition to be imposed on the *subsonic* outflow boundary. A wrong choice here will result in waves being reflected upstream, which will spoil the solution in the computational domain, and delay the convergence to steady state. Because of this reason, applying $p = p_\infty$ directly at the outflow may not be the best solution. Instead, we need a NRBC that

has the property of adjusting the outflow pressure in time so as to damp the waves trapped in the computational domain.

Rudy and Strikwerda [1981] have proposed the *linear, one parameter* boundary condition given by equation 4.12 to be applied at a subsonic outflow boundary to suppress the spurious reflection of pressure when attempting a time marching computational solution for the problem under consideration.

In this work, *new* NRBC's which can be considered generalizations of Rudy and Strikwerda NRBC are proposed. They are then studied with respect to their performance in calculating a steady state solution to the flat plate problem. The key term in the equation 4.12 which guarantees that at steady state the outflow pressure reaches the desired value of p_∞ is $(p - p_\infty)$. We manipulate this term so as to obtain a series of boundary conditions that have the similar property of guaranteeing $p = p_\infty$ at steady state, while adjusting the outflow pressure in time so as to damp the waves trapped in the computational domain, thus helping achieve a fast convergence to steady state.

4.4.5 Simple two parameter NRBC

The first NRBC proposed is:

$$\frac{\partial p}{\partial t} - \rho c \frac{\partial u}{\partial t} + \alpha \mid p - p_\infty \mid^z = 0 \tag{4.20}$$

which, in addition to the single parameter α of the Rudy and Strikwerda NRBC (equation 4.12), has a second parameter z, which can also be manipulated to achieve a different (hopefully, faster) rate of convergence to steady state.

This formulation can also be used to verify if the NRBC proposed by Rudy and Strikwerda (equation 4.12) is optimal. As the results presented later in this chapter show, equation 4.12 is not optimal. An analytical proof of this has not been attempted.

The following constraint on the values of the parameter z can be straightaway specified:

$$z > 0 \tag{4.21}$$

Also,

$$\alpha \neq 0 \tag{4.22}$$

Note that, under the condition of steady state, the first two terms involving the time derivative drop out and the above condition implies $p = p_\infty$ at the outflow boundary. If we allow z to take negative values, then dropping the time derivative terms will result in:

$$\frac{1}{(\mid p - p_\infty \mid)^{\mid z \mid}} = 0, \ (z < 0) \tag{4.23}$$

i.e., $p \to \infty$, which is a recipe for instability.

The reason for taking the absolute value before raising the term $(p - p_\infty)$ to z can be explained by considering fractional values of z, for example, $z = 1/2$. Since we are not interested in imaginary values of $(p - p_\infty)^z$, the absolute value sign is needed.

It may be argued that Rudy and Strikwerda NRBC does not contain any absolute value sign around the $(p - p_\infty)$ term, so one does not really get the same NRBC from the simple two parameter NRBC as that of Rudy and Strikwerda for the case of $z = 1$. In fact, for $z = 1$, an absolute value sign is not necessary around the term $(p - p_\infty)$. We took care of this case $(z = 1)$ by obtaining the results for both the situations– namely, with and without the absolute value sign– for various values of α tested. Identical results were obtained for N_{conv}, and indeed, for flow field $(u, v, T,$ etc.), for both these situations.

Intuitively, keeping a low α helps in reducing the effect of pressure fluctuations, a high value of z helps in a similar manner. Consider $\mid p - p_\infty \mid < 1$. $\mid p - p_\infty \mid^z$ is still smaller if $\mid z \mid > 1$, and $\alpha \mid p - p_\infty \mid^z$ is smaller still if $\alpha < 1$. However, minimum number of steps for convergence may not be achieved for $\alpha = 0+$, as seen from the recommendations of Rudy and Strikwerda [1981] in connection with their single parameter NRBC (equation 4.12) which corresponds to $z = 1$ in the NRBC proposed above (equation 4.20). They have carried out an analysis for an optimal α on *linearized* Navier Stokes equations. However, based on numerical experiments, they have suggested α in the range of $(0.3, 0.4)$ for their single parameter NRBC $(z = 1)$ for steady state calculations over the flat plate. There is a variance in the results obtained from linear analysis and experimentation. An interesting feature which emerges from

our results is that we have been able to achieve lower steps for convergence for $z \neq 1$ as compared to $z = 1$ (which corresponds to the Rudy and Strikwerda single parameter NRBC), while keeping α fixed, for certain values of α.

4.4.6 Exponentially adjusting NRBC

The other case we wish to consider is when the term $(p - p_\infty)$ appears under the exponential, the NRBC we propose is

$$\frac{\partial p}{\partial t} - \rho c \frac{\partial u}{\partial t} + \alpha \mid e^{(p-p_\infty)} - 1 \mid^z = 0 \tag{4.24}$$

with the following constraints on z and α

$$z > 0 \tag{4.25}$$

$$\alpha \neq 0 \tag{4.26}$$

When steady state is reached, the first two terms involving the time derivative drop out, which implies $e^{(p-p_\infty)} = 1$ (assuming $z > 0$), i.e., $p = p_\infty$ is guaranteed at the outflow boundary. For $z < 0$, instability will arise, because dropping the time derivative terms for negative values of z results in:

$$\frac{1}{(\mid e^{(p-p_\infty)} - 1 \mid)^{|z|}} = 0, \tag{4.27}$$

which requires the denominator to be infinitely large.

The use of absolute value is similar to that for equation 4.20, and has been explained above.

For the NRBC in equation 4.24, note that whatever be the value of $(p - p_\infty)$, $e^{(p-p_\infty)}$ is always positive. This has the additional advantage that when $(p - p_\infty)$ is large but negative, the tendency towards divergence can still be controlled as $e^{(p-p_\infty)}$ will be small in this case. To demonstrate the occurence of this situation in a practical computation is, however, a difficult job. A large positive difference will, on the other hand, worsen even more.

4.4.7 Logarithmically adjusting NRBC

In the following b.c., we consider the case when the evolution of the term $(p - p_\infty)$ is logarithmic:

$$\frac{\partial p}{\partial t} - \rho c \frac{\partial u}{\partial t} + \alpha [\mid \frac{1}{\ln \mid p - p_\infty \mid} \mid]^z = 0 \tag{4.28}$$

In the above,

$$z > 0 \tag{4.29}$$

and

$$\alpha \neq 0 \tag{4.30}$$

If the solution converges to steady state, the terms involving time derivatives can be dropped. Hence $[1/\ln \mid p - p_\infty \mid] = 0$, which guarantees $p \rightarrow p_\infty$, at the outflow boundary. The two absolute value signs have been introduced for the following reasons. The first one around $p - p_\infty$ ensures that we take the logarithm of a positive quantity. Since we are interested in the values of p such that $\mid p - p_\infty \mid < 1$, the logarithm of this quantity will be negative. Hence, we again take the absolute value before raising it to the power of z. The requirement $z > 0$ is explained as in the cases above.

One aspect is immediately clear: of the NRBC's listed above in equations 4.20, 4.24 and 4.28, the logarithmically adjusting NRBC (equation 4.28) will show the worst performance because of the following facts:

1. For $p = p_\infty$, which is what is required at steady state on the Subsonic Outflow Boundary, we have the expression $\ln 0 (= -\infty)$ in the above expression.

2. Logarithmic growth is the slowest of the three cases. For example, consider $\mid p - p_\infty \mid = 10^{-99}$. The logarithm of this is just $ln \mid p - p_\infty \mid = -227.9$. The inverse of this, $1/ln \mid p - p_\infty \mid$ is several orders of magnitude larger than what we started with (10^{-99}), it is $4.38\text{X}10^{-3}$. Hence large values of z will be required to ensure convergence as compared to the other two NRBC's. This is evident in the results presented below.

Constant pressure boundary condition

The 'reflecting' constant pressure b.c., which can be expressed as

$$p = p_\infty \tag{4.31}$$

has already been shown to be non-optimal by Rudy and Strikwerda [1981].

Additional b.c.'s for the numerical method

In the results presented in the following sections, NRBC's in equations 4.20, 4.24 and 4.28 have been used for various combination of values of α and z. For the three additional b.c.'s required for the implementation of the numerical method, zeroth order extrapolation for u, v and ρ, with T calculated from the e.o.s. has been used. The roles of ρ and T can be reversed, as is obvious.

4.4.8 Initial conditions

At $t = 0$, every x-location was assigned the same profile as the inflow profile. This inflow profile has been discussed above in section 4.4.3.

4.5 Results and discussions

Of interest is the number of steps required to reach convergence, N_{conv}. Pressure history at some point inside the domain is also of interest, as it gives an indication as to how well pressure reflections have been eliminated by the NRBC. The point chosen for this purpose lies close to the intersection of the Subsonic Outflow Boundary and the No Slip Boundary (the lower right hand corner). The choice of the neighbourhood of the No Slip Boundary is made because the largest fluctuations in the initial flow field occur near the rigid wall. Figure 4.1 shows this as the point 'A', its location is $(x_A, y_A) = (1.902439, 0.011265)$. The u-velocity profile at some x-location in the computational domain is also of interest, the results provided below plot this for $x = 1.560976$, which is about $75 percent$ of the total domain length downstream of the Subsonic Inflow Boundary.

4.5.1 Factors affecting convergence

The following five factors determine the convergence behaviour.

1. The NRBC (namely, the simple two parameter NRBC, the exponentially adjusting one, or the logarithmically adjusting one),
2. The value of the multiplicative parameter, α,
3. The value of the parameter which appears as the power, z,
4. The stability factor (Courant Friedrich Levy criteria) for the time marching numerical scheme. This is set to 0.7 for all calculations below.
5. The convergence criteria, ϵ. It is fixed at 10^{-6} in the calculations below.

4.5.2 Simple two parameter NRBC

Results for NRBC given in equation 4.20 are presented for the following values of α.

- $\alpha = 10^{-6}$
- $\alpha = 10^{-3}$
- $\alpha = 0.1$
- $\alpha = 0.3$

For each of the above, results for a set of values of z were computed.

Simple two parameter NRBC: $\alpha = 10^{-6}$

Results for $\alpha = 10^{-6}$ are presented in figures 4.3 – 4.11, and in table 4.1.

Table 4.1 summarizes the results of numerical experiments to determine the number of steps required for convergence. From the results we observe that for $\alpha = 10^{-6}$, as the value of z is increased, the number of steps required for convergence (N_{conv}) finally reaches a constant value. As already mentioned, there was no convergence for $z < 0$. Even for very small values of $z > 0$, the computations did not converge. Convergence was achieved only for $z \geq 0.223281$.

Figures 4.10 and 4.11 depict the variation in N_{conv} with z for $\alpha = 10^{-6}$. In figure 4.10, a log scale has been used on the x-axis to capture the x-range of values from 0 to 10000. Figure 4.11 shows the x-range where the variation in N_{conv} is the steepest, it uses a linear scale on both the axes. For this value of α ($\alpha = 10^{-6}$), the variation in N_{conv} with z is monotonically decreasing. Hence, the minimum value of $N_{conv}(= 27336)$ which is achieved at $z \geq 0.45$, is also the constant value of N_{conv} achieved when the curve flattens out. This does not turn out to be true for all values of α. In particular, it will be seen from the results presented for $\alpha = 0.1$ below that the constant value is slightly larger than the minimum value, and that $z = 1$ (which corresponds to the Rudy and Strikwerda NRBC) is not where N_{conv} is minimum. For values of z for which computations converge, N_{conv} quickly reaches its constant value as z increases (note the almost vertical initial slope of the curve).

As mentioned earlier (section 4.4.5), the argument that Rudy and Strikwerda NRBC does not contain any absolute value sign around the $(p - p_\infty)$ term, so one does not really get the same NRBC from the simple two parameter NRBC as that of Rudy and Strikwerda for the case of $z = 1$ needs to be taken care of. For the case of $z = 1$, results were obtained for both the situations– namely, with and without the absolute value sign. Identical values of N_{conv} and of flow variables (u, v, T, etc.) were obtained for these two situations.

Since N_{conv} can take only integer values, and since in the numerical experimentation convergence was checked only after every 50 steps, one can not expect these curves to be very smooth; figure 4.11 shows this jerkiness in the region $z = (0.2, 0.35)$.

Figure 4.3 shows the u velocity distribution with vertical distance y for $\alpha = 10^{-6}$, and a number of values of z. The plot is displayed for $x = 1.56$, which is about three fourths of the total length of the domain downstream of the inflow boundary on the left. The boundary layer is captured by the solution. The velocity profiles obtained for various values of z shown in figure 4.3 are identical at least to three decimal places, hence they overlap with each other in the figure. The profile is similar to the exponential inflow profile which approximates the fully developed self similar boundary layer profile for the velocity component u; indeed, the same profile exists for various x-locations once

the flow is fully developed. It will be seen from the results for other α values and also for the other proposed NRBC's that follow, that the u-velocity profiles are identical (at least upto the third decimal place). The same comment holds for different x-locations. This indicates that the steady state reached is the same for different combination of values of the two parameters and for different NRBC's, within the accuracy mentioned. In fact, for higher values of z, when N_{conv} becomes constant, the values, for different (α, z) combinations and for different NRBC's, are identical upto the sixth decimal place– that is within the ϵ value used to judge convergence. It must be remembered, however, that the result corresponds to the exponential inflow profile that has been used in these calculations (section 4.4.3).

Figures 4.4 – 4.9 show the behaviour of pressure p as one marches forward in time in the quest of a steady state. This pressure history is plotted for a point very near to the outflow (Non Reflecting) boundary (point 'A' of figure 4.1). Figure 4.4 plots this for $z = 0.22325$, for which the solution did not converge. The steep vertical slope of the curve as time increases indicates that pressure never reaches its steady state value. Figure 4.5 shows an exploded view of the pressure history for this case, where a definite trend in the curve with no indication of steadying out is visible. Figure 4.6 plots p versus time for $z = 0.223281$, for which $N_{conv} = 47634$. The other figures present the results for increasing values of z, that is for decreasing values of N_{conv}. Figure 4.7 shows this for $z = 0.225$ ($N_{conv} = 41871$), figure 4.8 for $z = 0.265$ ($N_{conv} = 32436$), and figure 4.9 for $z = 0.9$ ($N_{conv} = 27366$). All these curves flatten out to a steady state value. It is clear that lower the value of N_{conv}, lesser are the fluctuations in p.

For results that converged, CPU time utilized (on a Sun Sparc machine running on SunOS release 5.6 Generic) varied from 35 to 45 minutes.

Simple two parameter NRBC: $\alpha = 10^{-3}$

Results for $\alpha = 10^{-3}$ are presented in figures 4.12 – 4.17, and in table 4.2.

As for $\alpha = 10^{-6}$, the number of steps required for convergece (N_{conv}) finally reaches a constant value as z increases. For $z < 0.845$, there was no convergence. Table 4.2 summarizes the results of numerical experiments to determine the number of

steps required for convergence. Figures 4.16 and 4.17 depict the variation in N_{conv} with z for $\alpha = 10^{-3}$. In figure 4.16, a log scale has been used on the x-axis to capture the x-range of values from 0 to 10000. Figure 4.17 shows the x-range where the variation in N_{conv} is steepest, it uses a linear scale on both the axes. It is clearly demonstrated that $z = 1$ (which corresponds to the Rudy and Strikwerda NRBC, equation 4.12) is not where N_{conv} is lowest. At and in a small neighbourhood of $z = 1$, $N_{conv} = 27744$ is higher than the constant (and minimum) value $N_{conv} = 27336$. It must be noted that even a slight increase in z from $z = 1$ results in this minimum value.

As already mentioned (section 4.4.5), results have been obtained for two cases– with and without the absolute value sign– for $z = 1$. Identical results were obtained for N_{conv}, and indeed, for flow field (u, v, T, etc.), for both these situations.

Figure 4.12 shows the u velocity distribution with vertical distance y for a number of values of z, $\alpha = 10^{-3}$. The plot is displayed for $x = 1.56$, which is about three fourths of the total length of the domain downstream of the inflow boundary on the left. The results are similar to those obtained for $\alpha = 10^{-6}$.

Figures 4.13, 4.14 and 4.15 show the behaviour of pressure p as one marches forward in time in the quest of a steady state. The point whose pressure history is plotted is shown as 'A' in figure 4.1. Figure 4.13 plots this for $z = 0.1$, for which the solution did not converge. The almost constant downward slope of the curve as time steps increase indicates that pressure never reaches its steady state value. Figure 4.14 plots p versus time for $z = 0.9$, for which $N_{conv} = 29325$. Figure 4.15 shows this for $z = 5$ ($N_{conv} = 27336$). These two curves flatten out to a steady state value. For the lower value of N_{conv}, lesser fluctuations in p are observed. As for the figures for $\alpha = 10^{-6}$, fluctuations are all on the $+y$ side of the steady state value.

Simple two parameter NRBC: $\alpha = 0.1$

Results for $\alpha = 0.1$ are presented in figures 4.18, 4.19, 4.20, and in table 4.3.

As for the results for $\alpha = 10^{-6}$ and 10^{-3}, the number of steps required for convergece (N_{conv}) finally reaches a constant value as z increases. For $z < 0$, there was no convergence. Table 4.3 summarizes the results of numerical experiments to

determine the number of steps required for convergence. Figures 4.19 and 4.20 depict the variation in N_{conv} with z. In figure 4.19, a log scale has been used on the x-axis to capture the x-range of values from 0 to 10000. Figure 4.20 shows the x-range where the variation in N_{conv} is most interesting, it uses a linear scale on both the axes.

Two remarkable observations can be made from the results:

1. the minimum value of $N_{conv} = 27234$ is not equal to the constant value ($N_{conv} = 27336$) that is obtained as $z \to \infty$, and

2. There is a local spike in the curve of N_{conv} *vs.* z (figure 4.20), where N_{conv} takes the *high* value of 28611 *at* $z = 1$.

The minimum in N_{conv} (=27234) is observed in the region $0.5 < z < 0.895$. For $z \in [0.899, 1)$, $N_{conv} = 27336$, it is so also for $z > 1$. For z exactly equal to 1, N_{conv} jumps to 28611. In the above, the usual meaning of the symbols '(', ')', '[' and ']' pertaining to open and closed intervals hold.

As already mentioned (section 4.4.5), results have been obtained for two cases– with and without the absolute value sign– for $z = 1$. Identical values of N_{conv} and of flow variables (u, v, T, etc.) were obtained for these two situations.

It is thus clearly demonstrated that $z = 1$ (which corresponds to the Rudy and Strikwerda NRBC, equation 4.12) is not where N_{conv} is minimum, in fact this value of z leads to a *local maximum* in N_{conv}.

For $\alpha = 10^{-1}$, the variation in N_{conv} with z is *not* throughout monotonically decreasing as was the case for $\alpha = 10^{-6}$ and $\alpha = 10^{-3}$.

Figure 4.18 shows the u velocity distribution with vertical distance y for a number of values of z, $\alpha = 10^{-1}$. The results are similar to that obtained for $\alpha = 10^{-6}$. The plot is displayed for $x = 1.56$, which is about three fourths of the total length of the domain downstream of the inflow boundary on the left.

Simple two parameter NRBC: $\alpha = 0.3$

Results for $\alpha = 0.3$ are presented in figures 4.21, 4.22, 4.23, and in table 4.4.

As for the results for other values of α, N_{conv} finally reaches a constant value as z increases. For $z < 0$, there was no convergence. Table 4.4 summarizes the results of numerical experiments to determine the number of steps required for convergence. Figures 4.22 and 4.23 depict the variation in N_{conv} with z for $\alpha = 0.3$. In figure 4.22, a log scale has been used on the x-axis to capture the x-range of values from 0 to 1000. Figure 4.23 shows the x-range where the variation in N_{conv} is of greatest interest, it uses a linear scale on both the axes.

As for other values of α, and as mentioned in section 4.4.5, results for $z = 1$ have been obtained for two cases: with and without the absolute value sign in the simple two parameter NRBC. Identical results were obtained for N_{conv} and also for flow field $(u, v, T,$ etc.) for these two situations.

Following observations stand out for $\alpha = 0.3$:

1. the minimum value of $N_{conv} = 27132$ is not equal to the constant value ($N_{conv} = 27336$) that is obtained as $z \to \infty$,

2. There is a local spike in the curve of N_{conv} *vs.* z (figure 4.23) at $z = 1$, but now it is in the downward direction and results in a minimum in N_{conv} $(= 27132)$,

3. A step like behaviour is observed on both the sides of $z = 1$ (figure 4.23), with the spike at $z = 1$ forming a local (and global) minimum. For $z \in [0.2, 1)$, $N_{conv} = 27234$. When z is exactly equal to 1, N_{conv} jumps *down* to 27132. For $z \in (1, 1.0024991]$, $N_{conv} = 27234$, while for $z > 1.0024991$, N_{conv} attains its constant value of 272336. In the above, the usual meaning of the symbols '(', ')', '[' and ']' pertaining to open and closed intervals hold.

Unlike the case of $\alpha = 0.1$, minimum of N_{conv} occurs at $z = 1$ (which corresponds to the Rudy and Strikwerda NRBC, equation 4.12). Choosing z even slightly different from 1 results in a small increase in N_{conv}.

For $\alpha = 0.3$, the variation in N_{conv} with z is not throughout monotonically decreasing as was the case for $\alpha = 10^{-6}$.

Figure 4.21 shows the u velocity distribution with vertical distance y for a number of values of z, $\alpha = 0.3$. Results are similar to that obtained for the other cases

($\alpha = 10^{-6}, 0.001, 0.1$). The plot is displayed for $x = 1.56$, which is about three fourths of the total length of the domain downstream of the inflow boundary on the left.

4.5.3 Exponentially adjusting NRBC: $\alpha = 10^{-3}$

Results for the exponentially adjusting NRBC (equation 4.24) for $\alpha = 10^{-3}$ are presented in figures 4.24 – 4.31 and in table 4.5.

From the results we observe that for a fixed α, as the value of z is increased, the number of steps required for convergece (N_{conv}) finally reaches a constant value. As already mentioned, for $z < 0$, there was no convergence, in fact, calculations diverged for $z \leq 0.8$. Table 4.5 summarizes the results of numerical experiments to determine the number of steps required for convergence.

Since the variation in N_{conv} with z is monotonically decreasing, the minimum value of $N_{conv}(= 27336)$ which is achieved for $z \geq 1.08$, is also the constant value of N_{conv} when the curve flattens out. In the region near $z = 1$, N_{conv} is very sensitive to minute changes in z. In particular, minimum of N_{conv} is obtained for z just slightly greater than one (figures 4.30 and 4.31). In figure 4.30, a log scale has been used on the x-axis to capture the x-range of values from 0 to 10000. Figure 4.31 shows the x-range where the variation in N_{conv} is the steepest, it uses a linear scale on both the axes. The monotonic decrease is evident. It is also seen that once convergence sets in, N_{conv} quickly reaches its constant value as z increases; in fact it happens much faster than what was obtained for similar α value for the simple two parameter NRBC (figures 4.16 and 4.30 corresponding to the cases of simple two parameter NRBC and the exponentially adjusting NRBC respectively, and similarly tables 4.2 and 4.5). Since N_{conv} can take only integer values, and since in the numerical experimentation convergence was checked only after every 50 steps, these curves are not expected to be very smooth; figure 4.31 shows this jerkiness in the region $z = (0.96, 1.1)$.

Figure 4.24 shows the u velocity distribution with vertical distance y for a number of values of z, for the exponentially adjusting NRBC with $\alpha = 10^{-3}$. The plot is displayed for $x = 1.56$, which is about three fourths of the total length of the domain downstream of the inflow boundary on the left. The results are similar to the

simple two parameter NRBC, the solution captures the boundary layer. It must be remembered, however, that the result corresponds to the exponential inflow profile that has been used in these calculations.

Figures 4.25 – 4.29 show the behaviour of pressure p very near to the outflow (Non Reflecting) boundary (at the point 'A' of figure 4.1). Figure 4.25 plots this for $z = 0.8$, for which the solution did not converge. The steep vertical slope of the curve as time increases indicates that pressure never reaches its steady state value. Figure 4.26 shows an exploded view of the same figure, where a vertical slope in the curve with no indication of steadying out is visible. Figure 4.27 plots p versus time for $z = 0.85$, for which $N_{conv} = 33762$. The other figures present the results for increasing values of z, that is for decreasing values of N_{conv}. Figure 4.28 shows this for $z = 1.000001$ ($N_{conv} = 27744$), and figure 4.29 for $z = 4.2$ ($N_{conv} = 27366$). All these curves flatten out to a steady state value. The lesser the value of N_{conv}, lesser are the fluctuations in p. Fluctuations are all on the $+y$ side of the steady state value, this is because of the absolute value sign in the NRBC.

4.5.4 Logarithmically adjusting NRBC: $\alpha = 10^{-3}$

Results for the logarithmically adjusting NRBC (equation 4.28) for $\alpha = 10^{-3}$ are presented in figures 4.32 – 4.38, and in table 4.6

Table 4.6 summarizes the results of numerical experiments to determine the number of steps required for convergence. The most important observation about the logarithmically adjusting NRBC is that it has the worst convergence characteristics as compared to the simple two parameter NRBC (equation 4.20) and the exponentially adjusting NRBC (equation 4.24). From the results for $\alpha = 0.001$ for the three NRBC's proposed in this chapter, we find that the value of z for which the log NRBC starts resulting in convergence is much *higher* than that for any of the two others. The other two NRBC's start to converge for values of z even less than one (for $\alpha = 0.001$), while for the log NRBC, convergence is achieved only for $z > 3.9$. This happens because logarithmic growth is the slowest of the three cases, as illustrated in section 4.4.7

Figures 4.37 and 4.38 present the results in a graphical form. In figure 4.37, a

log scale has been used on the x-axis to capture the x-range of values from 0 to 10000. Figure 4.38 shows the x-range where the variation in N_{conv} is the steepest, it uses a linear scale on both the axes. The monotonic decrease is evident. It is also seen that once convergence sets in, N_{conv} quickly decreases to its minimum value of 27336, which is also the value at which the N_{conv} *vs.* z curve flattens out.

Figure 4.32 shows the u velocity distribution with vertical distance y for a number of values of z, for the logarithmically adjusting NRBC with $\alpha = 10^{-3}$. The plot is displayed for $x = 1.56$, which is about three fourths of the total length of the domain downstream of the inflow boundary on the left. The results are similar to the results for the other NRBC's, the solution captures the boundary layer. It must be remembered, however, that the result corresponds to the exponential inflow profile (a good approximation to the fully developed boundary layer profile) that has been used in these calculations.

Figures 4.33 – 4.36 show the behaviour of pressure p very near to the outflow (Non Reflecting) boundary (at the point 'A' of figure 4.1). Figure 4.33 plots this for $z = 3.5$, for which the solution did not converge. The steep downward slope of the curve as time steps increase indicates that pressure never reaches its steady state value. Figure 4.34 plots p versus time for $z = 3.99$, for which $N_{conv} = 33762$. The other figures present the results for increasing values of z, that is, for decreasing values of N_{conv}. Figure 4.35 shows this for $z = 4.05$ ($N_{conv} = 32946$), and figure 4.36 for $z = 8$ ($N_{conv} = 27336$). All these curves flatten out to a steady state value. The lesser the value of N_{conv}, lesser are the fluctuations in p. Fluctuations are all on the $+y$ side of the steady state value, this is because of the absolute value sign in the NRBC.

4.6 Summary of results

Tables 4.7 and 4.8 give an overview of the results for the application of the three proposed NRBC's to the geometry of figure 4.1.

Linearization for the purpose of subjecting them to analysis may destroy their essential characteristics, especially in view of the fact that the NRBC's themselves are non-linear; hence it has not been carried out. Numerical experimentation thus seems

to be the best option for studying them, the results for which have been presented in the previous sections.

Choosing a a high value of z (say 10000) for any NRBC for any α is, in general, safe, as it results in convergence. N_{conv} for such a choice is also usually sufficiently low, though it may not be the minimum for that α-value and NRBC. It is recommended that α be chosen less than unity. The logarithmically adjusting NRBC is not, in general, recommended.

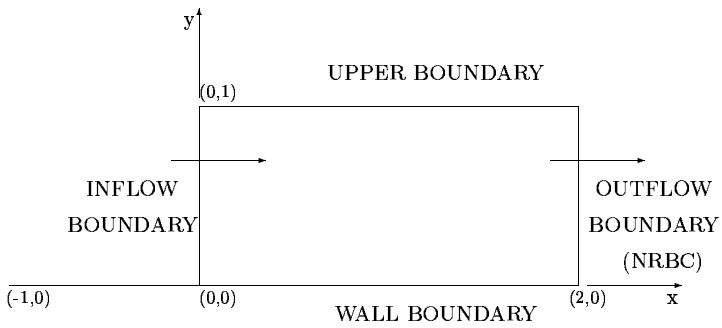

Figure 4.1: Solution domain for uniform subsonic flow over a flat plate

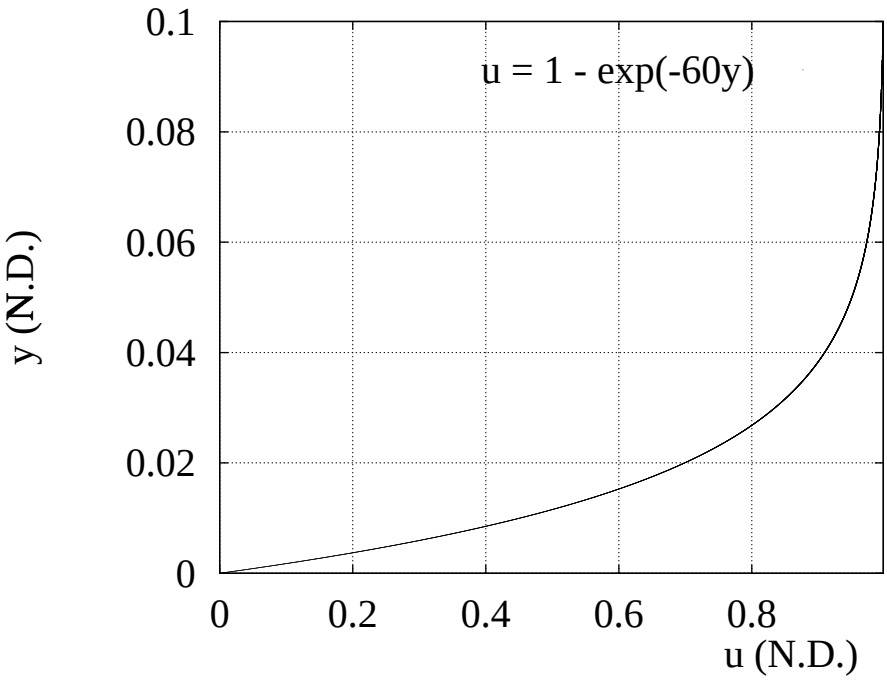

Figure 4.2: Exponential inflow velocity profile used

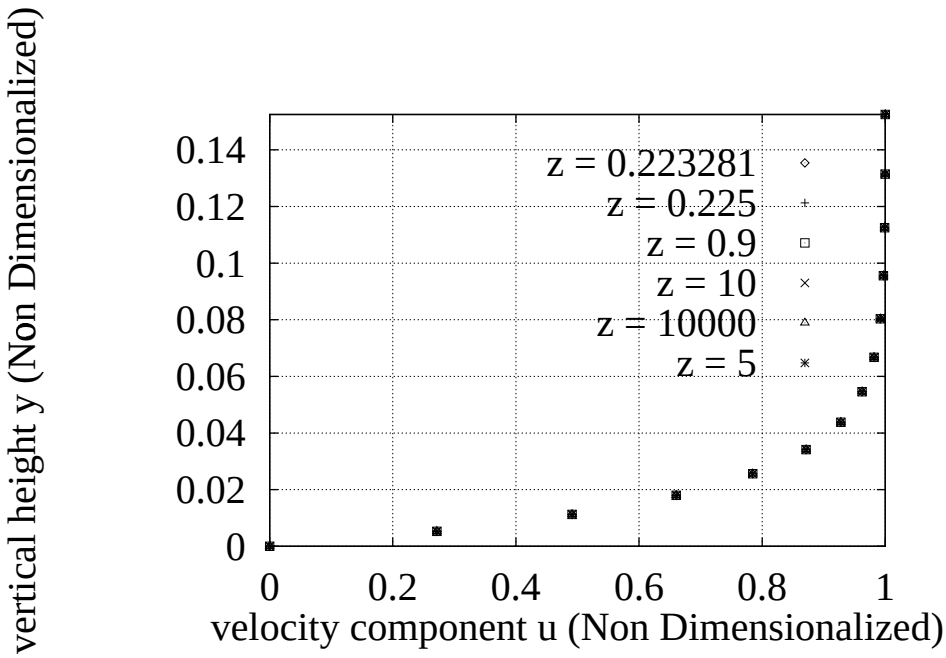

Figure 4.3: u velocity distribution with vertical distance y, $\alpha = 10^{-6}$, $x = 1.56$, simple two parameter NRBC.

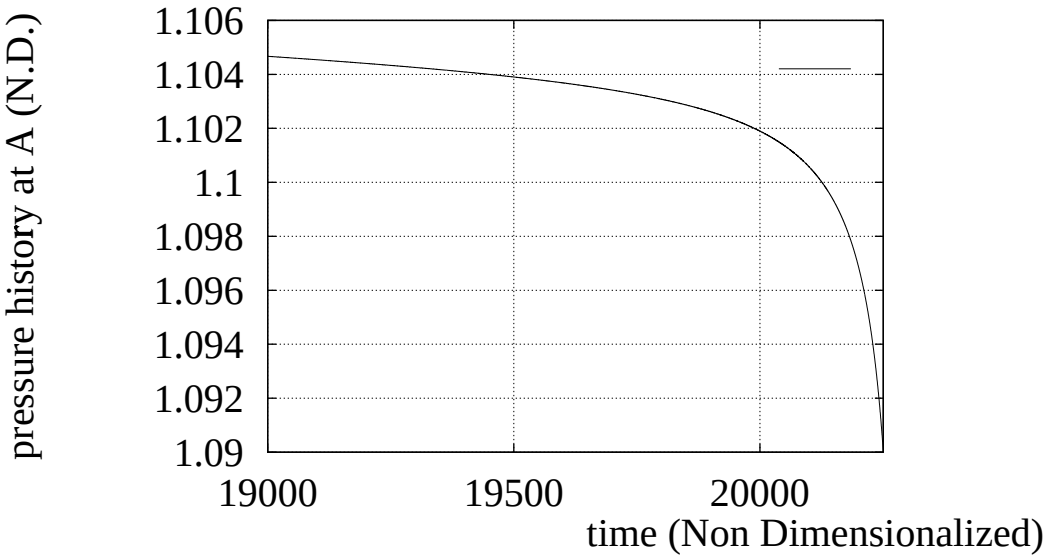

Figure 4.4: Pressure history at location A for $z = 0.22325$ which does not converge, $\alpha = 10^{-6}$, simple two parameter NRBC.

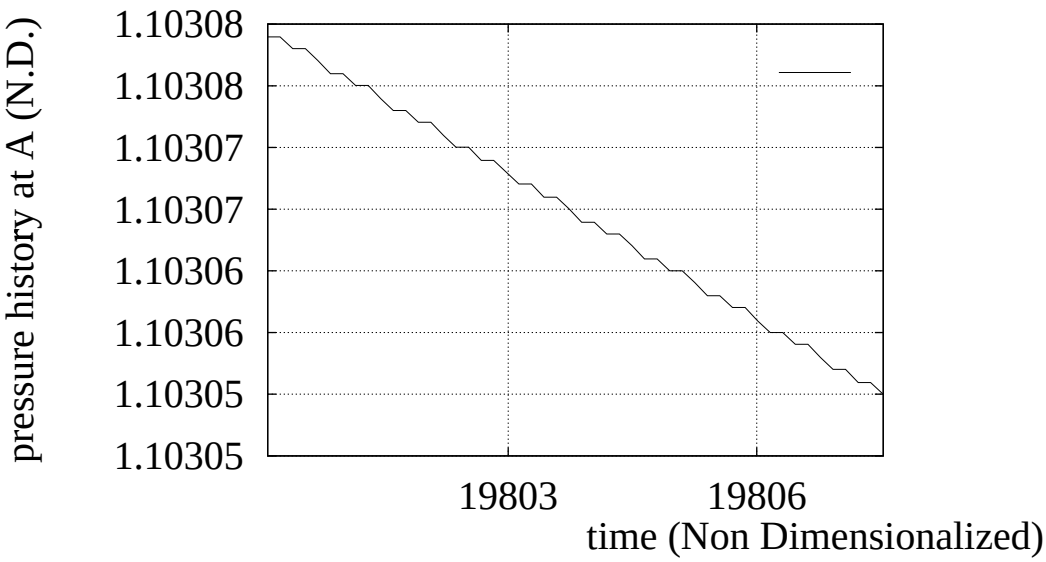

Figure 4.5: Pressure history at location A for $z = 0.22325$ which does not converge, exploded view, $\alpha = 10^{-6}$, simple two parameter NRBC

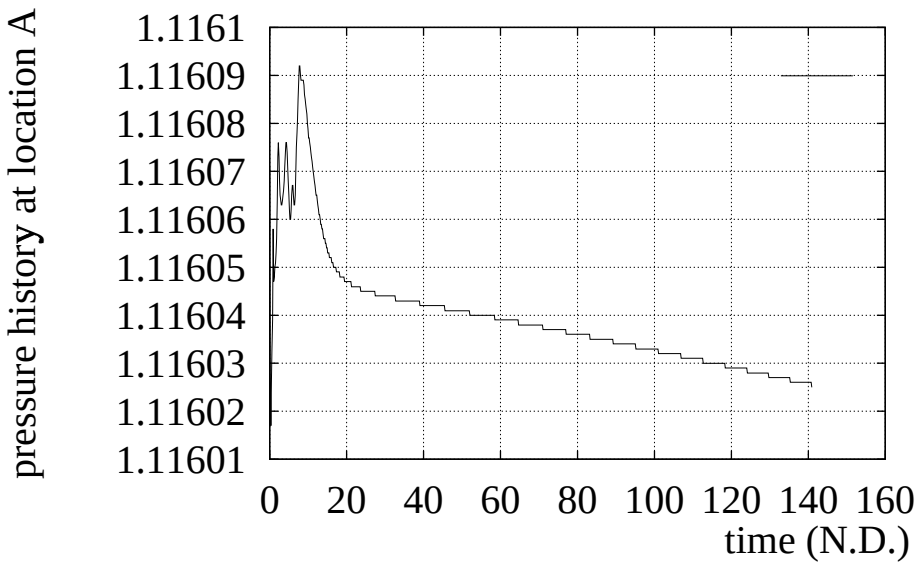

Figure 4.6: Pressure history at location A for $z = 0.223281$ which converges in 47634 steps, $\alpha = 10^{-6}$, simple two parameter NRBC

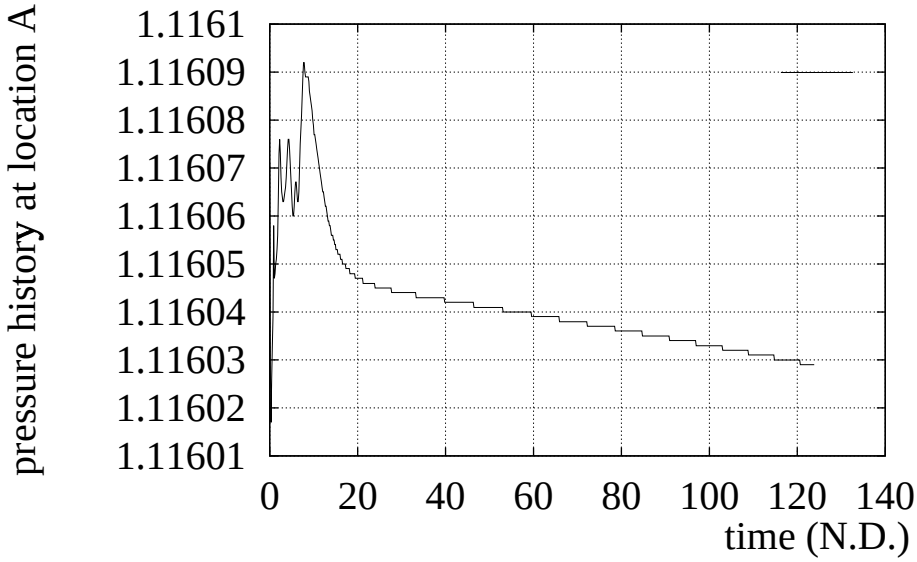

Figure 4.7: Pressure history at location A for $z = 0.225$ which converges in 41871 steps, $\alpha = 10^{-6}$, simple two parameter NRBC

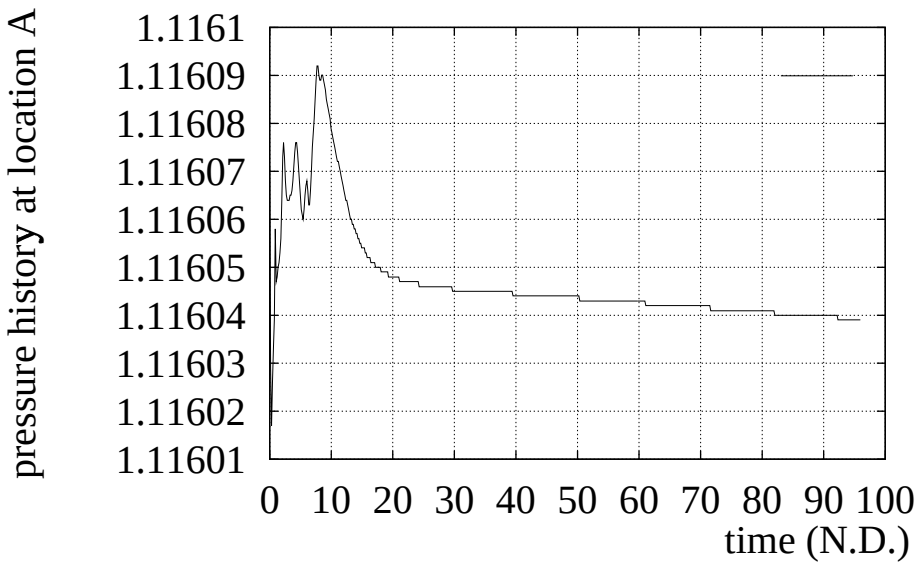

Figure 4.8: Pressure history at location A for $z = 0.265$ which converges in 32436 steps, $\alpha = 10^{-6}$, simple two parameter NRBC

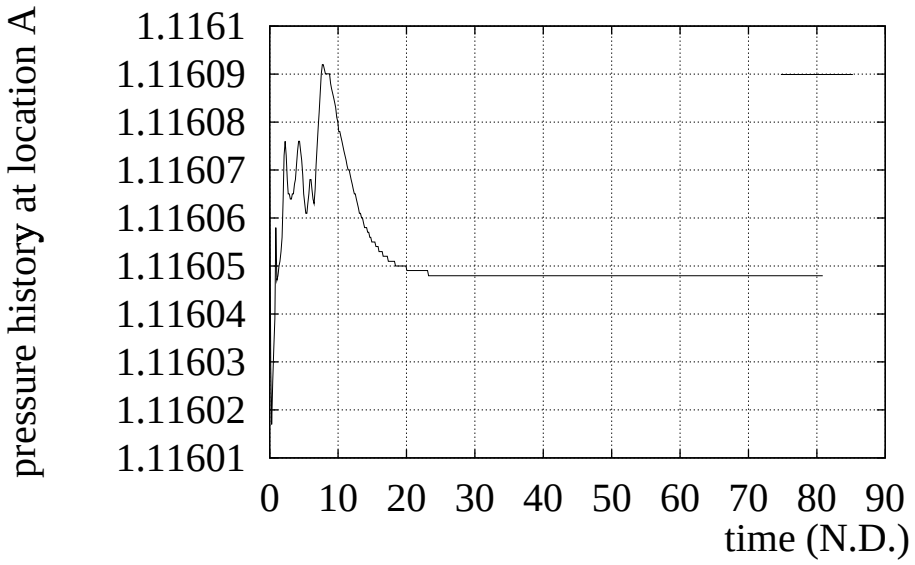

Figure 4.9: Pressure history at location A for $z = 0.9$ which converges in 27336 steps, $\alpha = 10^{-6}$, simple two parameter NRBC

z	Number of steps for convergence N_{conv}
< 0.223281	Does not converge
0.223281	47634
0.2233	47634
0.2234	47430
0.2235	47226
0.225	41871
0.228	39882
0.23	38199
0.24	33966
0.25	33558
0.26	32436
0.265	32436
0.27	30396
0.28	30294
0.29	29988
0.3	29682
0.35	27846
0.4	27846
0.45	27336
0.5	27336
0.95	27336
1	27336
1.1	27336
100	27336
10000	27336
10000.001	27336

Table 4.1: Typical values of steps for convergence (N_{conv}) vs. z for $\alpha = 10^{-6}$, simple two parameter NRBC

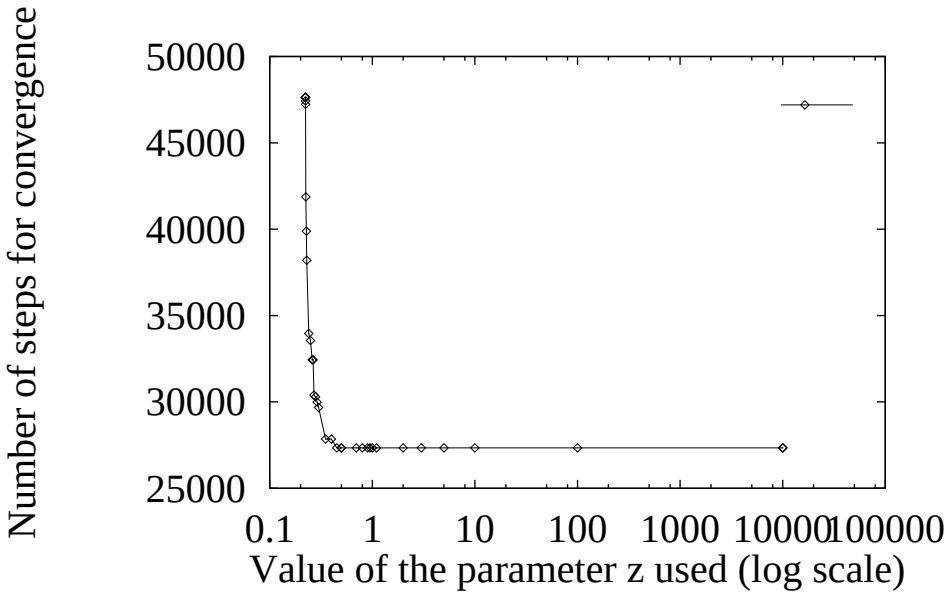

Figure 4.10: Number of steps required for convergence (N_{conv}) for different values of z, $\alpha = 10^{-6}$, simple two parameter NRBC

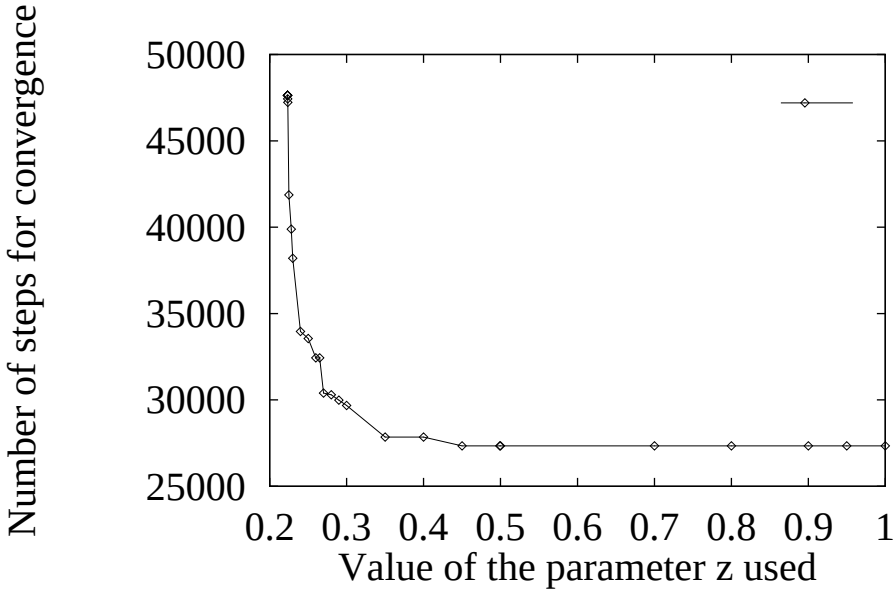

Figure 4.11: Number of steps required for convergence (N_{conv}) for different values of z, exploded view, $\alpha = 10^{-6}$, simple two parameter NRBC

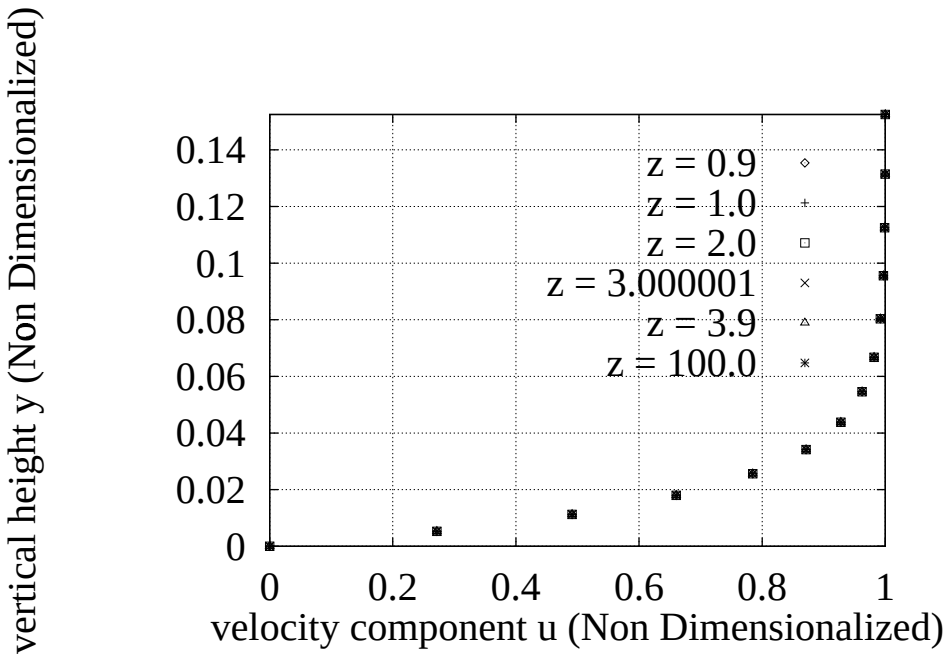

Figure 4.12: u velocity distribution with vertical distance y, $\alpha = 10^{-3}$, $x = 1.56$, simple two parameter NRBC

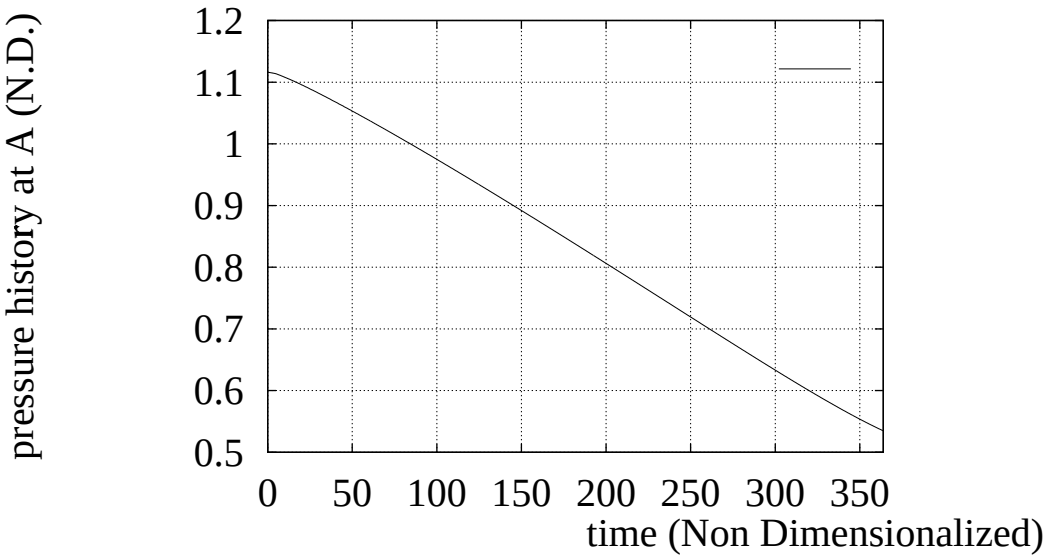

Figure 4.13: Pressure history at location A for $z = 0.1$ which diverges, $\alpha = 10^{-3}$, simple two parameter NRBC

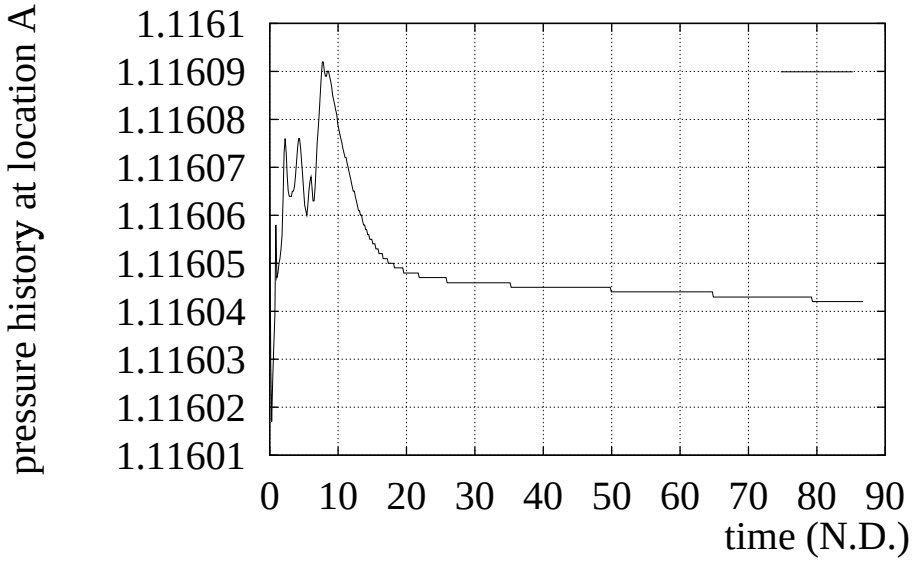

Figure 4.14: Pressure history at location A for $z = 0.9$ which converges in 29325 steps, $\alpha = 10^{-3}$, simple two parameter NRBC

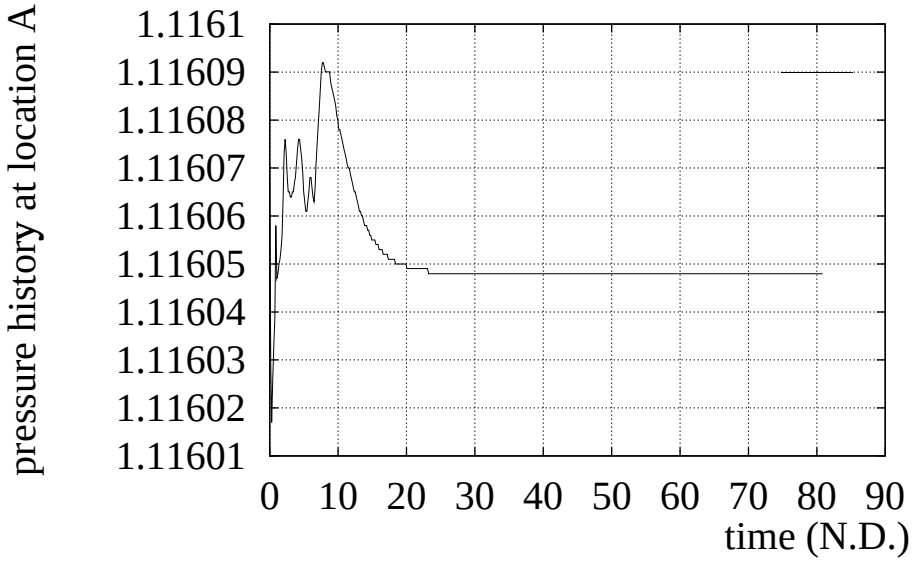

Figure 4.15: Pressure history at location A for $z = 5.0$ which converges in 27336 steps, $\alpha = 10^{-3}$, simple two parameter NRBC

z	Number of steps for convergence N_{conv}
≤ 0.845	Does not converge
0.85	33762
0.88	30396
0.9	29325
0.92	28254
0.95	27846
0.999	27846
0.9997	27744
0.999999	27744
0.9999999999	27744
1	27744
1.0000000001	27744
1.000001	27744
1.01	27744
1.0111	27744
1.0112	27540
1.019	27540
1.0199	27540
1.019922	27438
1.01995	27438
1.05	27438
1.0526	27438
1.0527	27336
1.053	27336
1.1	27336
2	27336
10000	27336

Table 4.2: Typical values of N_{conv} vs. z for $\alpha = 10^{-3}$, simple two parameter NRBC

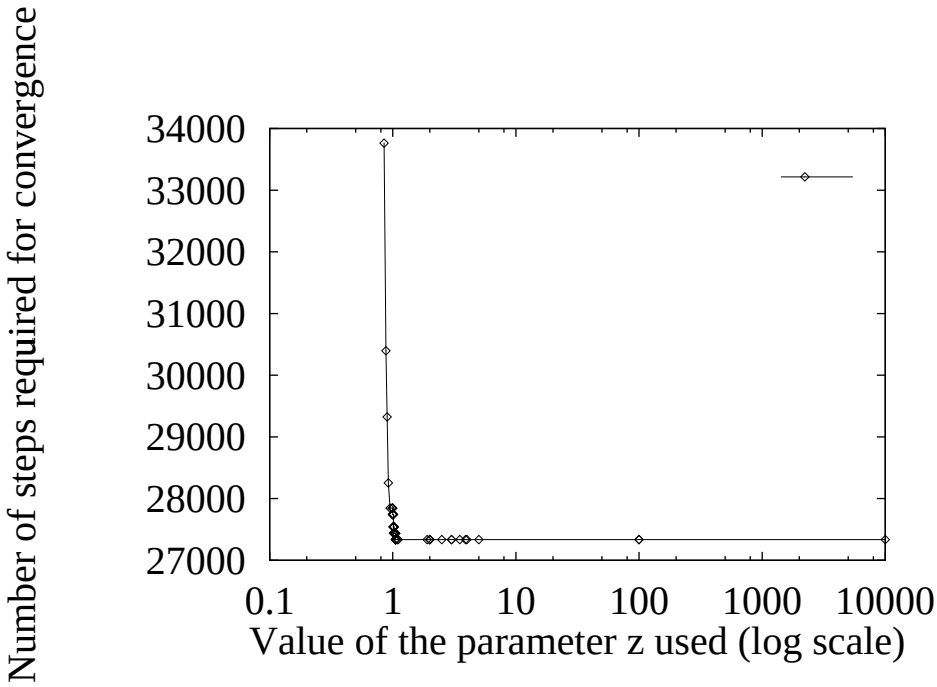

Figure 4.16: Number of steps required for convergence for different values of z, $\alpha = 10^{-3}$, simple two parameter NRBC

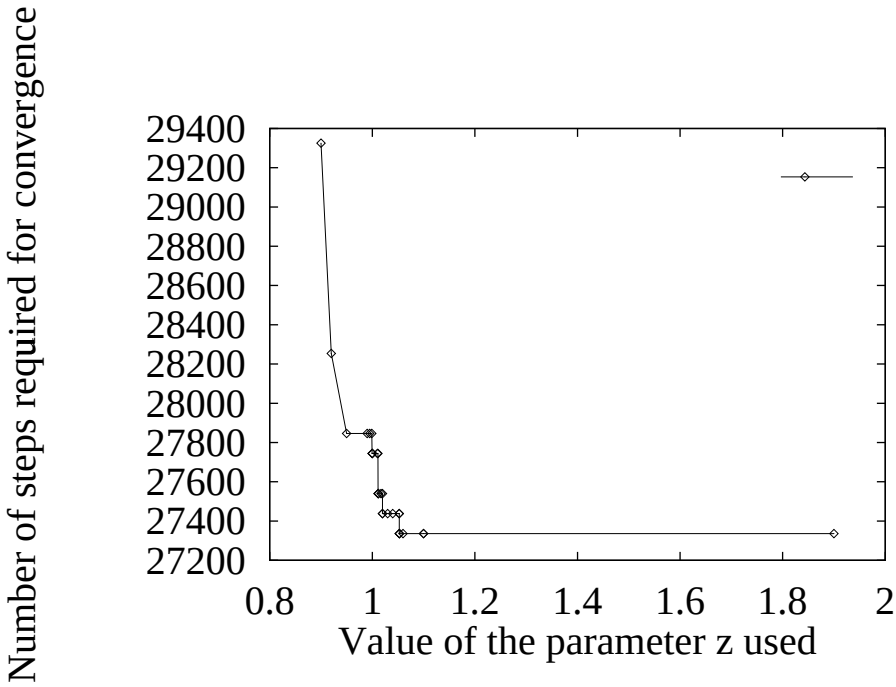

Figure 4.17: Number of steps required for convergence for different values of z, exploded view, $\alpha = 10^{-3}$, simple two parameter NRBC

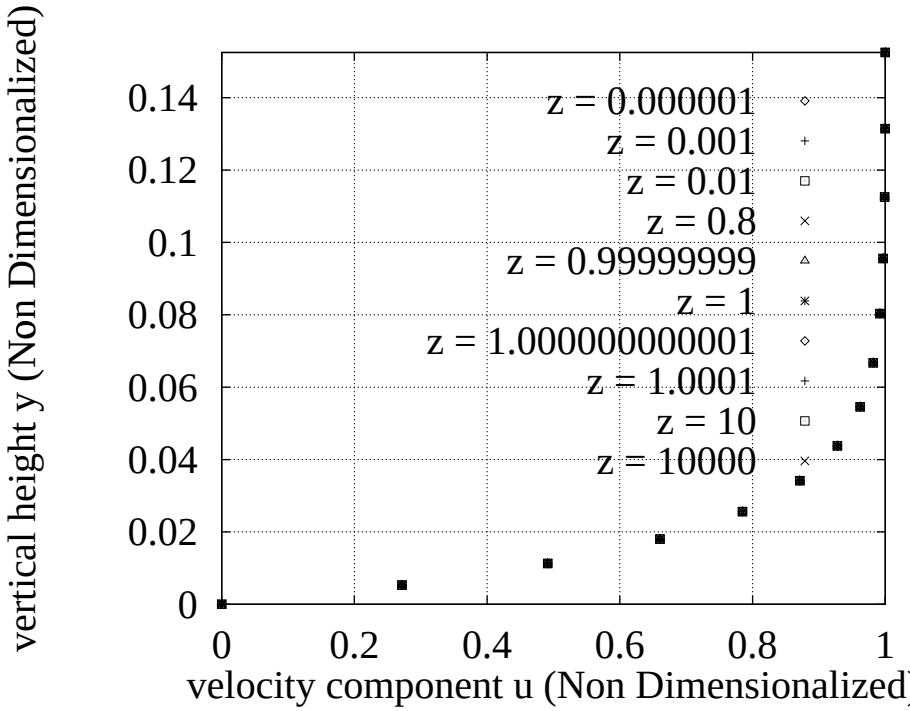

Figure 4.18: u velocity distribution with vertical distance y, $\alpha = 0.1$, $x = 1.56$, simple two parameter NRBC

z	Number of steps for convergence N_{conv}
< 0.0	Does not converge
0.000001	31467
0.00001	31467
0.0001	31467
0.001	31365
0.01	30702
0.5	27234
0.7	27234
0.8	27234
0.89	27234
0.895	27234
0.899	27336
0.99	27336
0.9999	27336
0.999999	27336
0.9999999	27336
0.99999999	27336
0.999999999999	27336
1.0	28611
1.000000000001	27336
1.00000001	27336
1.0000001	27336
1.000001	27336
1.0001	27336
1.01	27336
10	27336
10000	27336

Table 4.3: Typical values of N_{conv} vs. z, $\alpha = 0.1$, simple two parameter NRBC

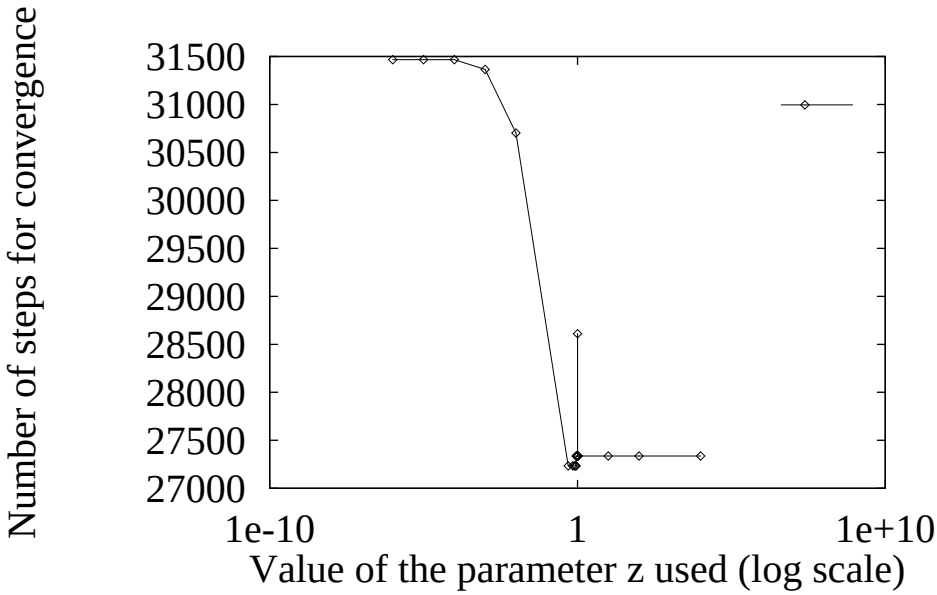

Figure 4.19: Number of steps required for convergence for different values of z, $\alpha = 0.1$, simple two parameter NRBC

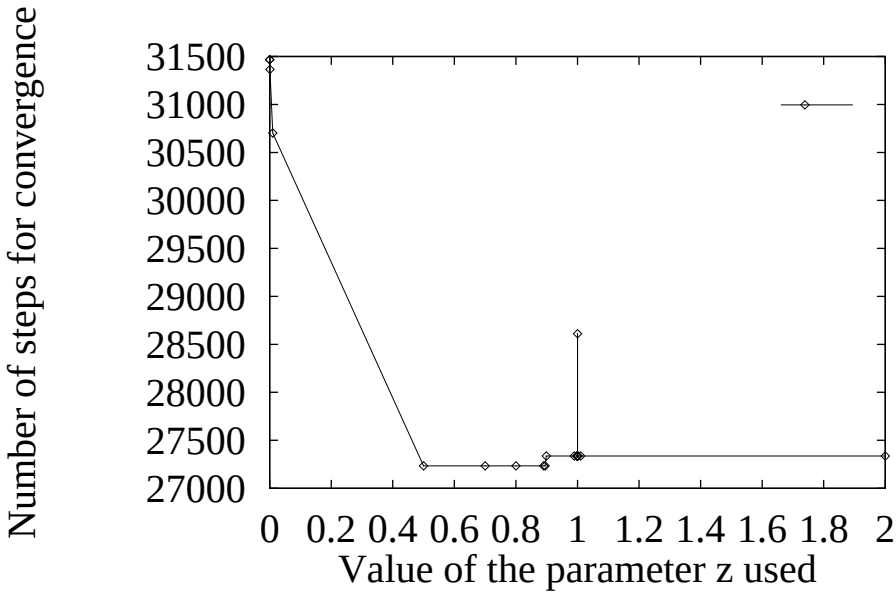

Figure 4.20: Number of steps required for convergence for different values of z, exploded view, $\alpha = 0.1$, simple two parameter NRBC

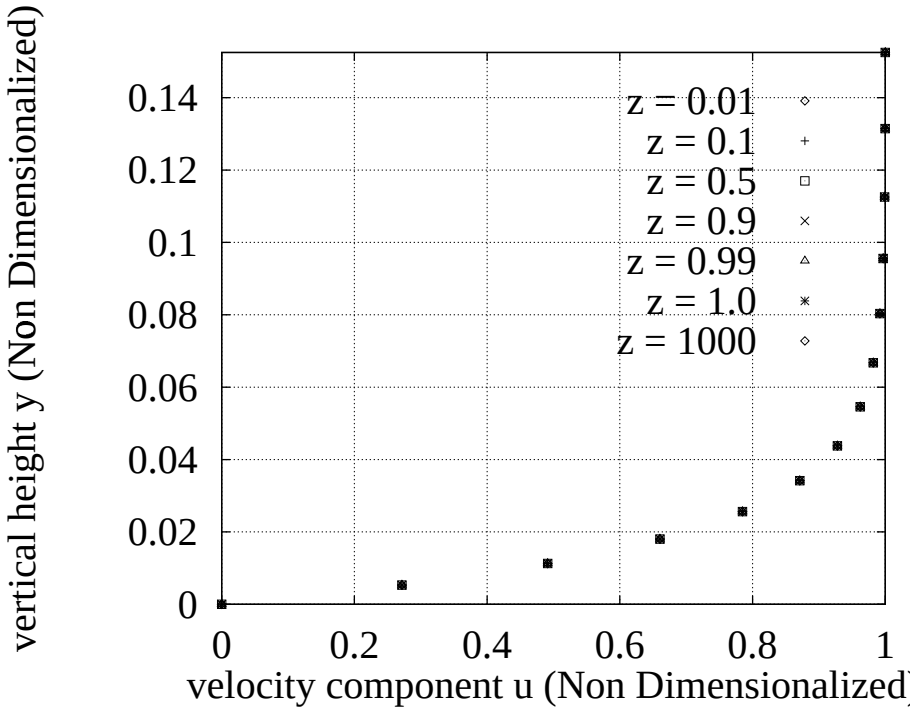

Figure 4.21: u velocity distribution with vertical distance y, $\alpha = 0.3$, $x = 1.56$, simple two parameter NRBC

z	Number of steps for convergence N_{conv}
< 0.0	Does not converge
0.0001	35292
0.001	35292
0.01	34629
0.05	32946
0.07	30804
0.1	27846
0.15	27846
0.2	27234
0.25	27234
0.9	27234
0.95	27234
0.99	27234
0.9999	27234
1.0	27132
1.0001	27234
1.001	27234
1.002	27234
1.0021	27234
1.002495	27234
1.002499	27234
1.0024991	27234
1.0024995	27336
1.0024999	27336
1.1	27336
10	27336
1000	27336

Table 4.4: Typical values of N_{conv} vs. z, $\alpha = 0.3$, simple two parameter NRBC

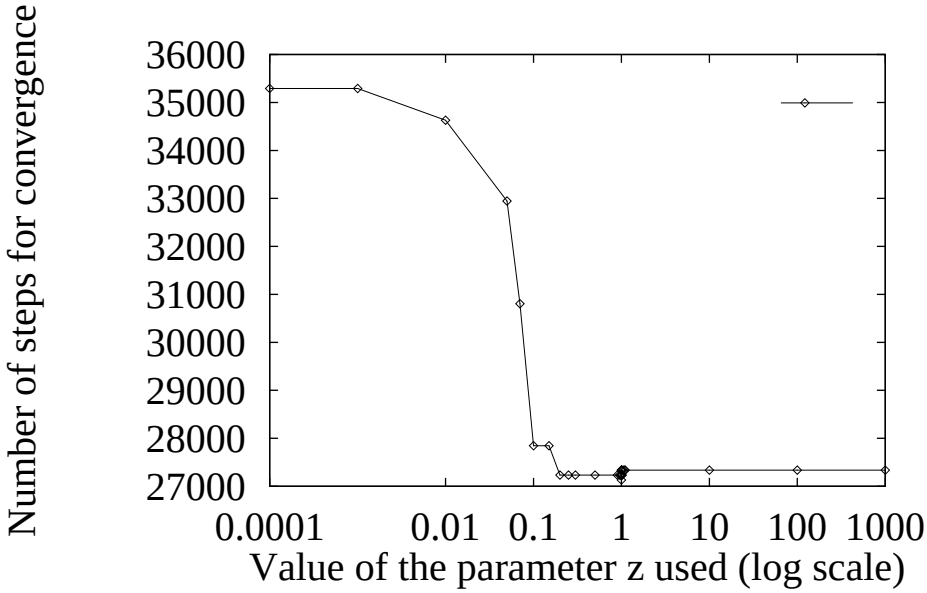

Figure 4.22: Number of steps required for convergence for different values of z, $\alpha = 0.3$, simple two parameter NRBC

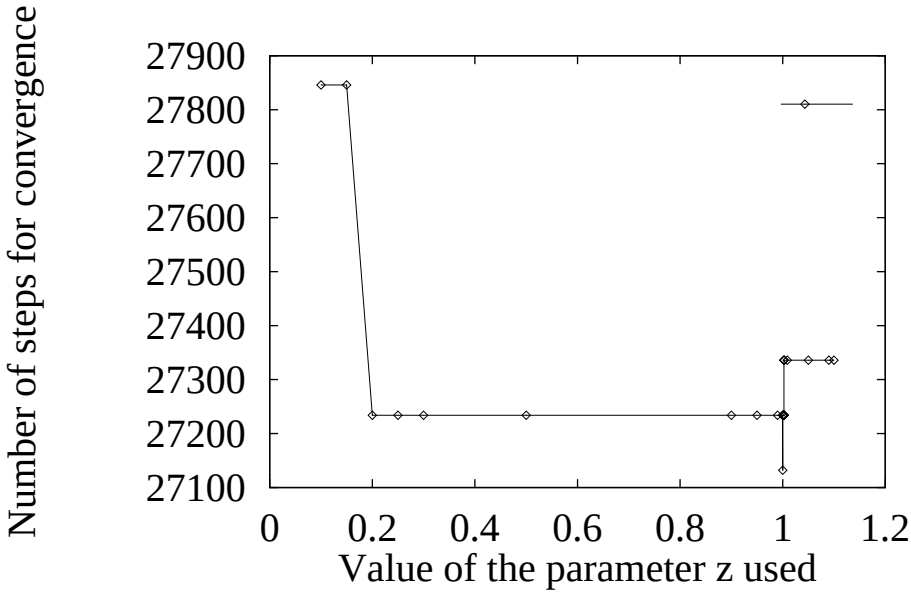

Figure 4.23: Number of steps required for convergence for different values of z, exploded view, $\alpha = 0.3$, simple two parameter NRBC

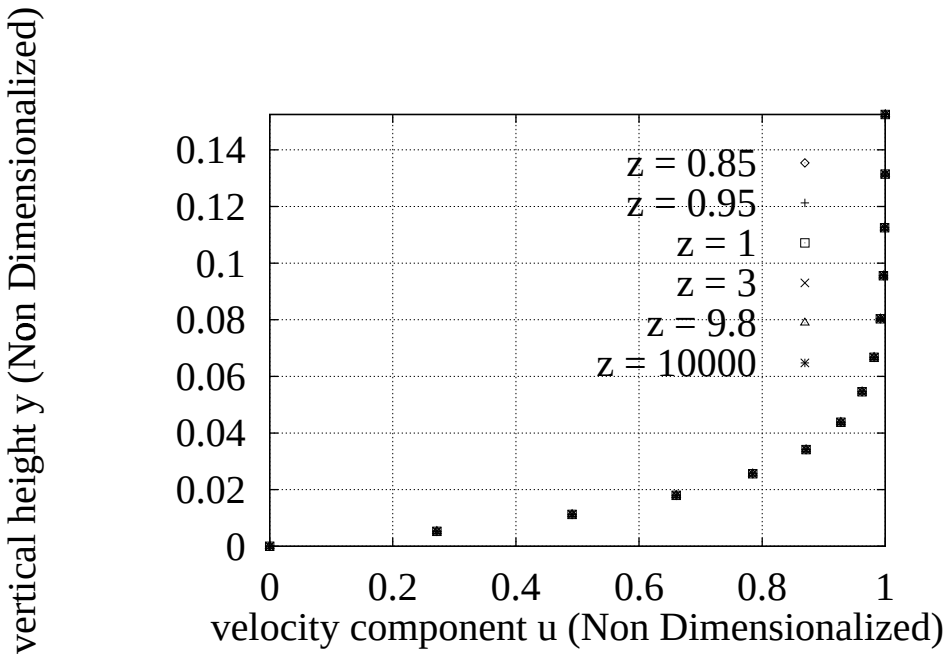

Figure 4.24: u velocity distribution with vertical distance y, $\alpha = 10^{-3}$,$x = 1.56$, exponentially adjusting NRBC

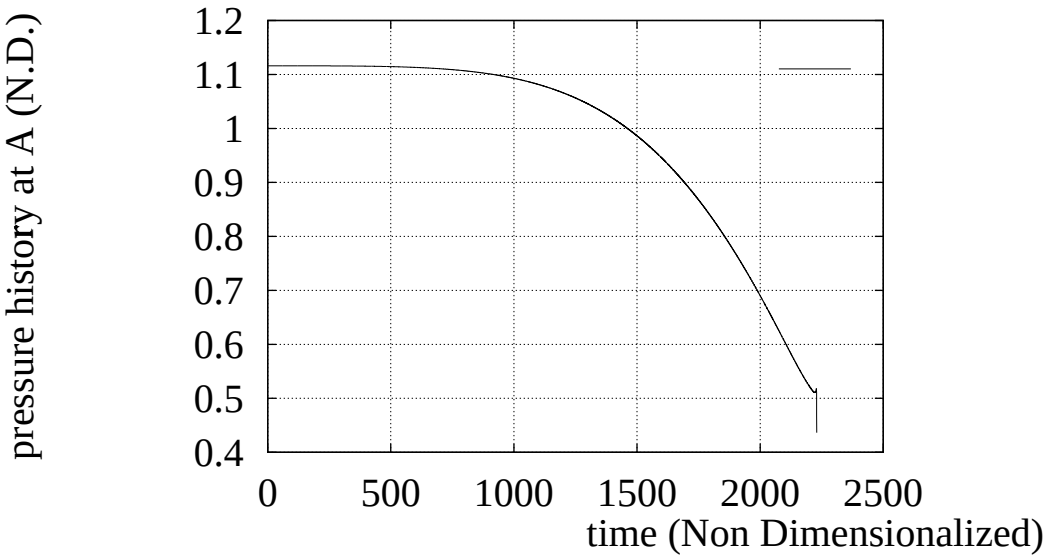

Figure 4.25: Pressure history at location A for $z = 0.8$ which diverges, $\alpha = 10^{-3}$, exponentially adjusting NRBC

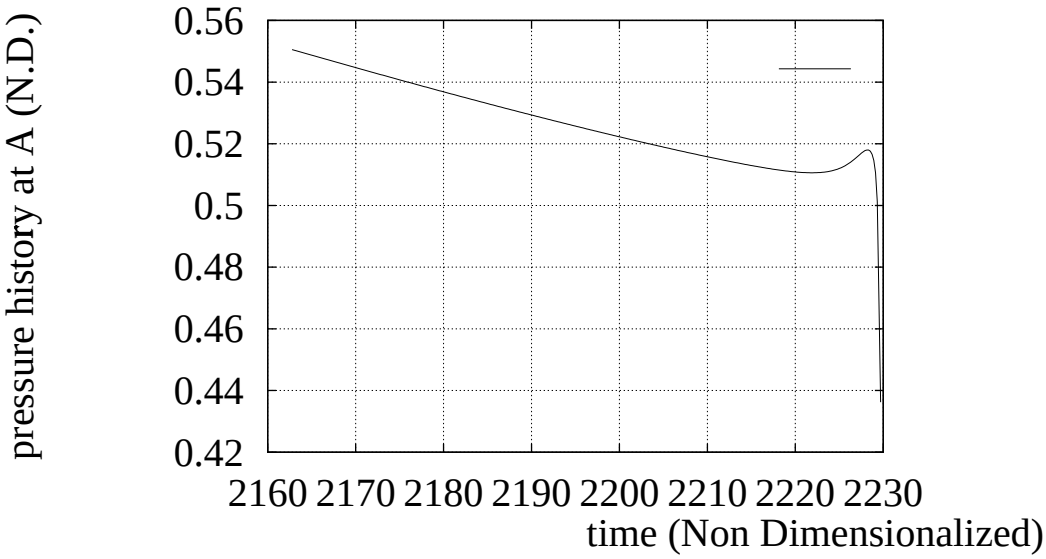

Figure 4.26: Pressure history at location A for $z = 0.8$ which diverges, exploded view, $\alpha = 10^{-3}$, exponentially adjusting NRBC

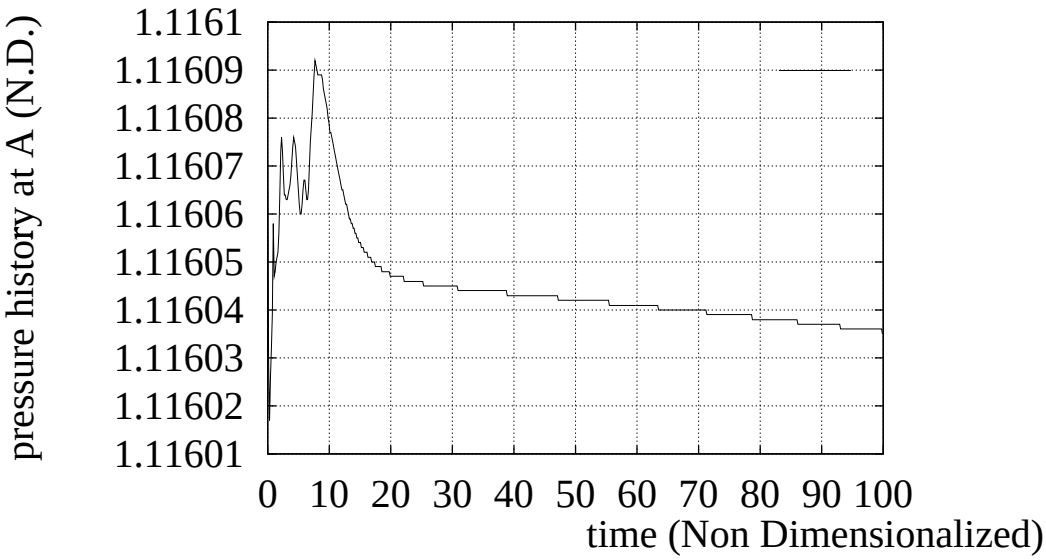

Figure 4.27: Pressure history at location A for $z = 0.85$ which converges in 33762 steps, $\alpha = 10^{-3}$, exponentially adjusting NRBC

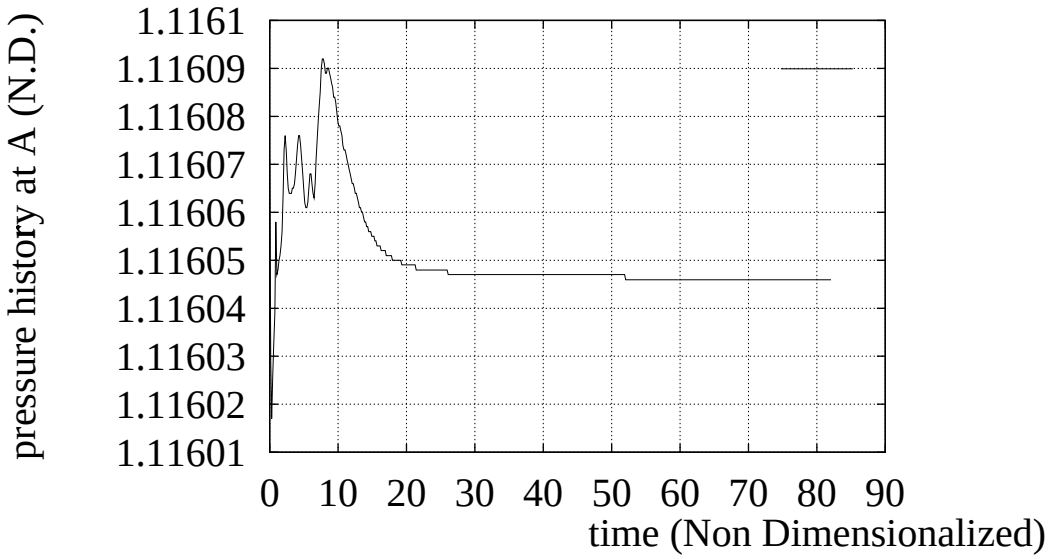

Figure 4.28: Pressure history at location A for $z = 1.000001$ which converges in 27744 steps, $\alpha = 10^{-3}$, exponentially adjusting NRBC

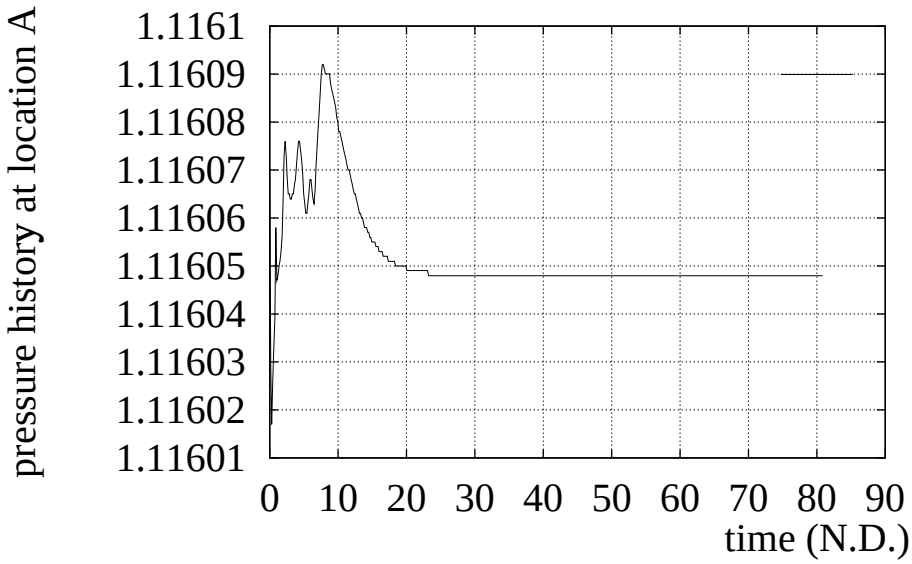

Figure 4.29: Pressure history at location A for $z = 4.2$ which converges in 27336 steps, $\alpha = 10^{-3}$, exponentially adjusting NRBC

z	Number of steps for convergence N_{conv}
≤ 0.8	Does not converge
0.85	33762
0.9	29325
0.95	27846
1	27744
1.000001	27744
1.001	27744
1.03	27438
1.05	27438
1.08	27336
1.1	27336
1.9	27336
2	27336
3	27336
4.2	27336
5	27336
9.8	27336
10000	27336

Table 4.5: Typical values of convergence steps (N_{conv}) vs. z, $\alpha = 0.001$, exponentially adjusting NRBC

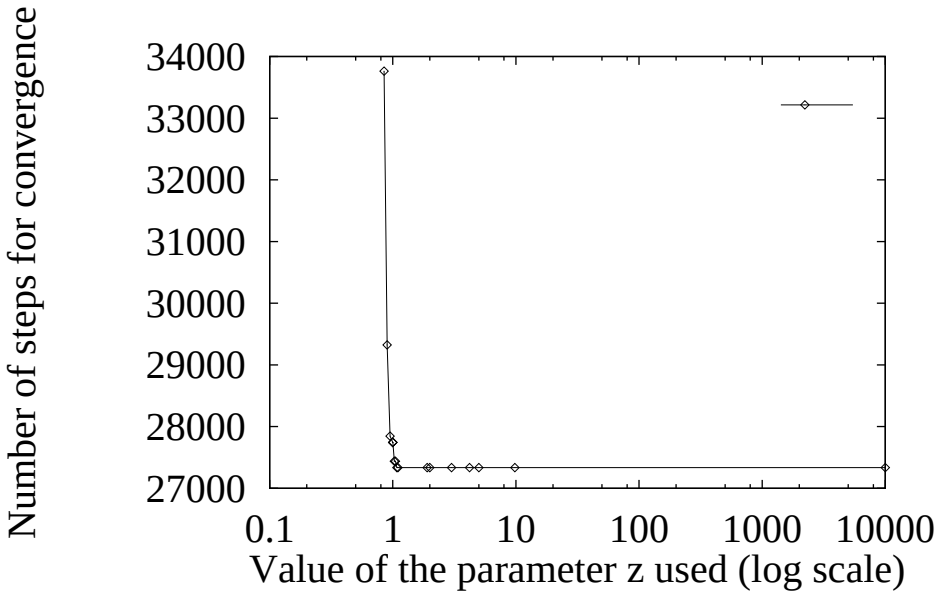

Figure 4.30: Number of steps required for convergence for different values of z, $\alpha = 10^{-3}$, exponentially adjusting NRBC

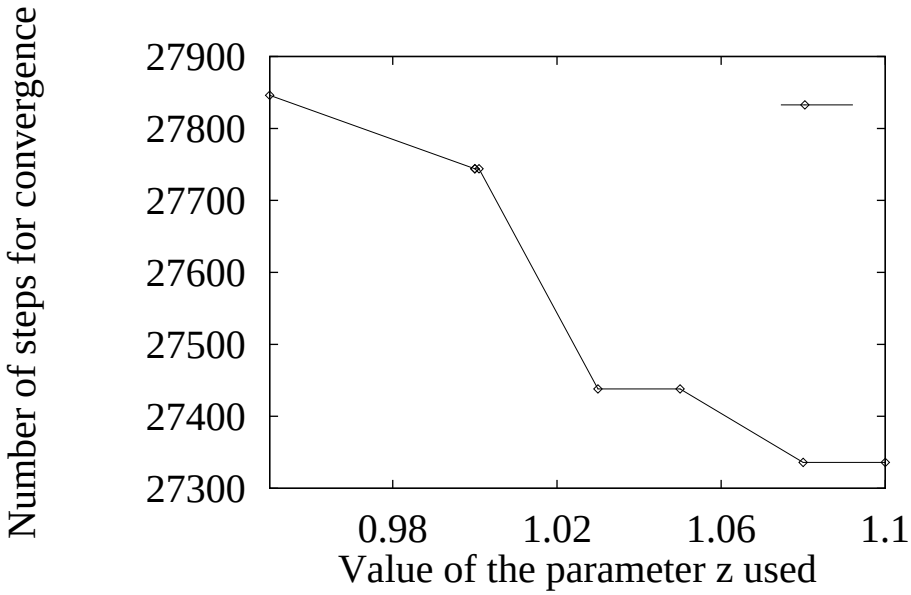

Figure 4.31: Number of steps required for convergence for different values of z, exploded view, $\alpha = 10^{-3}$, exponentially adjusting NRBC

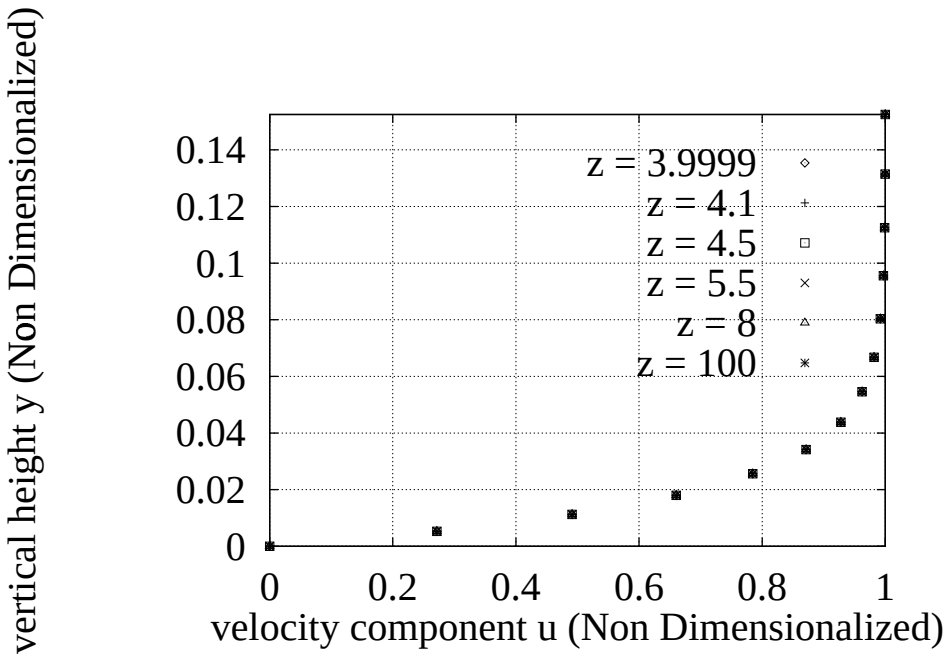

Figure 4.32: u velocity distribution with vertical distance y, $\alpha = 10^{-3}$,$x = 1.56$, logarithmically adjusting NRBC

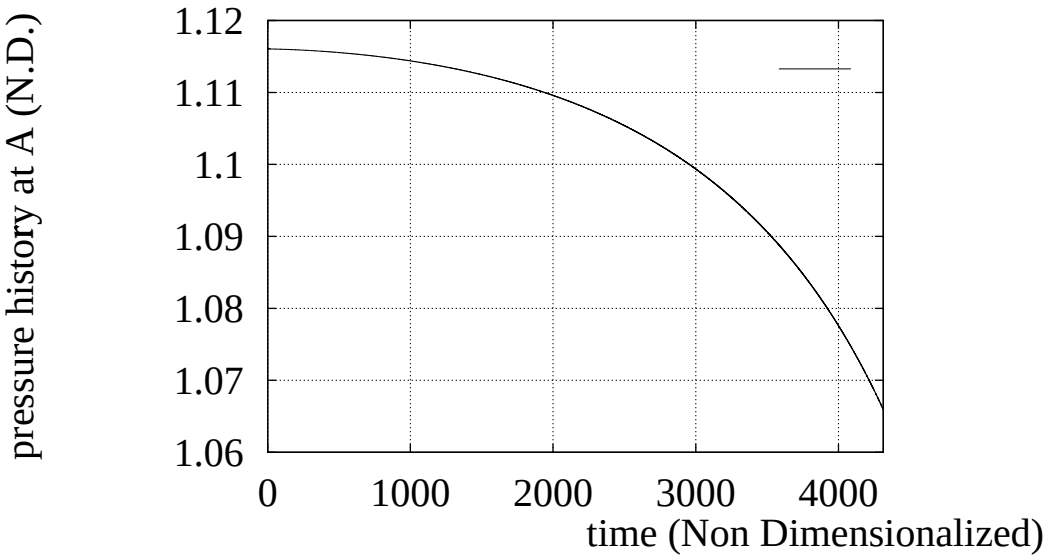

Figure 4.33: Pressure history at location A for $z = 3.5$ which diverges, $\alpha = 10^{-3}$, logarithmically adjusting NRBC

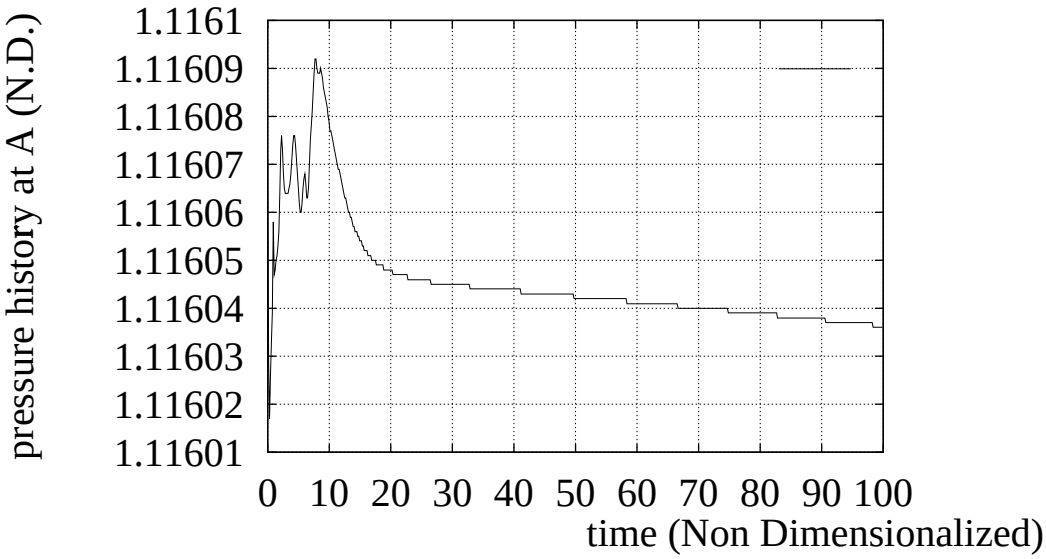

Figure 4.34: Pressure history at location A for $z = 3.99$ which converges in 33762 steps, $\alpha = 10^{-3}$, logarithmically adjusting NRBC

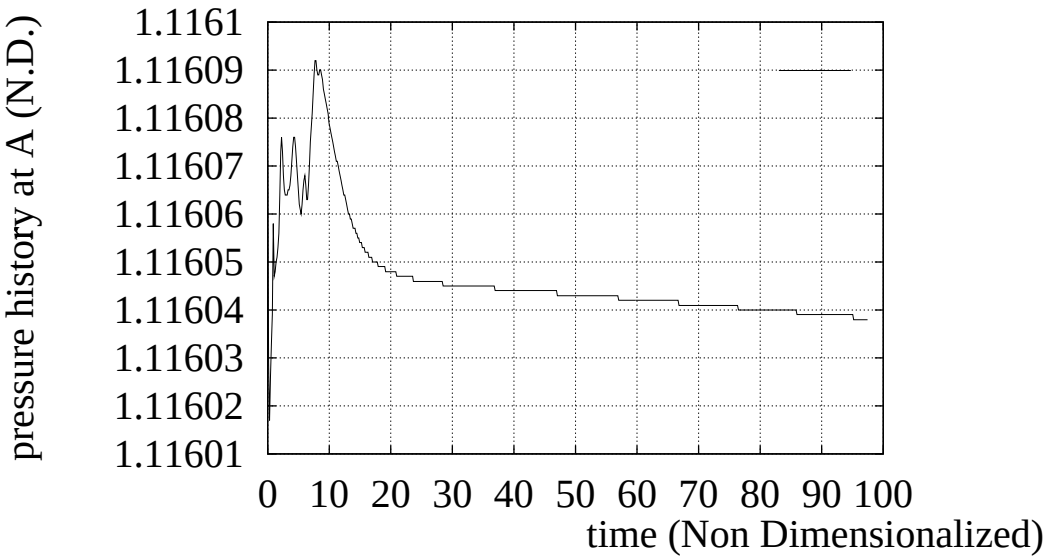

Figure 4.35: Pressure history at location A for $z = 4.05$ which converges in 32946 steps, $\alpha = 10^{-3}$, logarithmically adjusting NRBC

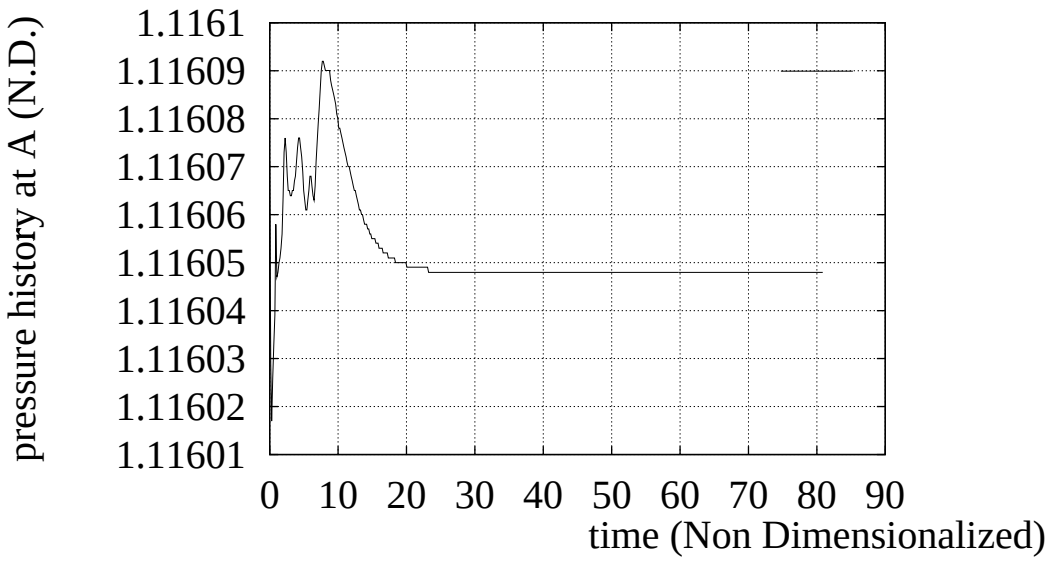

Figure 4.36: Pressure history at location A for $z = 8.0$ which converges in 27336 steps, $\alpha = 10^{-3}$, logarithmically adjusting NRBC

z	Number of steps for convergence N_{conv}
≤ 3.9	Does not converge
3.99	33762
3.999	33762
3.9999	33558
4.0	33558
4.0001	33558
4.05	32946
4.1	30396
4.15	30294
4.2	29682
4.22	29682
4.25	29325
4.4	27846
4.5	27846
4.6	27846
4.7	27846
4.8	27540
5	27336
5.5	27336
8	27336
100	27336
10000	27336

Table 4.6: Typical values of convergence steps (N_{conv}) vs. z, $\alpha = 0.001$, logarithmically adjusting NRBC

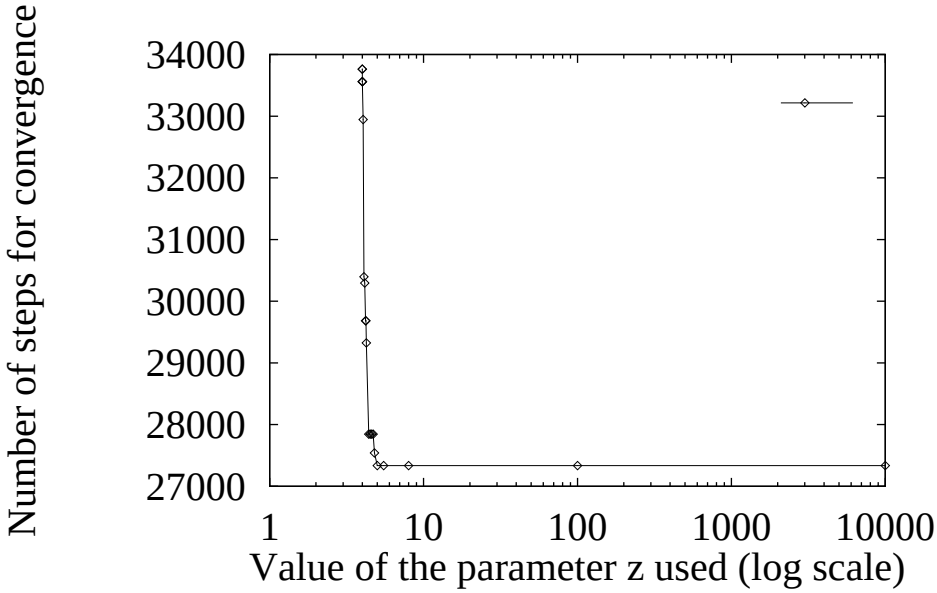

Figure 4.37: Number of steps required for convergence for different values of z, $\alpha = 10^{-3}$, logarithmically adjusting NRBC

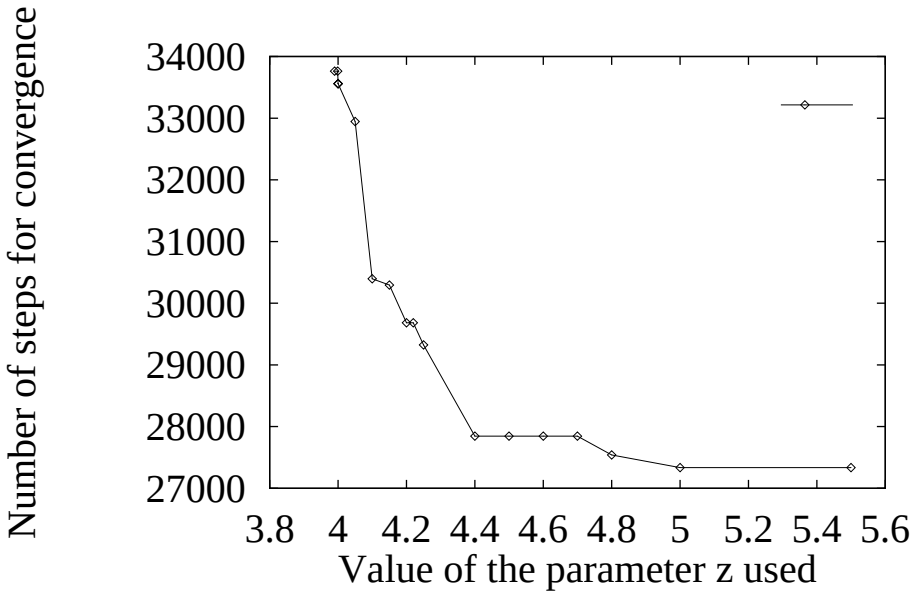

Figure 4.38: Number of steps required for convergence for different values of z, exploded view, $\alpha = 10^{-3}$, logarithmically adjusting NRBC

NRBC	α	minimum z for convergence	N_{conv} for this z
Simple 2 parameter	10^{-6}	0.223281	47634
Simple 2 parameter	10^{-3}	0.85	33762
Simple 2 parameter	0.1	10^{-6}	31467
Simple 2 parameter	0.3	10^{-3}	35292
Exponential	10^{-3}	0.85	33762
Logarithmic	10^{-3}	3.99	33762

Table 4.7: Minimum value of z required for convergence to occur

NRBC	α	minimum value of N_{conv}	z range for this N_{conv}
Simple 2 parameter	10^{-6}	27336	$z > 0.45$
Simple 2 parameter	10^{-3}	27336	$z > 1.0527$
Simple 2 parameter	0.1	27234	(0.5, 0.895)
Simple 2 parameter	0.3	27132	1
Exponential	10^{-3}	27336	$z \geq 1.08$
Logarithmic	10^{-3}	27336	$z \geq 5$

Table 4.8: Minimum value of N_{conv} and the corresponding z-range for various NRBC's and α-values

Chapter 5

Conclusion

5.1 Modeling of Unbounded Media

This dissertation deals with problems in the time domain, and the theme is obtaining solutions for wave fields in problems originally specified over unbounded/ large domains, by making use of NRBC's to truncate the domain to a finite size. The solution is obtained by applying an appropriate numerical method to the reformulated problem in terms of NRBC's.

Time dependent problems requiring the modeling of an infinite domain can be classified as those related to wave propagation and those related to diffusion. The prototype partial differential equation for the former is generally perceived to be hyperbolic, for the latter it is parabolic. But wave phenomena can be modeled/ exhibited by any of the three classes of equations. For example, paraxial wave equations that allow waves to propagate in one direction are usually parabolic, while statics (elliptic governing differential equations) as a special case of the time dependent problem (both wave propagation and diffusion) is also important.

The problems considered in this report deal with modeling of wave fields in infinite/ semi-infinite/ large media. The aim of research of this kind is to be able to solve practical problems efficiently and accurately. The region of interest in the spatial domain is generally the near (interior) region around the sources/scatterers. The far (exterior) region excluded is generally assumed to be regular. In this situation, the waves that result propagate from the structure-medium interface towards infinity (in the unbounded medium). The boundary condition applicable at infinity for wave propagation problems is a radiation condition. NRBC's are required at the truncation boundary to model the combination of an infinite domain and a radiation condition.

In this report, NRBC's have been formulated and used for two different problems. The first involves the time dependent wave equation in two dimensions for a complex geometry, the second deals with transonic flow of a Newtonian fluid over a flat plate. The first one is a second order linear partial differential equation with constant coefficients, the second one consists of compressible Navier Stoke's equations which are nonlinear.

In general, the particular NRBC for a given situation is dependent on the system of governing differential equations (g.d.e.). For each situation one may have to follow a different procedure to formulate a correct NRBC. In the case where the g.d.e. is linear, the procedure to arrive at an NRBC can be better formalized compared to the nonlinear case. A similar statement can be made about analysis carried out on the NRBC thus arrived at. The work related to the two problems reported in this dissertation amply demonstrates these general observations with regard to NRBC's.

5.2 Reported work

The work reported in this dissertation can be divided into two parts.

In the first part, a methodolgy has been developed to compute the interaction of failure induced pressure waves emanating first from a burst high pressure tube, then spreading through a low pressure liquid, and reflecting from the neighbouring pressure tubes. The proposed method affords significant economic improvement for computation by reducing the spatial domain of computation through the use of truncating boundaries where appropriate NRBC's are applied. These NRBC's simulate the behaviour of the large expanse of the low pressure fluid outside the computational domain. Well posedness analysis of the IBVP obtained when the problem is posed with these new set of boundary conditions applicable at the artificial boundary introduced at a finite distance from the source(s) and scatterer(s), rather than the original IBVP posed in terms of the Sommerfeld radiation condition which is applicable only at large distances from the sources/scatterers, is presented. Computational results obtained for a simplified domain are compared with the corresponding analytical solution to verify the applicability of the method before using the method for the complex geometry of

the PHWR. An elaborate computer experimentation is carried out on the placement of truncating boundaries. Transient phase of the solution is concentrated upon. The g.d.e. used is the scalar wave equation. The problem is linear.

This work has been reported in Chaturvedi and Roy [1999].

In the second part, a set of new NRBC's for the compressible Navier Stoke's equations are proposed. The motivation for these new two parameter NRBC's arises from the work of Rudy and Strikwerda [1980, 1981] who have proposed a single parameter NRBC. Their NRBC is a generalization of that proposed by Hedstrom [1979], which is more suitable for transient calculations. Rudy and Strikwerda added a term containing a parameter α to the Hedstrom NRBC to make it suitable for calculating steady state solutions (using time marching techniques) for subsonic compressible flow of a Newtonian fluid. The NRBC's proposed in this work involve two parameters (α and z), and can be viewed as generalizations of the Rudy and Strikwerda NRBC.

The choice of $z = 1$ in the first of these, the simple two parameter NRBC (equation 4.20), results in the Rudy and Strikwerda NRBC (equation 4.12), while $\alpha = 0$ can be used to reduce it to the Hedstrom NRBC. Hence the new NRBC's can be used to experimentally investigate the optimality of the Rudy and Strikwerda NRBC, where optimality is measured in terms of number of steps required for convergence. Use of NRBC's of this form is indicated for subsonic flow which requires the specification of a boundary condition at the outflow (which in many cases is the specification of pressure), and is especially useful in computing the steady state solution by a time marching technique. Numerical experiments carried out with these NRBC's for calculating the steady state solution for flow over a flat plate are presented. Thus we deal with a non linear set of governing differential equations and boundary conditions but a simple geometry in this part of the work. For certain values of α, it has been demonstrated that a choice of $z \neq 1$ results in faster convergence, in particular, for $\alpha = 0.1$ $z = 1$ results in a local maximum in N_{conv}. Results have been obtained for a number of combinations of the parameters α and z.

The other two NRBC's proposed and investigated are obtained by manipulating the pressure adjusting term $(p - p_\infty)$– it has been placed under the exponential

and logarithmic symbols to obtain them. Results of numerical experimentation with these NRBC's have been presented, which can serve as a guideline for the choice of the parameters for more complicated flowfields. An exponential evolution of the term $(p - p_\infty)$ leads to better convergence characteristics as compared to the logarithmic evolution of this term. Here, convergence characteristics are studied in terms of the minimum value of the parameter z required before the NRBC in question starts resulting in convergence for a fixed α. From this point of view, the logarithmically adjusting NRBC is not recommended.

The work that has thus been accomplished is enumerated below:

1. A critical review of the vast literature in the field of NRBC's.

2. Methodology for solving problems of wave propagation in a large domain (for a PHWR, for example), where the region of interest is much smaller than the total domain, and transient phase is of greater interest. This methodology is computationally efficient.

3. Formulation of NRBC's that can be applied for the scalar wave equation.

4. Their well posedness analysis, including well posedness at the corners. This analysis is largely based on the work of Kreiss.

5. Validation of the solution procedure for a simple geometry for which an analytical solution is available.

6. Numerical simulation of the failure event in a PHWR, based on the above model. Results obtained for various types of failure based on the model utilizing analyzed NRBC's.

7. Interpretation of the results obtained.

8. Determination of a suitable interior domain for simulating the PHWR problem, such that it is not too large.

9. Proposal of three new NRBC's for compressible Navier Stokes equations.

10. Placing these NRBC's in the appropriate context in literature on similar NRBC's (Hedstrom's NRBC and Rudy and Strikwerda NRBC).

11. Utilizing these NRBC's to obtain steady state solution for flow over a flat plate using a time marching technique.

12. Comparison of these NRBC's with their historical precursors– Rudy and Strikwerda NRBC's– of which they can be looked upon as generalizations.

13. Obtaining data on the performance of these NRBC's in terms of (a)iterations required to reach steady state and (b)pressure fluctuations at a point in the domain.

14. Interpretation of these results.

A fair amount of new contributions to knowledge is achieved in the points above.

5.3 Scope of further work

Regarding the problem of the Pressurized Heavy Water Reactor, an obvious direction of further work is the use of a fluid structure interaction code which will take into account the vibrations of the tubes (in two or three dimensions), and the effect of the movement of the structure on the pressure field in the moderator. Better models for the pressure field in the moderator may also be considered, and NRBC's developed for them.

In connection with the work on NRBC's for compressible Navier Stokes equations, an analysis was not provided. Examples of well posedness and other analyses do exist in literature, but such work has mainly been carried out on linearized equations, or equations otherwise simplified.

As far as an analysis of the optimal values of the parameters in the NRBC's for the Navier Stokes equations is concerned, Rudy and Strikwerda [1980, 1981] have provided results based on linearized Navier Stokes equations. However, the experimental results for the full Navier Stokes equations show a wide variance in the optimal

value of the parameter α from the result obtained from analysis. The new NRBC's that have been proposed in this report themselves are non linear, unlike the Rudy and Strikwerda NRBC which is linear. Hence, the linearization of the governing differential equations alone is not going to result in a linear system for analysis. This analysis may be considered in future work.

Also, the proposed NRBC's for the full Navier Stokes equations can be utilized for solving the flow field for more complex geometries than a flat plate, for example, a single airfoil or a cascade of airfoils. The results thus obtained can be compared with experimental values.

5.4 Publications

Following publications report the work presented in this dissertation:

1. R. Chaturvedi and D. P. Roy, Some formulations of local non reflecting boundary conditions, Proceedings of the 20th Fluid Mechanics and Fluid Power Conference, Dec. 1993, Fluid Control and Research Institute, Palakkad, India.

2. R. Chaturvedi and D. P. Roy, Non reflecting boundary conditions applied to water wave problems, Proceedings of the 21st Fluid Mechanics and Fluid Power Conference, Dec. 1994, Hyderabad, India.

3. R. Chaturvedi and D. P. Roy, Non reflecting boundary conditions and their use in estimating the effects of coolant channel failure in a PHWR, Nuclear Engineering and Design, 188, 345-360, 1999.

References

1. Bamberger, A., Chalinder, B., Jolly, P., Roberts, J. E., and Teron, J. L., Silent Boundary Methods for Transient Analysis, *SIAM J. Sci. Statist. Comput.*, **9**, 1016, (1988).

2. Bando, K., Bettes, P., and Emson, C., The Effectiveness of Dampers for the Analysis of Exterior Scalar Wave Diffraction by Cylinders and Ellipsoids, *Int. J. Numer. Methods Fluids*, **4**, 599, (1984).

3. Barry, A., Bielak, J., and MacCamy, R. C., On Absorbing Boundary Conditions for Wave Propagation, *J. Comput. Phys.*, **79**, 449, (1988).

4. Baskakov, V. A., and Popov, A. V., Transparent Boundary Conditions for Schrödinger-Type Equations, *Wave Motion*, **14**, 123, (1991).

5. Bayliss, A., and Turkel, E., Radiation Boundary Conditions for Wave Like Equations, *Commun. Pure Appl. Math.*, **33**, 707, (1980).

6. Bayliss, A., and Turkel, E., Far Field Boundary Conditions for Compressible Flows, *J. Comput. Phys.*, **48**, 182, (1982).

7. Blaschak, J. G., and Kriegsmann, G. A., A Comparative Study of Absorbing Boundary Conditions, *J. Comput. Phys.*, **77**, 109, (1988).

8. Canuto, C., Hariharan, S. I., and Lustman, L., Spectral Methods for Exterior Elliptic Problems, *Numerische Mathematik*, **46**, 505, (1985).

9. Carpenter, K. M., Note on the paper 'Radiation Conditions for the Lateral Boundaries of Limited Area Numerical Models' by M. J. Miller and A. J. Thorpe in *Q. J. Roy. Meteor. Soc.*, **107**, 615, Q. J. Roy. Meteor. Soc. 108, 717, (1982).

10. Castellani, A., Finite Element Method Accuracy for Wave Propagation Problems, *Meccanicca*, **9**, 199, (1974).

11. Cerjan, C., Kosloff, D., Kosloff, R., and Reshef, M., A Nonreflecting Boundary Condition for Discrete Acoustic and Elastic Wave Equations, *Geophysics*, **50**, 705, (1985).

12. Chaturvedi, R., and Roy, D. P., Non Reflecting Boundary Conditions Applied to Water Wave Problems, *Proceedings of 21st Fluid Mechanics and Fluid Power Conference*, Hyderabad, India, (1994).

13. Chaturvedi, R., and Roy, D. P., Non Reflecting Boundary Conditions and their Use in Estimating the Effects of Coolant Channel Failure in a PHWR, *Nuclear Engineering and Design*, **188**, 345, (1999).

14. Chen, Y. M., Numerical Computation of Dynamic Stress Intensity Factors by a Lagrangian Finite-Difference Method (the HEMP Code), *Engng. Fracture Mech.*, **7**, 653, (1975).

15. Chen, H. S., Infinite Elements for Water Wave Radiation and Scattering, *Int. J. for Num. Meth. in Fluids*, **11**, 555, (1990).

16. Chu, C. K., and Sereny, A., Boundary Conditions in Finite Difference Fluid Dynamics Codes, *J. Comput. Phy.*, **15**, 476, (1974).

17. Clarebout, J. E., *Imaging the Earth's Interior*, Blackwell Scientific Publishers, London, (1985).

18. Clayton, R., and Engquist, B., Absorbing Boundary Conditions for Wave Equation Migration, *Geophysics*, **45**, 895, (1980).

19. Clayton, R., and Engquist, B., Absorbing Boundary Conditions for Acoustic and Elastic Wave Equations, *Bull. of the Seismological Society of America*, **67**, 1529, (1977).

20. Cohen, M., and Jennings, P. C., 'Silent Boundary Methods for Transient Analysis', in *Computational Methods for Transient Analysis*, ed. Belytschko, T., and Hughes, T. J. R., Elsevier, Amsterdam, 301, (1983).

21. Elvius, T., and Sundström, A., Theoretical and Practical Aspects of Some Initial Boundary Value Problems in Fluid Dynamics, *Tellus*, **25**, 132, (1973).

22. Emerman, S. H., and Stephen, R. A., Comment on Absorbing Boundary Conditions for Acoustic and Elastic Wave Equations by R. Clayton and B. Engquist in Bull. of the Seismological Society of America 67 pg. 1529, *Bull. Seismol. Soc. Amer.*, **73**, 661, (1983).

23. Engquist, B., and Halpern, L., Absorbing Boundary Conditions for Dispersive Wave Equation, *Appl. Numer. Methods*, **4**, 21, (1988).

24. Engquist, B., and Majda, A., Absorbing Boundary Conditions for the Numerical Simulation of Waves, *Mathematics of Computation*, **31**, 629, (1977).

25. Engquist, B., and Majda, A., Radiation Boundary Conditions for Acoustic and Elastic Wave Equations, *Commun. Pure Appl. Math.*, **32**, 313, (1979).

26. Engquist, B., and Majda, A., Numerical Radiation Boundary Conditions for Unsteady Transonic Flow, *J. Comput. Phys.*, **40**, 91, (1981).

27. Feng, K., Finite Element Method and Natural Boundary Reduction, in *Proceedings of International Congress of Mathematicians*, Warsaw, Poland, 1439, (1983).

28. Fix, G. J., and Marin, S. P., Variational Methods for Underwater Acoustic Problems, *J. Comput. Phys.*, **28**, 253, (1978).

29. Foreman, M. G. G., An Accuracy Analysis of Boundary Conditions for the Forced Shallow Water Equations, *J. Comput. Phys.*, **64**, 334, (1986).

30. Givoli, D., and Keller, J. B., A Finite Element Method for Large Domains, *Comput. Methods Appl. Mech. Eng.*, **76**, 41, (1989).

31. Givoli, D., and Keller, J. B., Non-reflecting Boundary Conditions for Elastic Waves, *Wave Motion*, **12**, 261, (1990).

32. Givoli, D., Non-reflecting Boundary Conditions, *J. Comput. Phys.*, **94**, 1, (1991).

33. Goldstein, C. I., 'Numerical Methods for Helmholtz Type Equations in Unbounded Regions', in *Mathematical Methods and Applications of Scattering Theory*, ed. DeSanto, J. A., et. al., Lecture Notes in Physics Vol. 130, Springer Verlag, New York, (1980).

34. Grosch, G. E., and Orszag, S. A., Numerical Solution of Problems in Unbounded Regions: Coordinate Transforms, *J. Comput. Phys.*, **25**, 273, (1977).

35. Gurtin, M. E., The Linear Theory of Elasticity, Section 74, Mechanics of Solids II, Truesdell, C., ed., in *Encyclopedia of Physics*, Vol. VIa/2, Springer, Berlin, 257-264, (1972).

36. Hagstrom, T., Boundary Conditions for Parabolic Equations on Unbounded Domains, *SIAM J. Num. Anal.*, **23**, 948, (1986).

37. Hagstrom, T., and Hariharan, S. I., Accurate Boundary Conditions for Exterior Problems in Gas Dynamics, *Math. Comput.*, **51**, 581, (1988).

38. Hagstrom, T., and Keller, H. B., Exact Boundary Conditions at an Artificial Boundary for Partial Differential Equations in Cylinders, *SIAM J. Math. Anal.*, **17**, 322, (1986).

39. Halpern, L., Absorbing Boundary Conditions for the Discretization Schemes of the One-Dimensional Wave Equation, *Mathematics of Computation*, **38**, 415, (1982).

40. Halpern, L., Boundary Conditions for Mixed Parabolic-Hyperbolic Equations on Unbounded Domains, *SIAM J. Math. Anal.*, **22**, 1256, (1991).

41. Halpern, L., and Trefethen, L. N., Wide Angle One-way Wave Equations, *J. Acoust. Soc. Amer.*, **84**, 1397, (1988).

42. Hanson, M., and Petschek, A., Absorbing Boundary Conditions for Surface Waves, *J. Comput. Phys.*, **21**, 333, (1976).

43. Hariharan, S. I., 'Absorbing Boundary Conditions for Exterior Problems', in *Numerical Methods for Partial Differential Equations*, ed. Hariharan, S. I., and Moulden, T. H., Longman, Essex, (1986).

44. Hariharan, S. I., and Bayliss, A., *SIAM J. Sci. Statist. Comput.*, **6**, 285, (1985).

45. Hedstrom, G. W., Nonreflecting Boundary Conditions for Nonlinear Hyperbolic Systems, *J. Comput. Phys.*, **30**, 222, (1979).

46. Higdon, R. L., Absorbing Boundary Conditions for Difference Approximations to the Multi-dimensional Wave Equation, *Math. Comput.*, **47**, 437, (1986).

47. Higdon, R. L., Absorbing Boundary Conditions for Elastic Waves, *SIAM J. Numer. Anal.*, **27**, 831, (1990).

48. Hill, P. G., Hauptmann, E. G., and Lee, V., *Consequences of Pressure Tube Rupture on In-Core Components*, INFO-0115, Atomic Energy Control Board, Canada, (1985).

49. Howell, L. H., and Trefethen, L. N., Ill Posedness of Absorbing Boundary Conditions for Migration, *Geophysics*, **53**, 593, (1988).

50. Hu, F. Q., On Absorbing Boundary Conditions for Linearized Euler Equations by a Perfectly Matched Layer, *J. Comput. Phy.*, **129**, 1, (1996).

51. Israeli, M., and Orszag, S. A., Approximation of Radiation Boundary Conditions, *J. Comput. Phys.*, **41**, 115, (1981).

52. Jagannathan, S., *Nonlinear Free Surface Flows and Open Boundary Conditions*, Ph. D. Dissertation, University of California, Berkeley, (1985).

53. Jagannathan, S., Energy Flux Equalization: An Open Boundary Condition for Non-linear Free Surface Flows, *Int. J. for Numerical Methods in Fluids*, **14**, 793, (1992).

54. Jiang, H., and Wong, Y. S., Absorbing Boundary Conditions for Second-Order Hyperbolic Equations, *J. Comput. Phys.*, **88**, 205, (1990).

55. Jin, G. and Braza, M., A Non Reflecting Outlet Boundary Condition for Incompressible Unsteady Navier Stokes Calculations, *J. Comput. Phys.*, **107**, 239, (1993).

56. Keller, J. B., and Givoli, D., Exact Non-reflecting Boundary Conditions, *J. Comput. Phys.*, **82**, 172, (1989).

57. Keys, R. G., Absorbing Boundary Conditions for Acoustic Media, *Geophysics*, **50**, 892, (1985).

58. Kim, K. Y., Reid, R. O., and Whitaker, R. E., On an Open Radiational Boundary Condition for Weakly Dispersive Tsunami Waves, *J. Comput. Phys.*, **76**, 327, (1988).

59. Klemp, J. B., and Lilly, D. K., Radiation Conditions for the Lateral Boundaries of Limited-area Numerical Models, *J. Atmos. Sci.*, **35**, 78, (1978).

60. Kolakowski, H., Well Posedness of Absorbing Boundary Conditions, *Math. Methods Appl. Sci.*, **7**, 486, (1975).

61. Kolakowski, H., Well Posedness of Absorbing Boundary Conditions, *Math. Methods Appl. Sci.*, **8**, 41, (1986).

62. Kosloff, R., and Kosloff, D., Absorbing Boundaries for Wave Propagation Problems, *J. Comput. Phys.*, **63**, 363, (1986).

63. Kreiss, H. O., Initial Boundary Value Problems for Hyperbolic Systems, *Commun. of Pure Appl. Math.*, **23**, 277, (1970).

64. Kriegsmann, G., Solving the Helmholtz Equation for Exterior Problems with Variable Index of Refraction: II, *SIAM J. Sci. Statist. Comput.*, **3**, 318, (1982).

65. Kriegsmann, G., and Morawetz, C., Solving the Helmholtz Equation for Exterior Problems with Variable Index of Refraction: I, *SIAM J. Sci. Statist. Comput.*, **1**, 371, (1980).

66. Kriegsmann, G., Taflove, A., and Umashankar, K. R., A New Formulation of Electromagnetic Wave Scattering Using On-Surface Radiation Boundary Condition Approach, *IEEE Trans. on Antennas and Propagation* AP-35, 153, (1987).

67. Kuhlemeyer, R. L., and Lysmer, J., Finite Element Method Accuracy for Wave Propagation Problems, *J. Soil Mech. Foundations Div. Proc. ACSE*, Vol.**99** No.SM5, 421, (1973).

68. Kurihara, Y., and Bender, M. A., Filtering schemes in Weather Prediction Models, *Mon. Weather Rev.*, **111**, 445, (1983).

69. Liao, Z. P., and Wong, H. L., Extrapolation Boundaries in Elastodynamics, *Soil Dyn. Earthq. Eng.*, **3**, 174, (1984).

70. Lin, X., and Ballman, J., Re-consideration of Chen's Problem by Finite Difference Method, *Eng. Fracture Mechanics*, **44**, 735, (1993 a).

71. Lin, X., and Ballman, J., Numerical Method for Elastic-Plastic Waves in Cracked Solids, Part 1: Anti-plane Shear Problem, *Arch. Appl. Mech.*, **63**, 261, (1993 b).

72. Lin, X., and Ballman, J., Numerical Method for Elastic-Plastic Waves in Cracked Solids, Part 2: Plane Strain Problem, *Arch. Appl. Mech.*, **63**, 283, (1993 c).

73. Lin, X., and Ballman, J., Improved Bicharacteristic Schemes for Two-dimensional Elastodynamic Equations, *Quart. Appl. Maths.*, Vol. **LIII**, 383, (1995 a).

74. Lin, X., and Ballman, J., A Numerical Scheme for Axisymmetric Elastic Waves in Solids, *Wave Motion*, **21**, 115, (1995 b).

75. Lindman, E. L., Free Space Boundary Conditions for the Time Dependent Wave Equation, *J. Comput. Phys.*, **18**, 66, (1975).

76. Lysmer, J., and Kuhlemeyer, R. L., Finite Dynamic Model for Infinite Media, *J. Eng. Mech. Div. Proc. ASCE*, **95**, 859, (1969).

77. Mahrer, K. D., An Empirical Study of Instability and Improvement of Absorbing Boundary Conditions for the Elastic Wave Equations, *Geophysics*, **51**, 1499, (1986).

78. MacCamy, R. C., and Marin, S. P., Absorbing Boundaries for Wave Propagation, *Int. J. Math. Meth. Sci.*, **3**, 311, (1980).

79. MacCormack, R. W., The Effect of Viscosity in Hypervelocity Impact Cratering, *AIAA* Paper No. 69-354, (1969).

80. Macías, D., Brouard, S., and Muga, J. G., Artificial Absorbing Layers for Wave Propagation Problems, *Chem. Phys. Letters*, **228**, 672, (1995).

81. Miller, M. J., and Thorpe, A. J., Radiation Conditions for the Lateral Boundaries of Limited-area Numerical Models, *Q. J. Roy. Meteor. Soc.*, **107**, 615, (1981).

82. Moore, T. G., Blaschak, J. G., Taflove, A., and Kriegsmann, G. A., Theory and Application of Radiation Boundary Operators, *IEEE Trans. on Antennas. Propag.*, AP-**36**, 1797, (1988).

83. Mur, G., Absorbing Boundary Conditions for the Finite-difference Approximation of the Time-domain Electromagnetic-field Equations, *IEEE Trans. Electromagnetic Compatibility*, EMC-**23**, 377, (1981).

84. Niethammer, R. J., Kim, K. -S., and Ballman, J., Numerical Simulation of Shock Waves in Linear-Elastic Plates with Curvilinear Boundaries and Material Interfaces, *Int. J. Impact Engng.*, **16**, 711, (1995).

85. Oliger, J., and Sundtröm, A., Theoretical and Practical Aspects of Some Initial Boundary Value Problems in Fluid Dynamics, *SIAM J. Appl. Math.*, **35**, 3, 419, (1978).

86. Orlanski, I., Radiation Conditions for Incompressible Fluid Flow, *J. Comput. Phys.*, **21**, 251, (1976).

87. Pearson, R. A., Two Dimensional Incompressible Fluid Flow and Radiation Conditions, *J. Atmos. Sci.*, **31**, 1418, (1974).

88. Persillon, H., and Braza, M., Physical Analysis of Transition to Turbulence in the Wake of a Circular Cylinder by Three Dimensional Navier Stokes Simulation, *J. Fluid Mechanics*, **365**, 23, (1998).

89. Randall, C. J., Absorbing Boundary Condition for the Elastic Wave Equation, *Geophysics*, **53**, 611, (1988).

90. Raymond, W. H., and Kuo, H. L., Filtering schemes in Weather Prediction Models, *Q. J. Roy. Meteor. Soc.*, **110**, 535, (1984).

91. Robinson, A. R., 'The Transmitting Boundary– Again', in *Structural and Geotechnical Mechanics*, ed. Hall, W. J., Prentice Hall, Engelwood Cliffs, NJ, (1976).

92. Romate, J. E., Absorbing Boundary Conditions for Free Surface Waves, *J. Comput. Phys. Vol.*, **99**, 135, (1992).

93. Rudy, D. H., and Strikwerda, J. C., A Nonreflecting Outflow Boundary Condition for Subsonic Navier-Stokes Calculations, *J. Comput. Phys.*, **36**, 55, (1980).

94. Rudy, D. H., and Strikwerda, J. C., Boundary Conditions for Subsonic Compressible Navier-Stokes Calculations, *Computers and Fluids*, **9**, 327, (1981).

95. Scandrett, C. L., Kriegsmann, G. A., and Achenbach, J. D., Approximate Absorbing Boundary Conditions for Elastic Waves, *SIAM J. Sci. Statist. Comput.*, **7**, 571, (1986).

96. Schmidt, F., and Yevick, D., Discrete Transparent Boundary Conditions for Schrödinger-Type Equations, *J. Comput. Phys.*, **34**, 96, (1997).

97. Sharan, S. K., A Non-reflecting Boundary in Fluid Structure Interaction, *Computers and Structures*, **26**, 841, (1987).

98. Sharan, S. K., A Non-reflecting Boundary in Fluid Structure Interaction, *Commun. Appl. Numer. Methods*, **4**, 761, (1988).

99. Singh, R.K., Kant, T., and Kakodkar, A., Efficient Partitioning Schemes for Fluid-Structure Interaction Problems, *Eng. Comput.*, **7**, 101, (1990).

100. Singh, R.K., Kushwaha, H. S., Mahajan, S. C., and Kakodkar, A., Integrity of Neighbouring Coolant Channels in the Event of a Single Coolant Channel Failure in a PHWR, F11/2, *Proc. Structural Mechanics in Reactor Technology*, **12**, 189, Stuttgart, Germany, (1991 a).

101. Singh, R.K., Kant, T., and Kakodkar, A., Coupled Shell-Fluid Interaction Problems with Degenerate Shell and Three-Dimensional Fluid Elements, *Computers and Structures*, **38**, 515, (1991 b).

102. Smith, W. D., A Nonreflecting Plane Boundary for Wave Propagation Problems, *J. Comput. Phys.*, **15**, 492, (1974).

103. Sochacki, J., Absorbing Boundary Conditions for Elastic Waves, *Appl. Math. Comput.*, **28**, 1, (1988).

104. Sochacki, J., Kubichek, R., George, J., Fletcher, W. R., and Smithson, S., Absorbing Boundary Conditions for Surface Waves, *Geophysics*, **52**, 60, (1987).

105. Sommerfeld, A., *Partial Differential Equations in Physics*, Chapter 28, Academic Press, New York, (1949).

106. Sommerfeld, A., *Lectures on Theoretical Physics*, Academic Press, New York, (1964).

107. Tajima, T., Absorbing Boundary Condition and Budden Turning Point Technique for Electromagnetic Plasma Simulations, *J. Comput. Phys.*, **42**, 406, (1981).

108. Tappert, F. D., The Parabolic Approximation Method, in *Wave Propagation and Underwater Acoustics*, ed. Keller, J. B., and Papadkis, J. S., Springer Verlag, Berlin, (1977).

109. Thomson, K. W., Time Dependent Boundary Conditions for Hyperbolic Systems, *J. Comput. Phys.*, **68**, 1, (1987).

110. Thomson, K. W., Time Dependent Boundary Conditions for Hyperbolic Systems II, *J. Comput. Phys.*, **89**, 439, (1990).

111. Trautenberg, E. A., Gebauer, K., and Sachs, A., 'Numerical Simulation of Wave Propagation in Viscoelastic Media with Non-reflecting Boundary Conditions', in *Wave Propagation Viscoelastic Media*, ed. Mainardi, F., Pitman, London, 194, (1982).

112. Trefethen, L. N., and Halpern, L., Well Posedness of One-Way Wave Equations and Absorbing Boundary Conditions, *Math. Comput.*, **47**, 421, (1986).

113. Umashankar, K. R., and Taflove, A., A Novel Method to Analyze Electromagnetic Scattering of Complex Objects, *IEEE Trans. on Electromagn. Compat.*, EMC-**24**, 392, (1982).

114. van Dyke, M., *Perturbation Methods in Fluid Mechanics*, Academic Press, New York, (1964).

115. Vibók, *Á.*, and Balint-Kurti, G. D., Filtering schemes for Schrödinger Equation, *J. Chem. Phys.*, **96**, 7615, (1992).

116. von Neumann, J., and Richtmeyer, R. D., A Method for the Numerical Calculation of Hydrodynamic Shocks, *J. Applied Physics*, **21**, 232, (1950).

117. Wagatha, L., Approximation of Pseudodifferential Operators in Absorbing Boundary Conditions for Hyperbolic Equations, *Numerische Mathematik*, **42**, 51, (1983).

118. White, W., Valliappan, S., and Lee, I. K., Unified Boundary for Finite Dynamic Models, *J. Eng. Mech. Div. ASCE*, **103**, 949, (1977).

119. Whitham, G. B., *Linear and Nonlinear Waves*, Wiley Interscience, New York, (1974).

120. Wilson, J. C., Discrete Outflow Boundary Condition for Compressible Fluid Flow, *Proc. Edinburgh Math. Soc.*, **25**, 1, (1982).

121. Wurtele, M., Paegle, J., and Sielecki, A., Outflow Boundary Condition for Incompressible Fluid Flow, *Mon. Weather Rev.*, **99**, 537, (1971).

122. Yevick, D., Yu, J., and Yaon, Y., Filtering Schemes for Waves, *J. Opt. Soc. Am.*, **A12**, 107, (1995).

123. Zhang, Y. G., and Ballman, J., *Two Techniques for the Absorption of Elastic Waves Using and Artificial Transition Layer*, *Wave Motion*, **25**, (1997).

124. Zienkiewicz, O. C., *The Finite Element Method*, McGraw Hill, New York, (1977).

125. Zienkiewicz, O. C., and Newton, R. E., Coupled Vibrations of a Structure Submerged in a Compressible Fluid, in *Proc. Int. Symp. on Finite Element Techniques*, Univ. of Stuttgart, Germany, 359, 1969.